# ลักษณะสมบัติของ 4-α-GLUCANOTRANSFERASE รีคอมบิแนนท์จากมันสำปะหลัง *Manihot esculenta* Crantz และ *Arabidopsis thaliana*

นายกฤษณ์ ตันตนะรัตน์

วิทยานิพนธ์นี้เป็นส่วนหนึ่งของการศึกษาตามหลักสูตรปริญญาวิทยาศาสตรดุษฎีบัณฑิต

สาขาวิชาชีวเคมี ภาควิชาชีวเคมี

คณะวิทยาศาสตร์ จุฬาลงกรณ์มหาวิทยาลัย

ปีการศึกษา 2554

# CHARACTERIZATION OF RECOMBINANT 4-α-GLUCANOTRANSFERASE FROM CASSAVA *Manihot esculenta* Crantz AND *Arabidopsis thaliana*

Mr. Krit Tantanarat

A Dissertation Submitted in Partial Fulfillment of the Requirements

for the Degree of Doctor of Philosophy Program in Biochemistry

Department of Biochemistry

Faculty of Science

Chulalongkorn University

Academic Years 2011

| | |
|---|---|
| Thesis Title | CHARACTERIZATION OF RECOMBINANT 4-α-GLUCANOTRANSFERASE FROM CASSAVA *Manihot esculenta* Crantz AND *Arabidopsis thaliana* |
| By | Mr. Krit Tantanarat |
| Field of Study | Biochemistry |
| Thesis Advisor | Associate Professor Tipaporn Limpaseni, Ph.D |

---

Accepted by the Faculty of Science, Chulalongkorn University in Partial Fulfillment of the Requirements for the Doctoral Degree

..... Dean of the Faculty of Science

(Professor Supot Hannongbua, Dr.rer.nat)

THESIS COMMITTEE

.....Chairman

(Professor Anchalee Tassanakajon, Ph.D.)

.....Thesis Advisor

(Associate Professor Tipaporn Limpaseni, Ph.D.)

.....Examiner

(Associate Professor Teerapong Buaboocha, Ph.D.)

.....Examiner

(Assistant Professor Kanoktip Packdibamrung, Ph.D.)

.....External Examiner

(Associate Professor Jarunee Kaulpiboon, Ph.D.)

กฤษณ์ ตันตนะรัตน์ : ลักษณะสมบัติของ 4-α-GLUCANOTRANSFERASE รีคอมบิแนนท์จากมันสำปะหลัง *Manihot esculenta* Crantz และ *Arabidopsis thaliana* (CHARACTERIZATION OF RECOMBINANT 4-α GLUCANOTRANSFERASE FROM CASSAVA *Manihot esculenta* Crantz AND *Arabidopsis thaliana*) อ.ที่ปรึกษาวิทยานิพนธ์หลัก : รองศาสตราจารย์ ดร. ทิพาพร ลิมปเสนีย์, 159 หน้า

มันสำปะหลังเป็นแหล่งของแป้งที่สำคัญ ดังนั้นการศึกษากระบวนการสร้างและย่อยสลายแป้งในหัวมันสำปะหลังจึงมีความสำคัญ ในปัจจุบันกระบวนการเมแทบอลิซึมภายในหัวมันสำปะหลังยังไม่แน่ชัด เชื่อว่า disproportionating enzyme (4-α-glucanotransferase) (DPE1) (E.C. 2.4.1.25) ซึ่งเป็นเอนไซม์ที่พบในมันสำปะหลังมีความเกี่ยวข้องในกระบวนการสร้างและย่อยสลายแป้ง เอนไซม์นี้เร่งปฏิกิริยา disproportionation โดยทำการย้ายหมู่มอลโทส หรือกลูโคสสองเรสิดิวไปยังน้ำตาลตัวรับผ่านพันธะ α-1-4 glycosidic linkage เกิดเป็นน้ำตาลที่มีหน่วยของกลูโคสเพิ่มขึ้น จากการศึกษาใน *Arabidopsis* พบว่า DPE1 มีความจำเพาะต่อมอลโทไทรโอส และสามารถสร้างออลิโกแซคคาไรด์ขนาดยาวขึ้น ในงานวิจัยได้ทำการโคลนยีน *dpe1* จาก *Arabidopsis* และมันสำปะหลัง และแสดงออกใน *Escherichia coli* จากนั้นนำรีคอมบิแนนท์ DPE1 ที่ได้จาก *Arabidopsis* (AtDPE1) และมันสำปะหลัง (MeDPE1) มาทำให้บริสุทธิ์ และหาสมบัติทางชีวเคมี และจลนพลศาสตร์ของปฏิกิริยาที่มีมอลโทไทรโอสเป็นสารตั้งต้น รีคอมบิแนนท์ MeDPE1 และ AtDPE1 มีสมบัติในการย้ายหมู่มอลโทสจากมอลโทไทรโอสไปยังมอลโทไทรโอสอีกโมเลกุล เกิดเป็นน้ำตาลที่มีขนาดยาวขึ้น ซึ่งมีสมบัติต่างจากแอมิโลมอลเทสใน *Escherichia coli* และ DPE2 ใน *Arabidopsis* เมื่อใช้เทคนิค oligosaccharide array ในการหาชนิดและความจำเพาะของตัวรับ พบว่า AtDPE1 สามารถย้ายกลูแคนไปยังสาย α-1-4 กลูเคนได้ เอนไซม์ในกลุ่มนี้สามารถย้ายกลูแคนไปยังอนุพันธ์ฟลูออโรกลูโคสได้ทำการคัดแยกผลิตภัณฑ์ฟลูออโรมอลโทสที่เกิดจากการเร่งโดยAtDPE2 และศึกษาสมบัติของผลิตภัณฑ์ที่ได้โดยใช้เทคนิค $^{19}$F-NMR, $^{1}$H-NMR และ high resolution mass spectrometry รีคอมบิแนนท์ AtDPE1 และ MeDPE1 สามารถสร้างไซโคลเดกซ์ทรินวงใหญ่ (LR-CDs) จากแอมิโลสได้จากการตรวจสอบโดยเทคนิค HPAEC-PAD และ MALDI-TOF-MS ไซโคลเดกซ์ทรินวงใหญ่ที่สร้างได้สามารถจับกับโพลีอะนิลีน ทำให้เกิดการเปลี่ยนแปลงของ UV-Vis absorption

ภาควิชา :.....ชีวเคมี..... ลายมือชื่อนิสิต.....

สาขาวิชา :.....ชีวเคมี..... ลายมือชื่ออ.ที่ปรึกษาวิทยานิพนธ์หลัก.....

ปีการศึกษา :.....2554.....

# # 5073904823 : MAJOR BIOCHEMISTRY
KEYWORDS : DISPROPORTIONATING ENZYME/ GLYCOSIDE HYDROLASE FAMILY 77 / LARGE-RING CYCLODEXTRIN

KRIT TANTANARAT : CHARACTERIZATION OF RECOMBINANT 4-α-GLUCANOTRANSFERASE FROM CASSAVA *Manihot esculenta* Crantz AND *Arabidopsis thaliana*. THESIS ADVISOR : ASSOC. PROF. TIPAPORN LIMPASENI, Ph.D., 159 pp.

Cassava is one of the most important starch sources in tropical region. The synthesis and degradation pathway of starch in the tubers are considerable commercial important. Currently, there is no clear picture of the metabolic processes involved in cassava starch metabolism. One of the enzymes believed to be involved in the starch catabolic pathway is the disproportionating enzyme (4-α-glucanotransferase) (DPE1) (E.C. 2.4.1.25). DPE1 transfers a maltosyl unit of (1,4)-alpha-D-glucan to an acceptor sugar that can produce longer chain oligosaccharides. Previous report on DPE1 in leaves of *Arabidopsis thaliana* indicated that DPE1 can specifically use maltotriose as substrate to produce longer oligosaccharides and glucose. This work reports the cloning and expression of DPE1 from *Arabidopsis thaliana* (AtDPE1) and *Manihot esculenta* Crantz caltivar KU50 (MeDPE1) in *Escherichia coli*. Purified recombinant AtDPE1 and MeDPE1 were biochemically characterized on their molecular weight, optimum pHs, optimum temperatures, the stability of the enzymes and the enzyme kinetic parameters. Recombinant MeDPE1 and AtDPE1 were able to produce longer chain oligosaccharides from maltotriose by transferring maltosyl unit and showed different properties to amylomaltase (*E.coli)* and DPE2 from *Arabidopsis thaliana* (AtDPE2) in the same glycoside hydrolase family 77 (GH77). Enzyme in GH77 family can transfer glucan to fluoroglucose derivatives to produce longer chains, MeDPE1 was also able to produce fluorooligosaccharide derivatives. The fluoromaltose derivatives produced from AtDPE2 reaction mixture were purified and characterized by $^{19}$F-NMR, $^{1}$H-NMR and high resolution mass spectrometry. Oligosaccharide array was used to find the acceptor specificity of DPE1 which showed that AtDPE1 can use maltooligosaccharide with alpha-4-glucan as acceptor. Large ring cyclodextrins were produced from amylose and degree of polymerization analysed by HPAEC-PAD and MALDI-TOF-MS techniques. Mixture of cycloamyloses can form complexes with polyaniline which resulted in change of UV-Vis absorption.

Department:.....Biochemistry..... Student's Signature.....
Field of Study:.....Biochemistry..... Advisor's Signature.....
Academic Year:.....2011.....

# ACKNOWLEDGEMENTS

I would like to express my deepest gratitude to my advisor, Associate Professor Tipaporn Limpaseni, for her beautiful mind, excellent instruction, guidance, attention and support throughout this thesis.

My gratitude is also extended to Professor Anchalee Tassanakajon, Associate Professor Teerapong Buaboocha, Assistant Professor Kanoktip Packdibamrung, Associate Professor Jarunee Kaulpiboon for their valuable suggestion and comments and also dedicating valuable time for thesis examination.

The Department of Biochemistry, Faculty of Science gave support for chemicals and instruments. My appreciate is also expressed to Professor Alison Smith, Professor Robert A. Field, Martin Rejzek, Sergey Nepogodiev, Ellis O'Neill, Christian Ruzanski, Matthew Donaldson, Stephan Goetz, Sam Mugford and Department of Metabolic Biology, Department of Biological Chemistry, John Innes Centre, UK for the collaborative research. All members of Starch and Cyclodextrin Research Unit are also appreciated for their friendships, help and encouragement throughout my study.

This work was supported by the Grant from Thailand Research Fund, Royal Golden Jubilee, Ph.D. program and 90$^{th}$ Anniversary Chulalongkorn University Fund (Ratchadaphiseksomphot Endowment Fund), the Higher Education Research Promotion and National Research University Project of Thailand, Office of the Higher Education Commission (FW650B) and the Thai Government Stimulus Package 2 (TKK 2555) under the Project PERFECTA.

Finally, the greatest gratitude is expressed to my parents and my family for their infinite love, encouragement, understanding and everything giving to my life.

# CONTENTS

Pages

Pages

Pages

Pages

Pages

Pages

# LIST OF TABLES

# LIST OF FIGURES

Figure Pages

Figure Pages

Figure Pages

Figure Pages

# LIST OF ABBREVIATIONS

| | |
|---|---|
| 2FGlc | 2-Deoxy-2-fluoro-D-glucose |
| 3FGlc | 3-Deoxy-3-fluoro-D-glucose |
| 4FGlc | 4-Deoxy-4-fluoro-D-glucose |
| 6FGlc | 6-Deoxy-6-fluoro-D-glucose |
| A | absorbance |
| Amy | Amylomaltase |
| bp | base pair |
| BSA | bovine serum albumin |
| °C | degree Celsius |
| CDs | cyclodextrins |
| CAs | cycloamyloses |
| CGTase | cyclodextrin glycosyltransferase |
| cm | centimeter |
| Da | dalton |
| D-enzyme | Disproportionation enzyme |

| | |
|---|---|
| DP | degree of polymerization |
| DPEI | Disproportionation enzyme type I |
| DPE2 | Disproportionation enzyme type II |
| g | gram |
| GH | glycoside hydrolases family |
| Glc | Glucose |
| h | hour |
| kb | kilobase |
| kDa | kilodalton |
| l | litre |
| µl | microlitre |
| LR-CDs | large-ring cyclodextrins |
| M | molar |
| mA | milliampere |
| min | minute |
| mg | milligram |
| ml | millilitre |
| mM | millimolar |

| | |
|---|---|
| MW | molecular weight |
| MWCO | molecular weight cut off |
| MQ-Water | Milli-Q water |
| nm | nanometer |
| Rf | relative mobility |
| rpm | revolution per minute |
| µg | microgram |
| µM | micromolar |
| U | unit |
| V | volt |

# CHAPTER I

# INTRODUCTIONS

## 1.1 Cassava

Cassava,manioc or yuca are the common names of a plant with starch storage organ called tubers, the scientific name is *Manihot esculenta* Crantz Its scientific classification was detailed in Table1.1. Cassava originates in Brazil. It becomes one of the most important starch crops in tropical regions (Asia, Africa and part of Latin America) especially in africa which produces more than half of the world output (Nassar *et al.* 2010). Cassava is the world's third largest source of calories, after rice and wheat, which becomes the starch source for use in culinary, animal feed and starch base products. It requires at least 8 months of warm weather to produce harvestable tubers which can accumulate starch up to 30% fresh weight. Cassava plants tolerate drought acidic or infertile soils and quickly recovers from damage caused by pests and diseases. The sequencing of the cassava genome (estimate size 760 Mb), which has been published in draft sequence, will be one tool for cassava development (Phytozomev6.0).

## 1.2 *Arabidopsis thaliana*

*Arabidopsis thaliana* is a small plant found in Europe, asia and northwestern Africa. Its scientific classification is shown in Table 1.1. *Arabidopsis thaliana* was the first plant of which its genome was sequenced in 2000 by Arabidopsis Genome Initiative. Its genome size was small 157 megabase pairs in five chromosomes.

*Arabidopsis* has become a popular tool as model organism for research in plant biology and genetics because of its small genome size, small plant sized and short life cycle (six weeks).

**1.3 Starch**

Starch is a polysaccharide formed by glucose units joined together with glycosidic bonds to form long chain polymers. It is the storage form of energy for plants. Starch is stored as granules in amyloplast with varying diameter from 2-130 microns. The size and shape of starch granule is the characteristic of each plant form. Starch has become the common carbohydrate in human diet and is present in foods such as rice, wheat, corn, potato and cassava. Starch occurs in two main forms : amylose (linear and helical glucose polymer)(Figure 1.1) and amylopectin (Branched glucose polymer) (Figure 1.2). Both forms consist of polymers of α-D-glucose units. In amylose, α-D-glucose units are linked together with α-(1,4)glycosidic bonds. In amylopectin about one residue in every twenty α-(1,4)glucose unit is linked to another α-(1,4) oligosaccharide by α-(1,6) glycosidic bond forming branch-points. The ratio between amylose and amylopectin depends on the source of starch, for example, amylose content of chestnut starch (32.9%) (Attanasio *et al.* 2004), corn (24.5%) and cassava (18.6%).

**1.4 Transitory starch**

Plants store starch in leaf-chloroplasts during the day when photosynthesis activity is higher than mobilization rate during the day (Zeeman *et al.* 2004). This is called transitory starch. When photosynthesis stopped at night time, the transitory

starch is degraded and mobilized in the form of sucrose to other non-photosynthesis organs for energy metabolism and storage.

**Table 1.1 :** Scientific classification of cassava and *Arabidopsis*.

| **Scientific classification** | | |
|---|---|---|
| | **Cassava** | ***Arabidopsis*** |
| **Kingdom** | Plantae | Plantae |
| | Angiosperms | Angiosperms |
| | Eudicots | Eudicots |
| | Rosids | Rosids |
| **Order** | Malpighiales | Brassicales |
| **Family** | Euphorbiaceae | Brassicaceae |
| **Subfamily** | Crotonoideae | |
| **Tribe** | Manihoteae | |
| **Genus** | Manihot | *Arabidopsis* |
| **Species** | *M. esculenta* | *A. thaliana* |
| | **Binomial name** | |
| | *Manihot esculenta* Crantz | *Arabidopsis thaliana* |

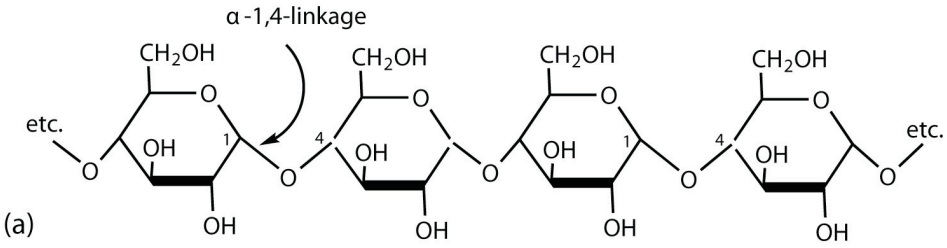


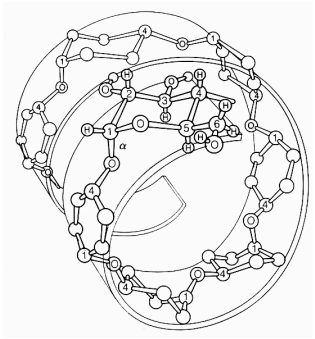

(b)

**Figure 1.1** Amylose structure (a) Amylose is a linear chain of α-D-glucose units joined together by α-1,4-glycosidic bonds. (b) secondary structure of amylose acquires a spiral structure that contains six glucose units per turn (http://www.nd.edu/~aseriann/amylose.html).

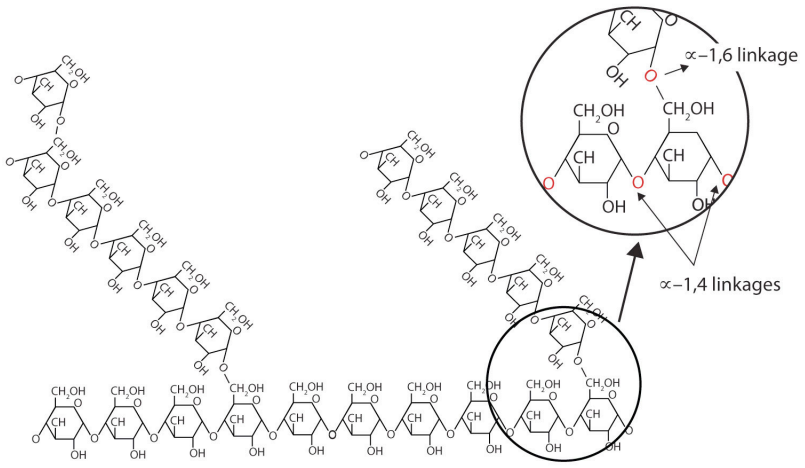


**Figure 1.2** Amylopectin structure : branching point in amylopectin formed by α-1,6-glycosidic bonds (Muhrbeck *et al.* 1987).

**1.5 Pathways of starch synthesis**

Carbon assimilated via the Calvin cycle is partitioned with a fraction exported to the cytosol for sucrose synthesis and retained fraction in the chloroplast for starch synthesis (Figure 1.3). The synthesis pathway of starch in plants starts with ADP-glucose pyrophosphorylase (AGPase) catalyses the formation of ADP-glucose from glucose-1-phosphate and ATP. Starch synthase uses ADP-glucose as substrate to add glucose units to the non-reducing end of the α-1,4-glucose polymers to form amylose molecule. Starch branching enzymes (SBE) create branch points on the amylose by hydrolyzing the 1,4-glycosidic bonds at appropriate chain length and transferring it to form 1,6 bonds at another glucose unit on the polymer to form branch point. De-branching enzyme (DBE), hydrolyzes 1, 6-glycosidic bonds and break apart branches in the polymer chains, in order to create new α-1,4 oligosaccharide with appropriate length.

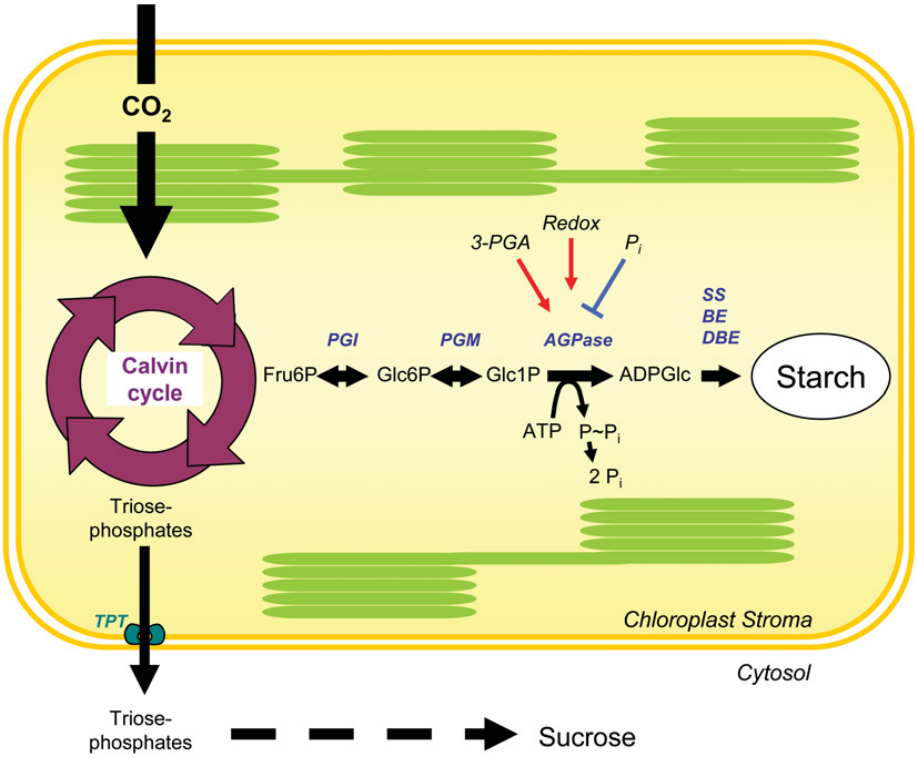


**Figure 1.3** Pathway of starch synthesis in chloroplasts. (fructose 6-phosphate (Fru6P), glucose 1-phosphate (Glc1P), glucose 6-phosphate (Glc6P), triose-phosphate/ phosphate translocator (TPT), ADP-Glucose Pyrophosphorylase (AGPase))(Zeeman *et al.* 2007).

**1.6 Pathways of starch breakdown**

In C3 plants, there are two pathways for starch degradation (hydrolytic and phosphorolytic pathway). In *Arabidopsis*, hydrolytic pathway is higher in chloroplast (Lin *et al.* 1988). Carbons released from starch by hydrolytic pathway are exported from chloroplast to cytosol as maltose and glucose transporters and converted to sucrose. In hydrolytic pathway (Figure 1.4), the first step involves the addition of phosphate to starch granule by glucan water dikinase (GWD). β-amylase and debranching enzyme or isoamylase hydrolyze starch granule to maltose and maltodextrin, β-amylase cannot hydrolyze maltotriose. Disproportionating enzyme type 1 (DPE1) produces one maltopentaose and one glucose from two maltotriose molecules via disproportionating activity (Figure 1.5). Maltose and glucose are transported out of the chloroplast to cytosol via maltose and glucose transporter at chloroplast membrane. In the cytosol, disproportionating enzyme type 2 (DPE2) transfers glucose unit from maltose to arabinogalactan or soluble heteroglycan (SHG). The glucose added to the SHG is released by an α-glucan phosphorylase (Pho2) to form glucose-1-phosphate, which is used in sucrose synthesis. Glucose in chloroplast was added phosphate group from ATP via hexokinase. The pathway through arabinogalactan or SHG can preserve energy from ATP in the glucose-glucose bond for use by hexokinase at night.

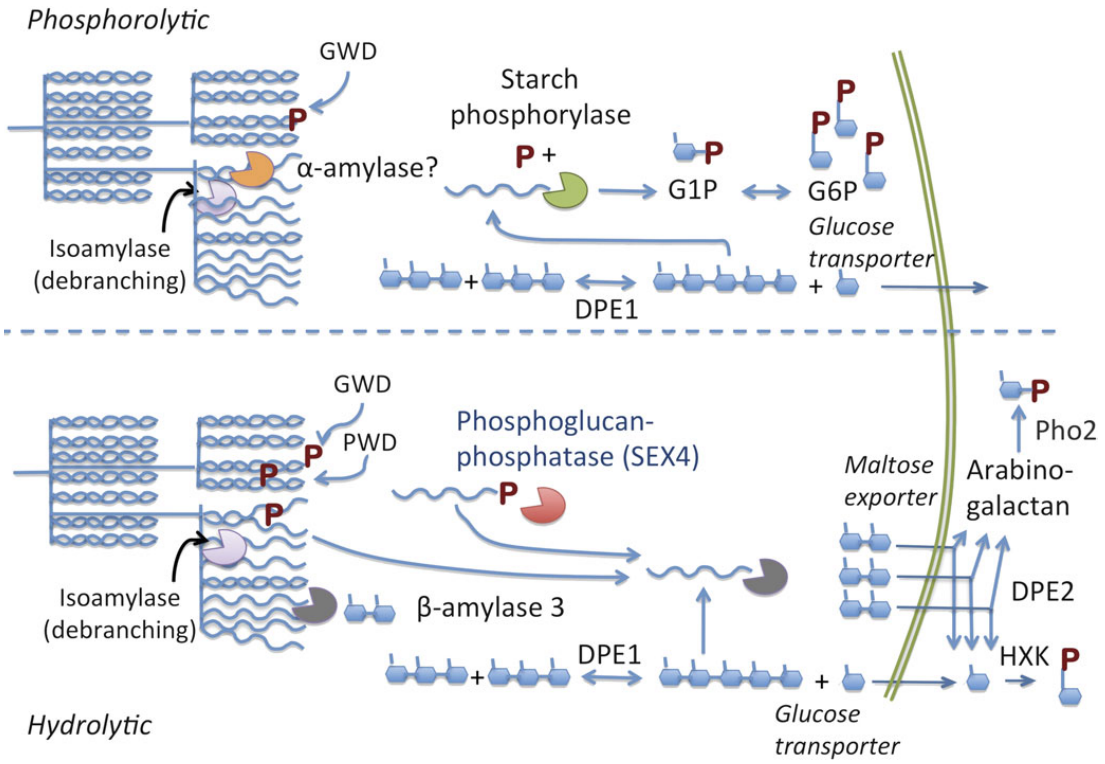


**Figure 1.4**: Phosphorolytic and hydrolytic pathways of starch breakdown in chloroplast and cytosol of C3 plant leaves. (glucan water dikinase (GWD), phosphoglucan water dikinase (PWD), Disproportionating enzyme (DPE1), Disproportionating enzyme 2 (DPE2), hexokinase (HXK), phosphoglucan phosphatase (SEX4)) Glucose on the arabinoglucan is cleaved phosphorolytically to make G1P. (Weise *et al.* 2011)

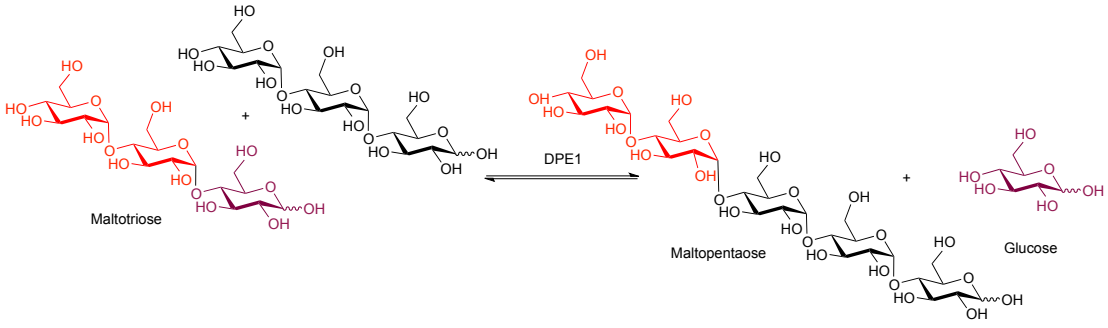


**Figure 1.5** Intermolecular transglycosylation (disproportionating activity) of D-enzyme with maltotriose ($Glc_3$) as substrate to produce maltopentaose ($Glc_5$) and one glucose unit.

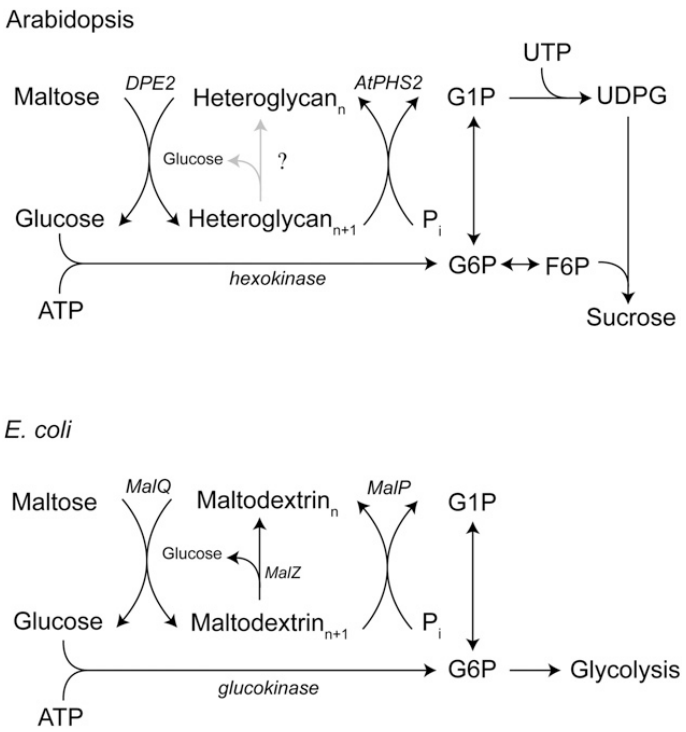


**Figure 1.6**. Schemes for maltose metabolism in *Arabidopsis* and *E. coli*. Top, Maltose conversion to Sucrose in *Arabidopsis*; bottom, maltose metabolism in *E. coli* conversion to Glycolysis. A hypothetical hydrolysis reaction to release Glucose from SHG (heteroglycan) is shown in gray with a question mark, α-glucan phosphorylase (AtPHS2), maltodextrin phosphorylase (MalP) (Lu *et al.* 2006).

**1.7 Functions of 4-α-glucanotransferase**

4-α-glucanotransferase (E.C. 2.4.1.25) can catalyze transfer of short chain maltooligosaccharide to oligosaccharide acceptor (glucose or alpha-1,4 glucan) via alpha-1,4 glycosidic bond to produce longer oligosaccharides (intermolecular transglycosylation) and synthesis of large cyclic glucan (intramolecular transglycosylation). Amylomaltase, disproportionating enzyme (D-enzyme) are glycosyl hydrolases belonging to glycoside hydrolase (GH) family 77 that show 4-α-glucanotransferase activity (Cantarel *et al.* 2009). D-enzyme (DPE1) having 4-α-glucanotransferase activity is found in many plants such as potato (Jones *et al.* 1969; Takaha *et al.* 1993; Takaha *et al.* 1998), *Arabidopsis* (Critchley *et al.* 2001; Stettler *et al.* 2009), pea (Kakefuda *et al.* 1989), sweet potato tuber (Suganuma *et al.* 1991), rice (Akdogan *et al.* 2011) and wheat endosperm (Bresolin *et al.* 2006) (Table 1.2). Disproportionating enzyme is found two isoforms ; DPE1 and DPE2.

**Table 1.2** DPE1, DPE2 and amylomaltase from various organism

| Source | Abbreviation | Accession number | Protein | LR* | References |
|---|---|---|---|---|---|
| Disproportionating enzyme isoform I | | | | | |
| *Arabidopsis thaliana* | AtDPE1 | AAK59831.1 | This study | 576 | (Critchley et al. 2001; Stettler et al. 2009) |
| *Chlamydomonas reinhardtii* | CrDPE1 | AAG29839 | Protein level | 585 | (Colleoni et al. 1999; Wattebled et al. 2003) |
| *Ostreococcus tauri* | OtDPE1 | AAS88889.1 | Hypothetical | 601 | - |
| *Solanum tuberosum* | StDPE1 | Q06801 | X-ray crystal structure (1X1N) | 576 | (Takaha et al. 1993) |
| *Triticum aestivum* | TaDPE1 | DQ068045 | Protein level | 574 | (Bresolin et al. 2006) |
| *Manihot esculenta* Crantz | MeDPE1 | cassava4.1_008552m.g | This study | | |
| *Zea mays* | ZmDPE1 | ACN26217 | Transcript level | 588 | - |
| *Ricinus communis* | RcDPE1 | XP_002528681 | Hypothetical | 584 | |
| *Oryza sativa* | OsDPE1 | NM_001066877 | protein level | 594 | (Akdogan et al. 2011) |
| Pea (*Pisum sativum* L.) | - | - | wild type | - | (Kakefuda et al. 1989) |
| Disproportionating enzyme isoform II | | | | | |
| *Arabidopsis thaliana* | AtDPE2 | NP_181616 | Transcript level | 955 | (Lin et al. 1999) |
| *Solanum tuberosum* | StDPE2 | AAR99599 | Transcript level | 948 | (Lloyd et al. 2004; Lu *et al.* 2004; Steichen et al. 2008) |

| Source | Abbreviation | Accession number | Protein | LR* | References |
|---|---|---|---|---|---|
| *Manihot esculenta* | MeDPE2 | cassava4.1_001086m | Hypothetic | 956 | - |
| *Ricinus communis* | RcDPE2 | XP_002523669 | Hypothetic | 901 | - |
| *Oryza sativa* | OsDPE2 | AK067082 | protein level | 946 | (Akdogan et al. 2011) |
| Amylomaltase (MalQ) | | | | | |
| *Aquifex aeolicus* VF5 | MalM | NP_213497 | X-ray crystal structure (1TZ7) | 485 | - |
| *Escherichia coli* CFT073 | EcMalQ | NP_756057 | Hypothetical | 694 | - |
| *Streptococcus pneumoniae* TIGR4 | SpMalQ | NP_346526 | Hypothetical | 505 | - |
| *Thermus aquaticus* ATCC 33923 | TaMalQ | BAA33728.1 | X-ray crystal structure (1CWY, 1ESW) | 500 | (Terada et al. 1999; Przylas et al. 2000; Przylas et al. 2000) |
| *Thermus thermophilus* HB8 | MalQ | BAD71084 | X-ray crystal structure (2OWX, 2OWW, 2OWC) | 500 | (Barends et al. 2007) |

*LR Length of protein (amino acid residue)

### 1.7.1 Amylomaltase

Amylomaltase (E.C. 2.4.1.25) or malQ involves in glycogen and maltooligosaccharides metabolism in microorganisms, catalyzes the transfer of short chain maltooligosaccharide to another oligosaccharide via alpha-1,4 glucan to form longer chain which glucan phosphorylase can act on (Figure 1.6). *Escherichia coli* lacking amylomaltase can not grow on maltose but its growth can be restored by transformed AtDPE2 and it was proposed that amylomaltase is similar in function to AtDPE2 (Lu et al. 2006). The genes for amylomaltase and glucan phosphorylase constituted the malPQ operon. Amylomaltase was found in many bacterial species such as *Thermus aquaticus* ATCC3392 (Terada *et al.* 1999), *Thermus thermophilus* HB8 (Kaper *et al.* 2007), *Thermus brockianus* (Bang *et al.* 2006) and *Aquifex aeolicus* VF5 (Deckert *et al.* 1998). Crystal structure of amylomaltase unbound and bound to acarbose from *Thermus aquaticus* ATCC3392 (PDB: 1CWY, 1ESW) was reported and the mechanism of the enzyme in production of cycloamylose was proposed (Przylas *et al.* 2000; Przylas *et al.* 2000). Crystal structure of amylomaltase (PDB: 2OWX, 2OWC, 2OWW) bound to acarbose and 4-deoxyglucose from *Thermus thermophilus* HB8 was also reported (Barends *et al.* 2007).

### 1.7.2 Disproportionating Enzyme 1 (DPE1)

In *Arabidopsis*, the gene coding for disproportionating enzyme 1 **(**D-enzyme) (DPE1) is located on chromosome 5 (AT5G64860) ((TAIR) 2012). DPE1 is involved in the metabolism of small maltooligosaccharides during starch degradation in

*Arabidopsis* leaves by converting small maltooligosaccharides, especially maltotriose into longer Oligosaccharides for starch-degrading enzymes such as β-amylase and starch phosphorylase. DPE1 transfers maltosyl unit from maltotriose to a second maltotriose to form maltopentaose and glucose. It was demonstrated in *Arabidopsis* that *dpe1* mutant accumulated maltooligosaccharides, especially maltotriose, which was its preferred substrate but no maltose was present (Critchley et al. 2001). Potato tuber with antisense D-enzyme (more than 98% of D-enzyme activity was eliminated) starch content or structure was not changed and it was proposed that D-enzyme was involved in starch degradation (Takaha et al. 1998). The study in *Chlamydomonas* showed different result from potato and *Arabidopsis*. The study on mutant of *Chlamydomonas* which D-enzyme was mutated let to the proposal that D-enzyme was involved in starch synthesis by transferring soluble maltooligosaccharides onto chains of the amylopectins (Colleoni *et al.* 1999; Wattebled *et al.* 2003).

#### 1.7.2.1 Intermolecular transglycosylation

Intermolecular transglycosylation which transfer glucan to the another α-1,4-D-glucan :

$$(\alpha\text{-}1,4\ \text{glucans})_m + (\alpha\text{-}1,4\ \text{glucans})_n = (\alpha\text{-}1,4\ \text{glucans})_{m-x} + (\alpha\text{-}1,4\ \text{glucans})_{n+x}$$

The enzyme in the group of glycosyltransferase (EC 2.4) were used to transfer glucan to produce longer chain of Oligosaccharide such as cyclodextrin glycosyltransferase (CGTase) (EC 2.4.1.19) which belongs to glucoside hydrolase

family 13 which low hydrolysis activity (Plou *et al.* 2007). DPE1, such as DPE1 from rice (Akdogan et al. 2011) and potato (Takaha et al. 1993) can catalyze intermolecular transglycosylation by transfer maltosyl unit between α-1,4 glucan via α-1,4 glycosidic bond. There was no report on using this enzyme for oligosaccharide synthesis.

#### 1.7.2.2 Intramolecular transglycosylation (cyclization activity)

Intramolecular transglycosylation or cyclization activity which transfer glucan on the same chain of amylose or amylopectin to produce cyclic α-1,4 glucans, large ring cyclodextrin or cycloamylose:

$$(\alpha\text{-}1,4\ \text{glucans})_m = \text{cyclic}(\alpha\text{-}1,4\ \text{glucans})_x + (\alpha\text{-}1,4\ \text{glucans})_{m-x}$$

Cyclodextrin glycosyltransferase (CGTase) catalyzed the cyclization activity (Zheng *et al.* 2002) but it produce smaller cycloamylose than DPE1 from potato (Takaha *et al.* 1996; Takaha *et al.* 1998) and amylomaltase from *thermus aquaticus* ATCC 3329 (Terada et al. 1999).

### 1.7.3 Disproportionating Enzyme 2 (DPE2)

DPE2 of *Arabidopsis thaliana* is located on chromosome 2 (AC002409) (Lin *et al.* 1999) and characterized to be involved in maltose metabolism in leaves (Steichen *et al.* 2008). A potato (*Solanum tuberosum*) encoding *dpe*2 (disproportionating enzyme isoforms 2) StDPE2 was present in chloroplast and accumulated at the time of starch degradation in potato tubers and leaves. In transgenic potato which StDPE2 activity was completely eliminated showed the accumulation of maltooligosaccharides during the dark period. The DPE2 transfers the non-reducing glucosyl unit of maltose to oyster glycogen and to a soluble

heteroglycan (SHG) found in cytosol of plant leaves (Lloyd *et al.* 2004). DPE2 transfers the non-reducing glucosyl unit from maltose to glycogen by a ping-pong mechanism and releases one free glucose. Glu-758 protonates the α-1,4-glycosidic oxygen in maltose while Asp-563 attacks C1 of the non-reducing end glucosyl unit, forming a covalent bond. Glucose leaves from the active site. Glu-758 to protonate the C4-hydroxyl group at the non-reducing end activating C4 for nucleophilic attack on C1 of the enzyme to reform an α-1,4-glycosidic bond (Figure 1.7).(Steichen et al. 2008). The forward reaction is specific to β-anomer of maltose while reverse reaction is not stereospecific to glucose acceptor (Steichen et al. 2008).

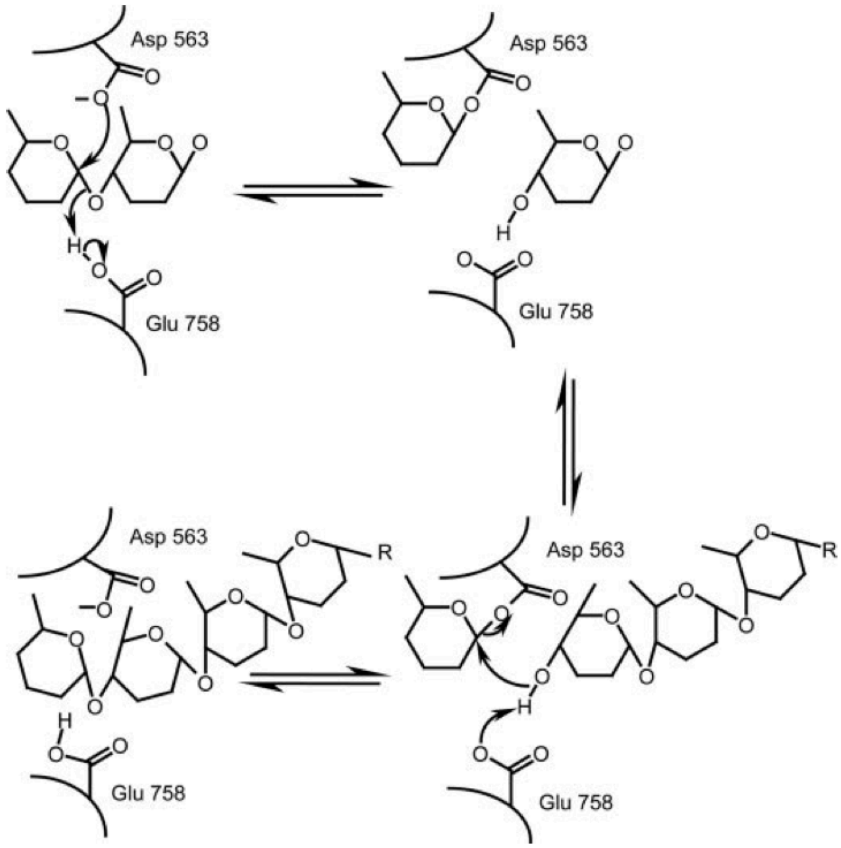


**Figure 1.7** The proposed reaction mechanism of DPE2 (Steichen et al. 2008).

**1.8 Protein domain structure of DPE1, DPE2 and amylomaltase.**

DPE1, DPE2 and amylomaltase are classified in the same glucoside hydrolase family 77 (GH77) but they have different protein domain structures. The protein structure of DPE1 contain signal peptide or plastid targeting sequence (CTP) at N-terminal and GH77 domain at C-terminal. DPE2 consists of a family 77 glycosyl hydrolase domain, similar to DPE1 but interrupted by a peptide insertion of >150 amino acids. The insert segment is at the surface of the enzyme and opposite the active site thus it can not interact with substrate at the active site. The N-terminal contains two carbohydrate binding domains (Steichen et al. 2008). This arrangements of DPE1 and DPE2 were found in all plants that have been sequenced. Amylomaltase contains only 77 glycosyl hydrolase domain same as DPE1 but has longer amino acid sequence than DPE1, without signal peptide at N-terminal (Figure 1.8).

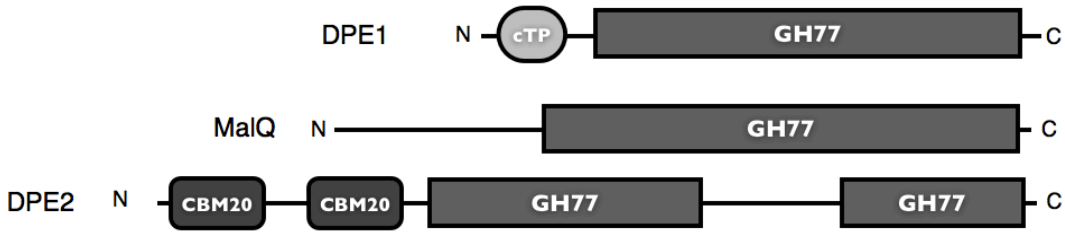


**Figure 1.8** Structure relationships of 4-α-glucanotransferases : DPE1, DPE2 and amylomaltase

**1.9 Structure of enzyme in GH77 family**

Crystal structures of the enzymes in this family were reported for amylomaltases from 4 bacterial (Henrissat 1991). Amylomaltase from *Thermus aquaticus* ATCC3392 in apo protein crystal (PDB: 1CWY) and acarbose bound with amylomaltase (PDB: 1ESW), amylomaltase from *Aquifex aeolicus* VF5 in apo protein crystal (PDB: 1TZ7), amylomaltase from *Thermus brockianus* in apo protein crystal (PDB: 2X1I), amylomaltase from *Thermus thermophilus* HB8 in apo crystal, acarbose and 4-deoxyglucose (2OWX, 2OWC, 2OWW). The only reported crystal structure of plant D-enzyme was D-enzyme from potato (*Solanum tuberosum*) in apo crystal (1X1N). The domains of amylomaltase were comparable to D-enzyme from potato (Figure 1.9). The general protein domains of α-amylase family in GH77 family contained the $(\beta/\alpha)_8$-chain fold barrel (domain A) and three subdomains (B1, B2 and B3) attached around the barrel (Figure 1.9). The catalytic residues were Asp (nucleophile), Glu (general acid/base catalyst) and Asp (third catalytic residue). When the amylomaltase was compared with pancreatic pig α-amylase and CGTase from *Bacillus circulans* in α-amylase family, it appeared that amylomaltase contained one domain $(\beta/\alpha)_8$-chain fold barrel as core and several inserts (subdomain B1, B2 and B3) between barrel core domain (Figure 10a). In amylomaltase, C-terminal domain (domain C, D and E) were absent which was different from pancreatic pig α-amylase and CGTase (Figure10 b,c). CGTase has two extra domains (domain D and E) while α-amylase has only three domains (A to C). Domain C of CGTase from *Bacillus circulans* appeared as an antiparallel β-sandwiched involved in maltose binding or

substrate binding sites. The function of domains D and E are not clear. Domain D may be involved in carbohydrate binding whereas domain E was believed to be important for attaching the enzyme to raw starch granules (Strokopytov *et al.* 1996).

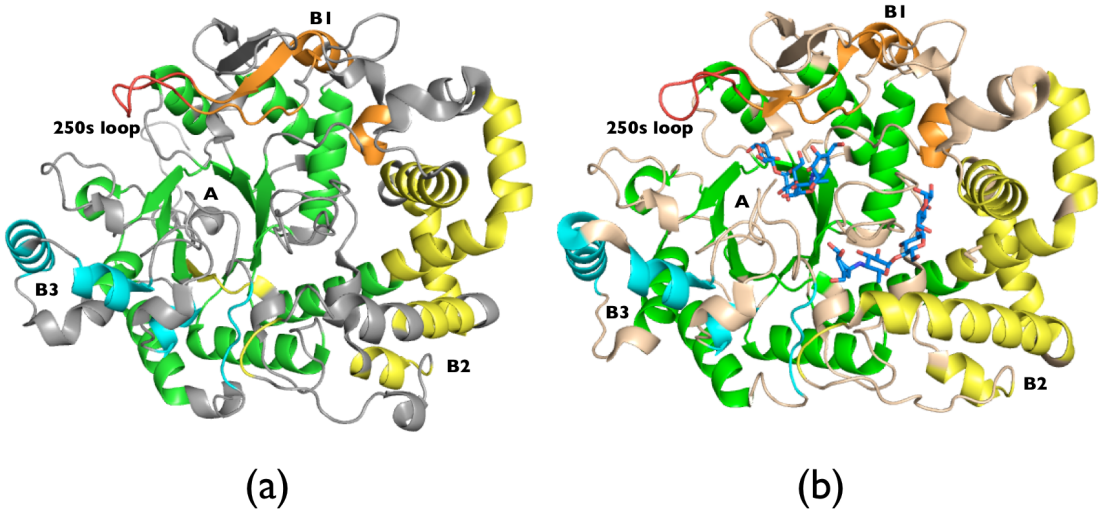


**Figure 1.9** Compare overall structure of (a) D-enzyme from potato (*Solanum tuberosum*) in apo crystal (1X1N) and (b) Amylomaltase from *Thermus aquaticus* ATCC3392 bound with acarbose (PDB: 1ESW) with domain A, 250s loop and three subdomain B1, B2 and B3.

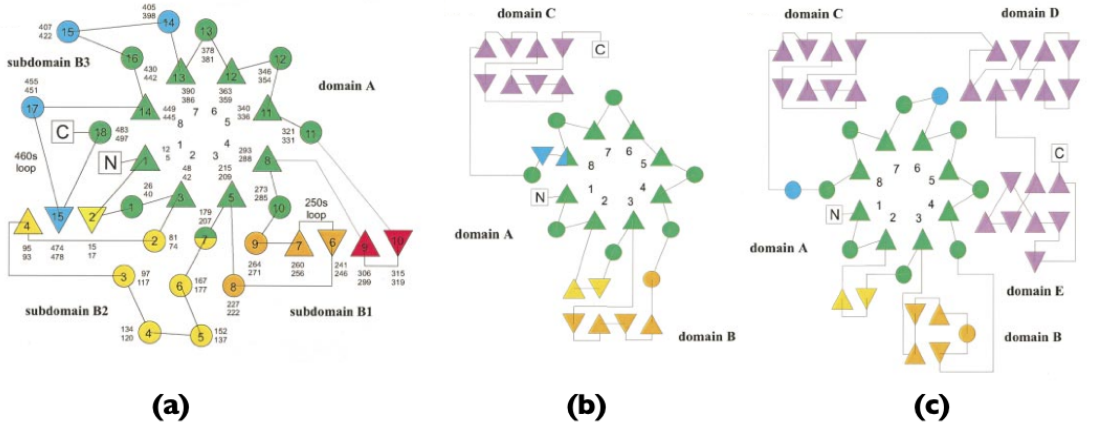


**Figure 1.10** Topography diagram compare between (a) amylomaltase from *Thermus aquaticus*, (b) pancreatic pig α-amylase and (c) CGTase from *Bacillus circulans*. (β-Strands are indicated by triangles, helices are marked by circles. The $(\beta/\alpha)_8$ barrel core structure (domain A) is colored in green, insertions between the first and fifth strand of the barrel (subdomain B2 and B1) are painted in a gradient going from yellow to red. Additional small insertions are shown in blue (subdomains B3). The additional C-terminal domains (C, D and E) are colored in purple) (Przylas et al. 2000).

## 1.10 Cyclodextrins

Cycloamylose also called cyclomaltodextrin is the cyclic α-1,4 glucans containing glucose units. Cyclodextrins (CDs) generally refer to small cyclic α-1,4 glucans numbers such as α-, β- and ɣ-CD which are composed of 6, 7 and 8 D-glucopyranose units, respectively. Each of the glucose units is in the rigid $^4C_1$-chair conformation, giving the macrocycle the shape of a hollow truncated cone (Figure 1.11). The cone is formed by the carbon skeletons of the glucose units and the glycosidic oxygen atoms in between glucose unit. The primary hydroxyls were on the narrow side of the cone and the secondary hydroxyls at the wide face. The hydroxyls make cyclodextrin water-soluble. The cavity of the cyclodextrin rings consist of a ring of C-H groups, make interior ring of cyclodextrin less polar. Structure of glucose molecule arrangement to from cyclodextrins is shown in Figure 1.11.

### 1.10.1 Large ring cyclodextrins or cycloamylose

Cyclodextrins with more than 9 D-glucopyranose units are called large-ring cyclodextrins (LR-CDs). LR-CDs will be abbreviated as $CD_n$, where n designated the number of D-glucopyranose units. The solubility of LR-CDs (except $CD_9$, $CD_{10}$, $CD_{14}$ and $CD_{26}$) are higher than α- and ɣ-CD. Some of the physicochemical properties of α-CD to $CD_{39}$ are listed in Table 1.3. $CD_9$, $CD_{10}$, $CD_{14}$ and $CD_{26}$ have been described using X-ray crystallographic analysis. Molecular structure of CD9 is a distorted elliptic boat-like shape while molecular structure of $CD_{10}$ and $CD_{14}$ exhibit a more elliptical macrocycle folded in a saddle-like shape (Figure 1.11)(Jacob *et al.* 1999). Structure of $CD_{26}$ is two antiparallel left-hand amylose like helices (Gessler *et al.*

1999). Other LR-CDs structures have not been reported because their single crystals cannot be prepared. Thus, conformational search with molecular dynamic simulation and principal component analysis were used instead (Ivanov 2010). The arrangement between two adjacent D-glucopyranose unit existed in two types : syn type conformation is commonly found in cyclodextrins which primary and secondary hydroxyl groups located on the same side. If they are located on different sides, they are called anti type conformation (band flip). $CD_{10}$, $CD_{14}$ and $CD_{26}$ are found in anti type conformation.

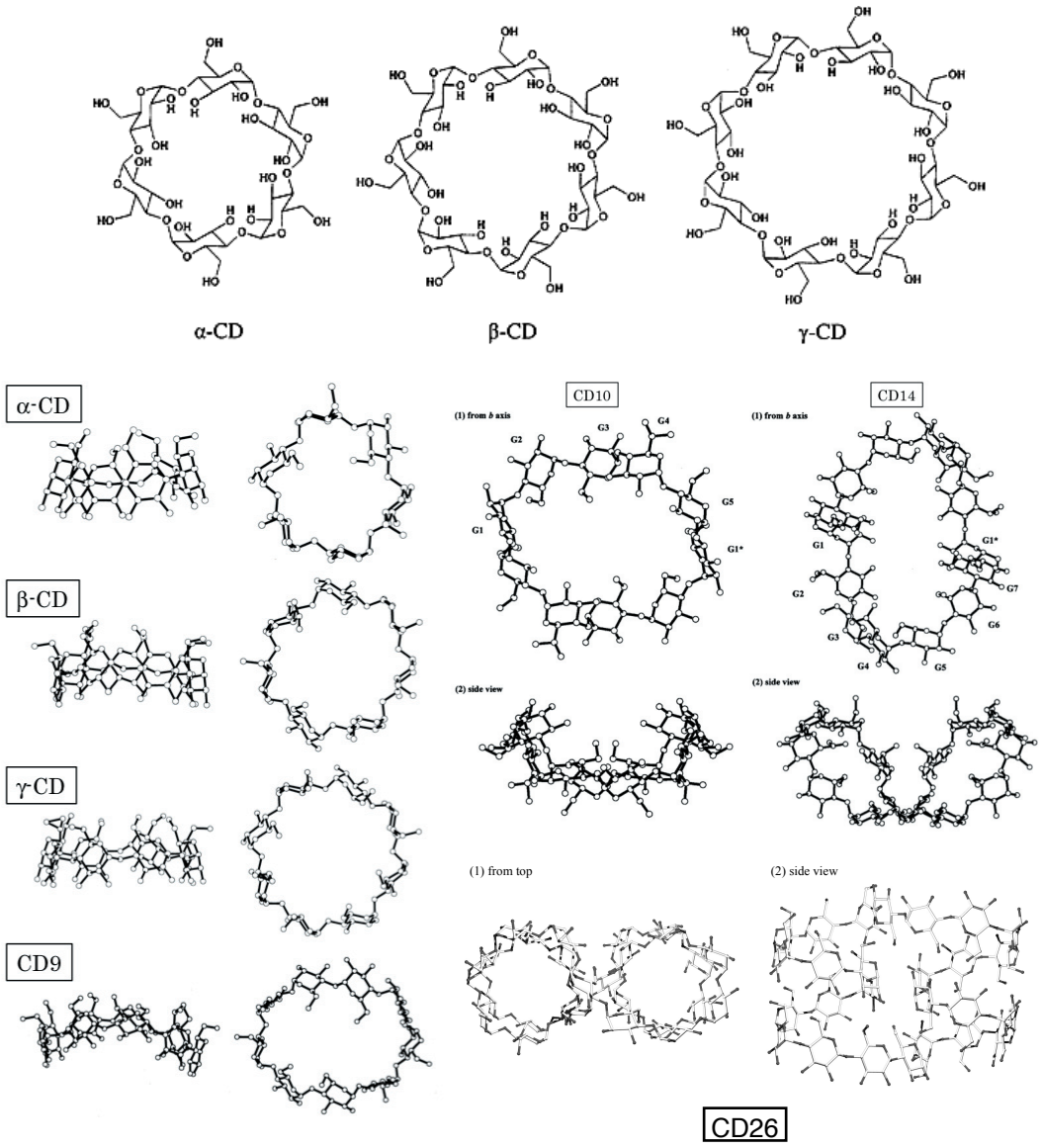


**Figure 1.11** Molecular structure of α-(alpha), β-(beta), γ-(gamma)-(CD), $CD_9$, $CD_{10}$, $CD_{14}$ and $CD_{26}$

**Table 1.3** : Physicochemical properties of native CDs and LR-CDs. (Endo 2011)

| | Theroritical [a] molecular weight | Aqueous [b] solubility (g/100 mL) | Surface [b] tension (mN/m) | Specific rotation $[\alpha]_D^{25}$ | Half-life of [c] ring opening (h) | | Theroritical [a] molecular weight | Aqueous [b] solubility (g/100 mL) | Surface [b] tension (mN/m) | Specific rotation $[\alpha]_D^{25}$ | Half-life of ring opening (h) |
|---|---|---|---|---|---|---|---|---|---|---|---|
| α-CD | 972.8 | 14.5 | 72 | +147.8 | 33 | CD23 | 3729.2 | >100 | 73 | +196.6 | 2.7 |
| β-CD | 1135.0 | 1.85 | 73 | +161.1 | 29 | CD24 | 3891.4 | >100 | 73 | +196.0 | 2.6 |
| γ-CD | 1297.1 | 23.2 | 73 | +175.9 | 15 | CD25 | 4053.5 | >100 | 73 | +190.8 | 2.8 |
| CD9 | 1459.3 | 8.19 | 72 | +187.5 | 4.2 | CD26 | 4215.7 | 22.4 | 73 | +201.4 | 2.9 |
| CD10 | 1621.4 | 2.82 | 72 | +204.9 | 3.2 | CD27 | 4377.8 | >125 | 72 | +189.4 | 2.8 |
| CD11 | 1783.5 | >150 | 72 | +200.8 | 3.4 | CD28 | 4539.9 | >125 | 72 | +191.2 | 2.6 |
| CD12 | 1945.7 | >150 | 72 | +197.3 | 3.7 | CD29 | 4702.1 | >125 | 72 | +190.2 | 2.5 |
| CD13 | 2107.8 | >150 | 72 | +198.1 | 3.7 | CD30 | 4864.2 | >125 | 72 | +189.1 | 2.3 |
| CD14 | 2270.0 | 2.30 | 73 | +199.7 | 3.6 | CD31 | 5026.4 | >125 | 71 | +189.0 | 2.4 |
| CD15 | 2432.1 | >120 | 73 | +203.9 | 2.9 | CD32 | 5188.5 | >125 | 71 | +192.7 | 2.4 |
| CD16 | 2594.2 | >120 | 73 | +204.2 | 2.5 | CD33 | 5350.6 | >125 | 71 | +192.1 | 2.2 |
| CD17 | 2756.4 | >120 | 72 | +201.0 | 2.5 | CD34 | 5512.8 | >125 | 72 | +189.6 | 2.2 |
| CD18 | 2918.5 | >100 | 73 | +204.0 | 3.0 | CD35 | 5674.9 | >125 | 71 | +193.7 | 2.1 |
| CD19 | 3080.7 | >100 | 73 | +201.0 | 3.4 | CD36 | 5837.1 | >100 | 71 | +190.6 | 1.9 |
| CD20 | 3242.8 | >100 | 73 | +199.7 | 3.4 | CD37 | 5999.2 | >100 | 71 | +189.9 | 1.8 |
| CD21 | 3405.0 | >100 | 73 | +205.3 | 3.2 | CD38 | 6161.3 | >100 | 71 | +190.1 | 1.9 |
| CD22 | 3567.1 | >100 | 73 | +197.7 | 2.6 | CD39 | 6323.5 | >100 | 70 | +188.1 | 1.8 |

a) Calculated as 162.1406 * *n*, where *n* is the number of glucopyranose unit.

b) Observed at 25 °C.

c) In 1 mol/L HCl at 50 °C.

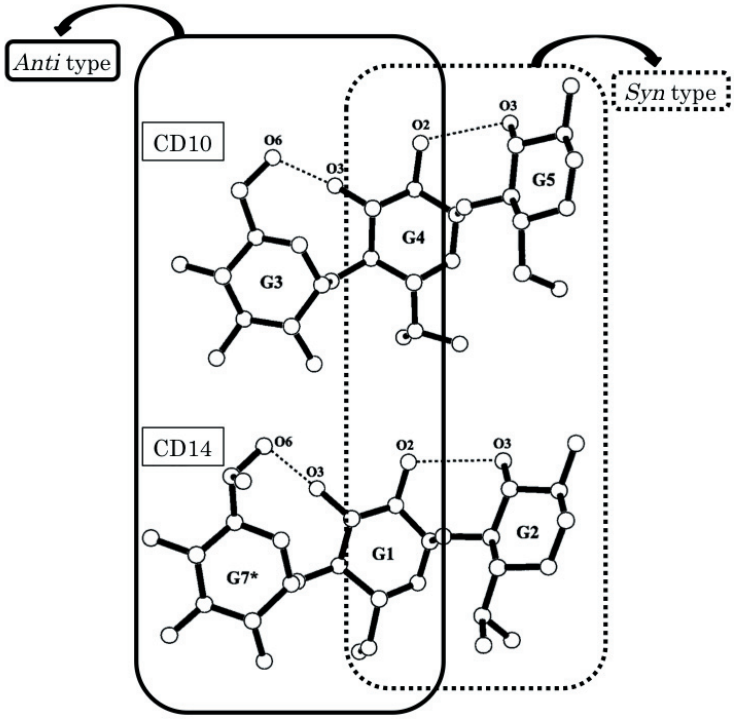


**Figure 1.12** syn and anti type conformations of α-1,4-linkage found in CDs. Dashed lines indicate hydrogen bond. (Endo 2011)

### 1.10.2 Inclusion complex of cycloamylose

Cycloamylose can form inclusion complex with many guest molecules. There were many reports on inclusion complexes with α-, β- and γ-CD. $CD_9$ has been reported to formed inclusion complexes with 22 drugs which showed improved solubility but complexes with α-, β- and γ-CD showed no solubility effect (Miyazawa *et al.* 1995). The interaction of cycloamylose with various drug was also reported (Tomono *et al.* 2002). Crystal structure of inclusion complex of $CD_9$ and cycloundecanone was studied. The structure of $CD_9$ was changed from elliptic boat like shape to truncated cone to fit the guest molecule. This is one of the most important evidences supporting the mechanism of inclusion complex formation (Harata *et al.* 2002). LR-CD mixture was used as artificial chaperone in protein refolding kit (Machida *et al.* 2000). This result suggestion that LR-CDs might be good host molecules for relatively large guest compounds in comparison with α-, β- and γ-CD.

### 1.10.3 Cycloamylose production

Large ring cyclodextrins (LR-CDs) were produced from stach or amylose by cyclodextrin glucanotransferase (CGTase, EC 2.4.1.19) (Terada *et al.* 1997) (Terada *et al.* 2001). 4-α-glucanotransferase (E.C. 2.4.1.25) (Takaha *et al.* 1999), especially D-enzyme from potato and amylomaltase from *Thermus aquaticus*, could produce LR-CD mixture when synthetic amylose was used as substrate (Takaha et al. 1996), (Terada et al. 1999). CGTase, D-enzyme and amylomaltase produced smallest CDs with the degree of polymerization 6, 17 and 22, respectively. Glycogen debranching

enzyme (GDE, E.C. 2.4.1.25/E.C. 3.2.1.33) from *Saccharomyces cerevisiae* which has 4-α-glucanotransferase and amylo-1,6-glucosidase activities in single peptide chain(Yanase *et al.* 2002) was also able to produce LR-CDs up to $CD_{50}$ from amylose and also produced cycloamylose from branched glucan substrate and branched starch. GDE did not use D-glucose or maltose as acceptor in coupling reaction.

**1.11 The objectives of this study**

In *Arabidopsis thaliana*, native DPE1 was reported to be involved in degradation of transitory starch in the chloroplast at night and it is one of the key enzymes in *Arabidopsis* carbohydrate metabolism. Native DPE1 from *Arabidopsis* (AtDPE1) has been well characterized. It will be useful to compare its properties with DPE1 from cassava (MeDPE1) and use the informations in understanding their involvement in both starch synthesis or degradation process in plant system. In addition, the ability of MeDPE1 and AtDPE1 in production of useful oligosaccharides is worth investigated since it has been reported that DPE1 from potato able to produce cycloamylose from amylose. We propose to clone and purify MeDPE1 and AtDPE1, characterize their properties and functions and study the possibility of using the enzyme for producing useful products.

**The objectives**:

1. To clone and express *dpe1* genes of *Manihot esculenta* Crantz and *Arabidopsis thaliana*

2. To purify and characterize DPE1 of both transformants

3. To apply transglycosylation reaction of D-enzyme in producing useful products such as production of cycloamylose and fluorinated compounds.

# CHAPTER II

# MATERIALS AND METHODS

## 2.1 Equipments

Autoclave: Model H-88LL, Kokusan Ensinki Co., Ltd., Japan

Autopipette: Pipetman, Gilson, France

Amicon Ultra-4 centrifugal filter unit MWCO 30,000: Millipore, USA

Centrifuge, refrigerated centrifuge: Model J2-21, Beckman Instrument Inc., USA

Electrophoresis unit:

-Mini protein, Bio-Rad, USA

- Submarine agarose gel electrophoresis unit, Bio-Rad, USA

FPLC AKTA Amersham Pharmacia Biotech unit:

Column: Amersham Biosciences HisTrap IMAC FF, HiLoad 26/60 seperdex 75 prep grade

HPAEC DX-600: Dionex Corp., Sunnydale, USA

Column: Carbopac PA-100TM 4 x 250 mm

Pulsed amperometry detector

DIONEX ED40 Autosampler:

DIONEX AS40 Column oven: DIONEX ICS-3000 SP

Incubator, waterbath: Model M20S, Lauda, Germany and BioChiller 2000,FOTODYNE Inc.,USA and ISOTEMP 210, Fisher Scientific, USA

Incubator shaker: Innova$^{TM}$ 4080, New Brunswick Scientific, USA

Light box: 2859 SHANDON, Shandon Scientific Co., Ltd., England

Laminar flow: HT123, ISSCO, USA

Magnetic stirrer: Model Fisherbrand, Fisher Scientific, USA

NanoVue UV/Visible spectrophotometer: GE Healthcare, UK

Orbital incubator: Model 1H-100, Gallenkamp, England

Orbital shaker: Orbital shaker 03, Stuart Scientif30ic, England

pH meter: Model PHM95, Radiometer Copenhegen, Denmark

Shaking waterbath: Model G-76, New Brunswick Scientific Co., Inc., USA

Spectrophotometer: DU Series 650, Beckman, USA

Thermal cycler: Mastercycler, Eppendorf, Germany

Vortex: Model K-550-GE, Scientific Industries, Inc, USA

**2.2 Chemicals**

2-Deoxy-2-fluoro-D-glucose (2FGlc): Fluorochem, UK

3-Deoxy-3-fluoro-D-glucose (3FGlc): Carbosynth, UK

6-Deoxy-6-fluoro-D-Glucose (6FGlc): Carbosynth, UK

Acrylamide: Merck, Germany

Agar: Merck, Germany

Agarose: SEKEM LE Agarose, FMC Bioproducts, USA

Ammonium persulphate: Sigma, USA

Ammonium sulphate: Carlo Erba Reagenti, Italy

Boric acid: Merck, Germany

Bromphenol blue: Merck, Germany

Coomassie brilliant blue R-250: Sigma, USA

di-Potassium hydrogen phosphate anhydrous: Carlo Erba Reagenti, Italy

Ethidium bromide: Sigma, USA

Ethyl alcohol absolute: Carlo Erba Reagenti, Italy

Ethylene diamine tetraacetic acid (EDTA): Merck, Germany

Glacial acetic acid: Carlo Erba Reagenti, Italy

Glucose: BDH, England

Glycerol: Merck, Germany

Glycine: Sigma, USA

Glycogen from oyster Type II: Sigma, USA

Hydrochloric acid: Carlo Erba Reagenti, Italy

Iodine: Baker chemical, USA

Isoamyl alcohol: Merck, Germany

Isopropanol: Merck, Germany

Maltose: Conda, Spain

Maltotriose: Fluka, Switzerland

MOPS (3-(N-morpholino)propanesulfonic acid): Sigma, UK

N,N-Dimethyl-formamide: Fluka, Switzerland

N,N'-Methylene-bis-acrylamide: Sigma, USA

N,N,N',N'-Tetramethyl-1, 2-diaminoethane (TEMED): Carlo Erba Reagenti, Italy

Peptone: Scharlau microbiology, Spain

Plasmid Mini Kit: Bio-Rad, USA

Potassium iodide: Mallinckrodt, USA

Potassium phosphate monobasic: Carlo Erba Reagenti, Italy

Pre-coated silica plates gel 60 $F_{254}$ plates 0.25mm: Merck, USA

QIA quick Gel Extraction Kit: QIAGEN, Germany

Sodium acetate: Merck, Germany

Sodium carbonate anhydrous: Carlo Erba Reagenti, Italy

Sodium chloride: Carlo Erba Reagenti, Italy

Sodium citrate: Carlo Erba Reagenti, Italy

Sodium dodecyl sulfate: Sigma, USA

Sodium hydroxide: Merck, Germany

Standard protein marker: Amersham Pharmacia Biotech Inc., USA

Tris (hydroxymethyl)-aminomethane: Carlo Erba Reagenti, Italy

Tryptone: Scharlau microbiology, Spain

Yeast extract: Scharlau microbiology, Spain

**2.3 Enzymes and restriction enzymes**

Restriction enzymes: New England BioLabs Inc., USA; Fermantas, Canada; Roche, UK

pTrcHis2C: Invitrogen, USA

Champion™ pET Directional TOPO® Expression Kits: Invitrogen, USA

Phusion™ DNA polymerase

RNaseA: Sigma, USA

$T_4$ DNA ligase: New England BioLabs, Inc, USA

Glucose-6-phosphate dehydrogenase (G6P-DH): Roche, UK

Amyloglucosidase from *Rhizopus* sp.: Cat on. E-AMGPU, Megazyme, UK

Hexokinase (HK) from yeast overproduction: Roche, UK

**2.4 Bacterial stains**

*E. coli* strain TOP10, For use as a vector for manipulating plasmids. Produces large quantities of plasmids.

**Genotype:** $F^-$ *mcr*A Δ(*mrr-hsd*RMS-*mcr*BC) φ80*lac*ZΔM15 Δ*lac*X74 *rec*A1 *ara*D139 Δ(*ara-leu*) 7697 *gal*U *gal*K *rps*L ($Str^R$) *end*A1 *nup*G λ-

*E.coli* strain DH5α, For use as a vector for Blue/white screening of transformants and expression of pTrcHis2C vector.

**Genotype**:F- φ80lacZΔM15 Δ(lacZYA-argF)U169 deoR recA1 endA1 hsdR17(rk-, mk+) phoA supE44 thi-1 gyrA96 relA1 λ

*E.coli* strain BL21 Star™(DE3), For use as a protein expression for pET151/D TOPO vector.

**Genotype**: F- *ompT hsdSB* (rB-mB-) *gal dcm rne131* (DE3)

## 2.5 Cloning of *medpeI* gene from Cassava (*Manihot esculenta* Crantz)

### 2.5.1 Amplification of *medpe1* gene using PCR technique

A pair of primers designed from sequence of D-enzyme from cassava (Phytozome, 2010) (online) was used in the PCR reaction. Forward primer (DTrcHis_F) was 5' – TTCGAAGCAGTTTCTTTATCCTCTACC –3' with *Bst*BI site and reverse primer (DTrc_R1) was 5' –GTCGACCACCCGCCCATACATTG -3' with *Sal*I site. The underlined letters were designed for the restriction sites. The $T_m$ of primers were 70 and 69°C, respectively. The *medpe1* gene was amplified using PCR method. Fifty microliters reaction mixture contained 1 unit of Phusion™ DNA polymerase, 0.2 mM dNTPs, 1X PCR buffer, 1.5 mM $MgCl_2$, cDNA template and 10 pmole of each primer. The PCR was performed with three rounds of temperature cycling. In the first round, pre-denaturation at 95°C for 2.0 minutes followed by adding Phusion™ DNA polymerase 1 unit and pre denaturation at 98°C for 30 seconds. In the second round, 32 cycles of denaturation at 98°C for 8 seconds, annealing at 70°C for 20 seconds, extension at 72°C for 1 minutes 45 seconds were performed. Finally the samples were incubated at 72°C for 10 minutes. The PCR product was analyzed by agarose gel electrophoresis.

### 2.5.2 Agarose gel electrophoresis

Agarose gel electrophoresis was employed to separate, identify and purify fragments of DNA using 1.0% agarose in TAE buffer (40 mM Tris-acetate, 1mM EDTA). DNA samples with 1X gel loading buffer were loaded into the wells. The gel was run at 100 volts for 1 hour or until bromophenol blue reached the bottom of the

gel. After electrophoresis, the gel was stained by immersing the gel in electrophoresis buffer or $H_2O$ containing ethidium bromide (0.5 µg/ml) for 30-45 minutes at room temperature. The stained gel was visualized with UV light.

**2.5.3 Ligation of PCR product with pGEM-T vector.**

PCR product was cleaned by using Gel/PCR DNA Fragments Extraction Kit from Geneaid. Cleaned PCR product was ligated into pGEM-T vector (Promega) in 10 µl reaction mixture containing 1x Rapid ligation buffer, 3 U of T4 DNA ligase, 50 ng of pGEM®-T vector and cleaned PCR product. The reaction was performed at 4°C 16 hours. Reaction mixture was transformed into *E.coli* DH5α with $CaCl_2$ methods.

**2.5.4 Plasmid transformation using $CaCl_2$ method**

**2.5.4.1 Preparation of competent cells**

A single well isolated colony of *E.coli* strain DH5α was incubated at 37°C overnight with shaking at 250 rpm in 10 ml of LB media. A 2 ml aliquot of the overnight culture was transferred to 200 ml of LB media and grown until the $OD_{600}$ was between 0.3-0.4. The cells were chilled on ice for 15 minutes followed by centrifugation at 3,500 xg 4°C for 15 minute. Cells were collected and resuspended in cold 10 ml of $CaCl_2$ buffer and left on ice for 15 minutes. Cells were collected by centrifugation at 3,500 xg 4°C for 15 minute. Cell pellet was resuspended in 1.5 ml of $CaCl_2$ buffer, 0.3 ml of 86% Glycerol. Aliquots of 100 µl were stored in sterilized 1.5 ml microcentrifuge tubes and immediately kept at -80°C for Heat-shock transformation.

#### 2.5.4.2 Heat-shock transformation

An aliquot of competent *E.coli* strain DH5α was thawed on ice for 5-10 minutes. The cells suspension was gently mixed with 2 µl of ligation reaction or plasmid mixture (section 2.5.3) and incubated on ice for 30 minutes. The cells were transformed by heat-shock at 42°C for 1 minute, then placed on ice for 2 minutes followed by addition of 900 µl of LB medium and incubated at 37°C with shaking at 250 rpm for 1 hour. The mixture was spread on the LB agar plates containing appropriate antibiotics and incubated at 37°C overnight. Colonies were selected for plasmid isolation using plasmid extraction kit from Geneaid.

### 2.5.5 Restriction enzyme digestion and ligation with pTrcHis2C vector

The expression vector pTrcHis2C (Invitrogen) (appendix C) and pGEM-T vector with insert were linearized with restriction enzyme *Bst*BI and *Sal*I in 20µl reaction mixture containing 1x Fastdigest® buffer, 1 U of *Bst*BI, 1U of *Sal*I and Vector template. The reaction was performed at 37°C for 5 min and reaction stopped by heating at 80°C for 5 minutes. The digested fragment from pGEM-T vector was ligated into pTrcHis2C vector to generate pTmedpe1. Recombinant plasmid was transformed into *E.coli* strain DH5α using $CaCl_2$ method for protein expression.

## 2.6 Cloning of *atdpeI* gene from *Arabidopsis thaliana*

### 2.6.1 Amplification of *atdpeI* gene using PCR technique

A pair of primers designed from sequence of *atdpeI* gene from *Arabidopsis thaliana* (Joint Genome Institute, 2010)(online) was used in the PCR reaction. The forward primer (AtDPE1_F) was 5' – **CACC**ATGGAGGTCGTTTCGAGTAATTCC

–3’ with CACC for directional cloning.The sequence of reverse primer (AtDPE1_R) was 5’ -TCAAAGCCGTCCG TACAATGACAAAAGATC -3’. The $T_m$ of primers were 73 and 74°C, respectively. The *atdpeI* gene was amplified using PCR method. Fifty microliters reaction mixture contained 1 unit of Phusion™ DNA polymerase, 0.2 mM dNTPs, 1X PCR buffer, 1.5 mM $MgCl_2$, cDNA template and 10 pmole of each primer. The PCR was carried out as described in section 2.5.1. The PCR product was analyzed by agarose gel electrophoresis.

### 2.6.2 Ligation with pET151/D-TOPO® expression vector

The amplified fragment was ligated into pET151/D-TOPO® vector (Invitrogen) (appendix D) using Champion™ pET151 Directional TOPO® Expression Kit with BL21 Star™ (DE3) One Shot® by incubated at room temperature for 15 minutes. Ligation mixture were transformed into *E. coli* strain TOP10 from kit using $CaCl_2$ method and selected recombinant plasmid in LB plate containing 50 μg/ml carbenicillin. Recombinant plasmid (pEatdpe1) was sequenced to confirm insertion of *atdpeI* gene and transformed into *E.coli* BL21 Star™(DE3) using $CaCl_2$ method.

## 2.7 Expression and purification of MeDPE1 and AtDPE1

### 2.7.1 Starter media

The *E. coli* transformed colony from section 2.5.5 and 2.6.2 were transferred into LB medium containing 50 μg/ml carbenicillin and incubated at 37°C with 250 rpm rotary shaking overnight.

### 2.7.2 Media cultivation and crude enzyme preparation

Each starter medium (1%) was transferred into Auto Induction Media (AIM) medium (appendix F) containing 50 μg/ml carbenicillin in Erlenmeyer flask and cultured at 37°C with shaking. When $A_{600}$ of the culture reached 0.4-0.6, it was transferred and cultured at 16°C with shaking overnight and harvested by centrifugation at 5,000 xg for 15 minutes. Bacterial cells were resuspended in lysis solution (appendix G) then disrupted with cell lysis machine at 25 kPsi. Cell debris was removed by centrifugation at 12,000 xg for 30 minutes. The supernatants were crude enzymes of MeDPE1 and AtDPE1 when were used for enzyme purifications.

### 2.7.3 Purification of recombinant DPE1

Both crude enzyme extracts from section 2.7.2 were initially purified at 4°C by 5 ml nickel-charged HisTrap IMAC FF™ column followed by HiLoad 26/60 seperdex 75 prep grade attached to an Åkta fast protein liquid chromatography (FPLC, GE Healthcare Ltd, UK). The enzymes were eluted from nickel-charged HiTrap IMAC FF column using washing buffer (0.5 M NaCl and 30 mM Immidazole in 50 mM Tris pH 8.0) and enzyme eluted with linear gradient of elution buffer (0.5 M NaCl and 500 mM Immidazole in 50 mM Tris pH 8.0). Pooled fractions from nickel-charged HiTrap IMAC FF column was loaded on HiLoad 26/60 seperdex 75 prep grade column using gel filtration buffer (100 mM NaCl in 50 mM HEPES pH 7.5). Elution time was used to calculate molecular weight as described in section 2.10.1.1. Fractions with enzyme activity were pooled, concentrated and buffer was

changed to 50 mM HEPES pH 7.5 using Amicon Ultra-4 centrifugal filter unit MWCO 30,000. Protein concentration was measured using NanoVue spectrophotometer. The enzymes were stored in aliquots at -80°C.

## 2.8 Assay of DPE1 activity

### 2.8.1 Disproportionating reaction

Reaction mixture was prepared in Eppendorfs (total volume 135 µl) containing 100µl of 100mM MOPS-NaOH pH 7.0 (c=74 mM), 25 µl of 100mM maltotriose (c=18.5 mM) and 10 µl of MeDPE1 or AtDPE1 (0.2 µg of purified enzyme) and incubated at 37°C for 15 minutes. Reaction was stopped by boiling for 5 minutes. In control reaction, the reaction mixture was boiled immediately after addition of enzyme. The glucose released was measured by hexokinase-G6P dehydrogenase method.

### 2.8.2 Measurement of glucose by hexokinase-G6P dehydrogenase method

The reaction mixture in section 2.8.1 (10µl) was pipetted into each well of microtiter plate (3 wells per Eppendorfs) containing 188µl of hexokinase assay cocktail (Appendix E). Absorbance at 340nm as recorded as start absorbance (Abs1), glucose-6-phosphate dehydrogenase (0.23 unit) was then added and incubated for 10 minutes and absorbance at 340 nm was recored as end absorbance (Abs2). Change in OD at 340 nm (Abs2-Abs1) was compared with glucose standard curve. (Appendix E). Standard curve of glucose was prepared (appendix E). One unit activity of DPE1

was defined as the amount of enzyme which produced 1 μmol of glucose per minute under described condition.

## 2.9 Polyacrylamide gel electrophoresis (PAGE)

Two types of PAGE were performed for analysis of enzyme purification, the denaturing and non-denaturing gels. The gels were visualised by coomassie blue staining. For non-denaturing gel, glycogen disproportionation activity stain was also undertaken.

### 2.9.1 SDS-polyacrylamide gel electrophoresis (SDS-PAGE)

The slab gel system consisted of 0.1% SDS (w/v) in 10.0% (w/v) acrylamide separating and 5.0% (w/v) acrylamide stacking gel with Tris-glycine buffer, pH 8.0 containing 0.1% SDS as electrode buffer. The gel preparation solutions were described in appendix A. Samples to be analysed were treated with sample buffer and boiled for 5 minutes prior to loading to the gel.The electrophoresis was run from anode towards cathode at constant current of 20 mA per slab at room temperature on a Mini-Gel electrophoresis unit (Bio-rad). Standard molecular weight markers were run and used to prepare calibration curve for protein molecular weights. After electrophoresis, proteins in the gel were visualised by coomassie blue staining solution. Molecular weight of both DPE1 were determined from the calibration curve.

### 2.9.2 Non-denaturing polyacrylamide gel electrophoresis (Native-PAGE)

Native-PAGE was performed on the slab gel of 10.0% (w/v) acrylamide separating gel contained 0.3% glycogen and 5% (w/v) acrylamide on stacking gel. Tris-glycine buffer pH 8.3 was used as electrode buffer. Preparation of solutions and polyacrylamide gel were described in appendix B. Samples to be analyzed were treated with sample buffer prior to loading to the gel. The electrophoresis was run from anode towards cathode at constant current of 16 mA per slab, at 4°C on a Mini-Gel electrophoresis unit (Bio-rad). For activity staining, the gel was incubated in substrate solution buffer (50 mM Tris-HCl pH 8.0, 8 mM EDTA, 0.3% maltodextrin) at room temperature (25°C) overnight. The gel was rinsed several times with distilled water and stained with iodine solution (0.2% $I_2$ in 2% KI). The activity gel was compared with the protein gel to determine the position of DPE1.

## 2.10 Characterisation of MeDPE1 and AtDPE1

### 2.10.1 Molecular weight determination

Molecular weights of recombinant MeDPE1 and AtDPE1 were determined using gel filtration and SDS-PAGE

#### 2.10.1.1 Molecular weight determination from gel filtration column chromatography

The molecular weight of each purified DPE1 was determined by gel filtration on HiLoad 26/60 seperdex 75 prep grade column. The marker proteins used were Vitamin B12(1.355 kDa), Aprotinin(6.5 kDa), Cytochrome C (12.4 kDa),

RNAse A (13.7 kDa), Myoglobin (17.6 kDa), Carbonic anhydrase (29.0 kDa), HPLF +7 monomer (56.8 kDa), BSA (66.0 kDa) and ADH (150.0 kDa). The calibration curve of protein markers was constructed from log molecular weight of the standard proteins and elution time.

**2.10.1.2 Molecular weight determination from SDS-polyacrylamide gel electrophoresis (SDS-PAGE)**

The molecular weight of both purified DPE1 were determined by SDS-PAGE. The standard curve of protein markers was constructed from the molecular weight of the standard proteins and their relative mobility ($R_f$).

**2.10.2 Optimum pH**

The effect of pH on the disproportionating activity of each DPE1 was determined at 37°C at various pHs for 15 minutes. The buffers used for controlling pH were 0.1M acetate buffer, pH 3-5; 0.1M phosphate buffer, pH 5-7; 0.1 M Tris-HCl pH 7-9; 0.1 M MOPS pH 7-8 and 0.1 M Glycine pH 8-10. The disproportionating activity was determined as described in section 2.8. The results were shown as percentage of the relative activity. The pH at which maximum activity was observed was set as 100%.

**2.10.3 Optimum Temperature**

The disproportionating activity of DPE1 was assayed in 0.1 M MOPS buffer, pH 7.0 at various temperatures in the range of 20-60°C. The results were shown as a percentage of the relative activity. The temperature at which maximum activity was observed was set as 100%.

### 2.10.4 Effect of temperature on DPE1 stability

The effect of temperature on the stability of the enzymes was determined at 25°C and 37°C. The purified enzymes were incubated at each temperature for 0-16 hours in MOPS buffer pH 7.0 the disproportionating activity was determined at different time point. The results were shown as a percentage of relative activity. The highest activity was defined as 100%.

### 2.10.5 Determination of kinetic parameters

Kinetic parameters of the disproportionation activity were determined by incubating various concentrations of maltotriose ($Glc_3$), ranging from 2-60 mM in 250 µl reaction contain 190 µl of hexokinase assay cocktail with G6PDH, 50 µl of maltotriose at various concentrations and 10 µl of MeDPE1 or AtDPE1 (0.1 µg of purified enzyme) at 25°C from 0-25 minutes by measuring the absorbent at $A_{340}$ every 1 minute. The suitable time for calculated initial velocity was 1 minutes of incubation. Kinetic parameters were determined from the Michaelis-Menten equation, using Lineweaver-Burk plot.

## 2.11 Determination of oligosaccharide products

### 2.11.1 Oligosaccharides detection using HPAEC-PAD technique

Purified MeDPE1, AtDPE1,AtDPE2 and amylomaltase (final concentration 10 µg/ml) were incubated in 10 mM MOPS pH 7.0 containing 25 mM maltotriose ($Glc_3$) in 100 µl total volume for 15 minutes at 37°C and reactions stopped by boiling for 5 minute. The reactions were analysed by High Performance Anion Exchange

chromatography (HPAEC-PAD) DX-600 system (Dionex, Cambridge, UK). For separation, the column (CarboPac-PA100) was flushed with 100 mM NaOH 1 M NaOAc for 10 minutes and was then equilibrated with 100 mM NaOH for 60 min. Oligosaccharides were eluted using a linear gradient of NaOAc (0 to 300 mM in 25 minutes), followed by elution with 1 M NaOAc dissolved in 100 mM NaOH (10 minutes).

## 2.12 Identified acceptor specific using oligosaccharide array

Oligosaccharide array was used to monitor acceptor specificity of recombinant MeDPE1 and AtDPE1. $^{14}$C-glycogen solution was used as donor while oligosaccharide printed on membrane was used as acceptor.

### 2.12.1 $^{14}$C-glycogen solution preparation

$^{14}$C-glycogen solution was prepared by incubated reaction mixture (500 µl) containing 100 µl of 100 mM MOPS pH 7.0, 160 µl of 25 mg/ml glycogen solution (appendix H), 90 µl water, 100 µl of recombinant PHS2 (cytosolic α-1,4-glucan phosphorylase)(50 µg protein) and 50 µl of $^{14}$C-Glucose-1-Phosphate (3.7kBq/µl) for 1hour at 37°C and boiled to stop reaction. $^{14}$C-Glycogen Separated by gel filtration NAP™-5 columns (Sephadex™ G-25)(from GE healthcare) using 10 mM MOPS pH 7.0 as buffer.

### 2.12.2 Oligosaccharide array preparation and detection

Oligosaccharide array type I and type II were contained many types of oligosaccharides printed on membrane (Appendix I) were used as acceptors. Stock solutions were prepared : TBS solution (50 mM Tris-HCl, pH 7.4 and 150 mM NaCl), TBST (50 mM Tris-HCl, pH 7.4 and 150 mM NaCl add 1 ml of 0.1% Tween 20 in 1 litre). Experimental steps for preparing membrane and reactions were follow:

1st step : Add 5%BSA on TBS solution (block space on membrane) shake for 1 hour

2nd step : Wash with TBS solution for 10 min twice and wash membrane with 50 mM MOPS pH7.0

3rd step : Add $^{14}$C-glycogen solution (100 µl) and 50mM MOPS pH7.0 (4ml) followed by add DPE1 (MeDPE1 150 µg and AtDPE1 150 µg) and incubated at room temperature for 4 hours.

4th step : Wash with TBST solution for 10 min 3 times.

The membrane was dried, wrapped in plastic paper and exposed to phosphorimage plate (10 days) and scanned the spot intensity

## 2.13 Large-ring cyclodextrins production

The synthesis of large-ring cyclodextrins was performed using amylose from corn. Product were detected by using HPEAC-PAD and MALDI-TOF MS.

### 2.13.1 Large-ring cyclodextrins preparation

The reaction mixtures (10 ml) contained 9 ml of 2% amylose from corn incubated with 1 mg protein of recombinant MeDPE1 and AtDPE1 in 5 mM triethylamine-acetate pH 7.5. The reaction mixtures were incubated at room temperature (25°C) with shaking overnight and reaction stopped by boiling for 15 minutes. Then, 1.25 mg of amyloglucosidase from *Rhizopus* sp. (35 U/mg protein) were added to reaction mixtures and incubated at room temperature overnight. Reactions were stopped by boiling for 15 minutes. The reaction mixtures were concentrated and fractionated into three partitions by centricon centrifugal Filter Units (MWCO 5000 cut off and MWCO 3000 cut off). The partition1 was retained in filter MWCO5000. The partition2 was passed through filter MWCO5000 but retained in filter molecular weight 3000. The partition3 was passed through filter MWCO3000. Each partition was freeze-dried to eliminate buffer and concentrated. The products were analysed by HPAEC-PAD and MALDI-TOF-MS.

### 2.13.2 Detection of large-ring cyclodextrins using HPAEC-PAD

Large-ring cyclodextrins mixtures were analyzed on high performance anion exchange chromatography with pulsed amperometric detector (HPAEC-PAD,

Dionex-500, USA). A CarboPac PA-100 column (4x250 mm, Dionex). Elution was performed by a linear gradient of sodium nitrate (0–2 min, increasing from 4 to 8% at 2–10 min, increasing from 8 to 18% at 10–20 min, increasing from 18 to 28% at 20–40 min, increasing from 28 to 35% for 40–55 min, increasing from 35 to 45% at 55–60 min, increasing from 45 to 63%) in 150 mM NaOH with a flow rate of 1 ml/min. The size of LR-CD products were compared with standard LR-CDs.

### 2.13.3 Detection of large-ring cyclodextrins using MALDI-TOF-MS

Molecular mass spectrum of cycloamylose mixture was obtained by matrix-assisted laser desorption ionization-time of flight mass spectrometry (MALDI-TOF-MS). One microliter of sample was mixed with 1 µl of matrix (10 mg/ml of 2,4,6-trihydroxyacetophenone monohydrate in 70:30 MeCN:$H_2O$), dropped on ground steel target plate and detected on MALDI-TOF-MS.

## 2.14 Inclusion complex of LR-CDs mixture with polyaniline.

Polyaniline solution was prepared and filtered thought to centrifugal filter unit MWCO 5,000. Then mixed with LR-CDs mixture (partition 2) from section 2.13.1. This reaction was filtered thought the centrifugal filter unit MWCO 5,000 and the reaction remained on filter was collected. This retained fraction was analyzed by UV-Vis spectrophotometer to scan at wavelength from 200 nm to 850 nm in comparison with polyaniline mixture and cycloamylose mixture.

## 2.15 Synthesis and detection of fluoro-oligosaccharide products

Transglycosylation reaction of recombinant enzymes were used to produce fluoro-oligosaccharide products. Fluoroglucose derivatives (2-Deoxy-2-fluoro-D-glucose (2FGlc), 3-Deoxy-3-fluoro-D-glucose (3FGlc) and 6-Deoxy-6-fluoro-D-Glucose (6FGlc)) were used as acceptor. Glycogen was used as donor.

### 2.15.1 Transglycosylation reaction (small scale reaction)

Recombinant enzymes (MeDPE1, AtDPE1, AtDPE2 and amylomaltase)(1µg protein) were added into 20 µl buffer solution (50 mM MOPS pH7.0) containing 12.5 mg/ml glycogen solution (appendix H) and 10mM (1.82 mg/ml) of fluoroglucose derivatives (2-Deoxy-2-fluoro-D-glucose (2FGlc), 3-deoxy-3-fluoro-D-glucose (3FGlc), 4-Deoxy-4-fluoro-D-glucose (4FGlc), and 6-deoxy-6-fluoro-D-Glucose (6FGlc)). The reaction mixture were incubated overnight at 37°C and boiled for 5 minutes to stop the reaction. One microlitre reaction mixtures were spotted on pre-coated silica plates gel 60 $F_{254}$ plates 0.25mm and developed on acetonitrile:ethyl acetate:isopropanol:water (85:20:50:50). The TLC plate was air dried and then dipped into orcinol solution (appendix H) prepared by mixing 20 ml of conc. sulphuric acid with cold solution of 3,5-dihydroxytoluene (360 mg) in ethanol (150 ml) and water (10 ml) and heated with hot-air gun to visualise the compounds. $R_f$ value of each on TLC plate were calculated.

### 2.15.2 Transglycosylation reaction (preparative scale)

Recombinant AtDPE2 (0.9 mg) was added to a glycogen solution (125 mg) in 10 ml of 50 mM triethylamine acetate pH 7.0 contained 25 mg of fluoroglucose derivatives acceptor (2FGlc, 3FGlc and 6FGlc). The mixture was incubated at 25°C for 18 hours with gentle shaking. The reaction was quenched by heating in boiling water for 5 min. The remaining glycogen was removed by filtration using Amicon spin filter (MWCO 30,000) and freeze-dried. The crude mixtures were re-dissolved in MQ water (1.5 ml) and applied in three portions (0.5 ml) onto TSK-HW40S column (length 50 cm diameter 2.5 cm). The column was eluted with MQ water at a flow rate 0.5 ml/min using RID detector and collected 1.0 ml fractions Fractions containing the product of the transglycosylation reaction were monitored by TLC (section 2.15.1). Fluoro-oligosaccharide products were pooled and freeze-dried.

### 2.15.3 Characterisation of fluoromaltose derivatives

NMR spectra were recorded on a Bruker Avance III spectrometer at 400 MHz ($^{1}H$) or 376 MHz ($^{19}F$). Chemical shifts of $^{1}H$ NMR signals recorded in $D_2O$ were reported with respect to proton resonance of residual HDO at $\delta_H$ 4.70 ppm. Chemical shifts of $^{19}F$ NMR signals recorded in $D_2O$ were reported with respect to external $CFCl_3$ at $\delta_H$ 0 ppm. Assignments were made with the aid of COSY and HSQC experiments.

Optical rotations were measured at ambient temperature on a Perkin-Elmer model 141 polarimeter using a sodium lamp. High-resolution accurate mass spectra were obtained using a Thermo LTQ Orbitrap mass spectrometer using positive electrospray ionisation.

# CHAPTER III

# RESULTS

## 3.1 Cloning and expression of *medpe1* gene from *Manihot esculenta* Crantz and *atdpeI* gene from *Arabidopsis thaliana*

### 3.1.1 Cloning of *medpe1* gene from *Manihot esculenta* Crantz

#### 3.1.1.1 *medpe*1 gene amplification and preparation

PCR product of *medpeI gene* amplification was detected as single band on 1% agarose gel in Figure 3.1 lane1. The size of PCR product was 1.7 kb. The PCR product was cleaned and ligated into pGEM-T vector.

#### 3.1.1.2 Recombinant plasmid vector

The pGEM-T vector with inserted PCR product was shown on agarose gel in Figure 3.1 lane 2. The pGEM-T with insert was digested with restriction enzymes *Bst*BI and *Sal*I. The digested pGEM-T product was shown in Figure 3.1 lane 3. The insert in pGEM-T was digested at the same size as PCR product. The extracted plasmid pTrcHis2C was shown by agarose gel electrophoresis in Figure 3.1 lane 4. The pTrcHis2C plasmid was subjected to digestion with *Bst*BI and *Sal*I. The size of the linear form of this plasmid vector was shown to be 4.4 kb (Figure 3.1 lane 5).

#### 3.1.1.3 Transformation and colony selection

The digested PCR product and the linear form of plasmid vector were ligated by T4 DNA ligase. The recombinant plasmid was constructed and transformed into the competent cell of *E. coli* DH5α following the method in section 2.5.4. Extracted plasmid was checked for plasmid on agarose gel electrophoresis (Figure 3.1

lane 6). The vector subjected to *BstB*I and *Sal*I digestions was shown in lane7. It comprised of two bands: 4.4 kb corresponded to the size of linear form of the pTrcHis2C vector and 1.7 kb corresponded to the PCR product of *medpeI* gene. Restriction map of pTmedpe1 was shown in Figure 3.2.

**3.1.1.4 Nucleotide sequencing**

To confirm whether the inserted fragment was *medpe1* gene, the recombinant plasmid was subjected to DNA sequencing using the pTrc_forward and pTrc_reverse primers which enabled sequencing through the 5'-terminus and 3'-terminus of the *medpe1* inserted gene in the plasmid. The nucleotide sequence of *medpe1* and predicted signal peptide sequence were shown in Figure 3.3. The 585 amino acid residues was deduced from the *medpeI* which had an open reading frame of 1,758 bp length. The 56 amino acid residues at N-terminal was predicted to be signal peptide by using Chlorop v1.1. Expressed MeDPE1 protein sequence included only mature enzyme and Histidine-Tag. (Figure 3.7 (A))

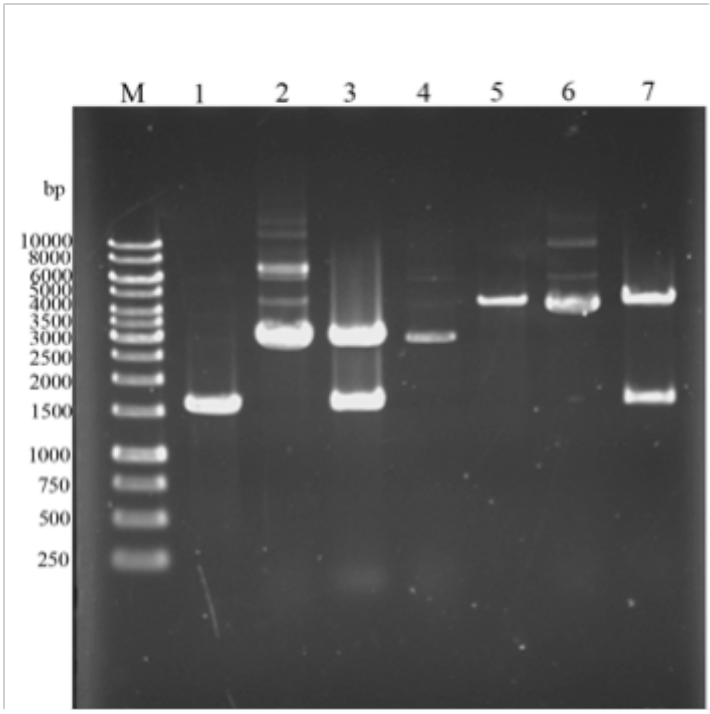


**Figure 3.1** Agarose gel electrophoresis of PCR product and recombinant plasmids of *medpeI* gene. Lane M, 1 kb ladder; Lane 1, PCR product; Lane 2, pGEM-T with insert; Lane 3, pGEM-T with insert cut with *Bst*B I and *Sal* I; Lane 4, pTrcHis2C vector; Lane 5:pTrcHis2C cut with *Bst*B I and *Sal* I; Lane 6, pTmedpe1; Lane 7, pTmedpe1 cut with *Bst*B I and *Sal* I

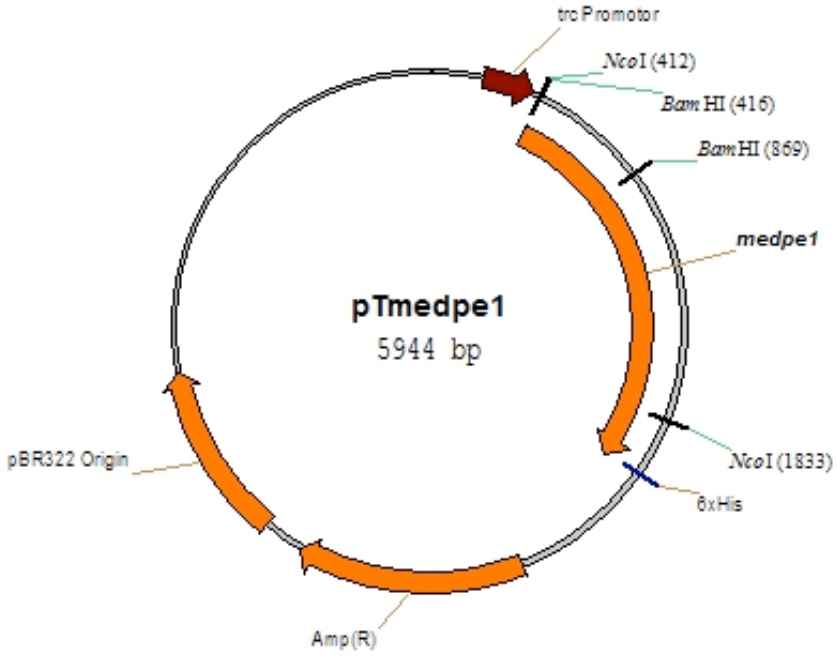


**Figure 3.2** Restriction map of pTmedpeI (pTrcHis2C vector inserted with *medpe1* gene).

```
atggcgctacatagctctcacttcgtccttttcttcttcttcttcttcttctcttttc
 M  A  L  H  S  S  H  F  V  L  S  S  S  S  S  S  S  S  L  F
tgttccaaaaagctcgatctctcctcttatccaccttcttcaatttccttgcctctcttc
 C  S  K  K  L  D  L  S  S  Y  P  P  S  S  I  S  L  P  L  F
aattcccaacccaaactccacgcctctaaactcattttcagaaccgacgcagtttcttta
 N  S  Q  P  K  L  H  A  S  K  L  I  F  R  T  D  A  V  S  L
tcctctaccatcggcgtcggcgaggacttgcctgctgattacgacgaatggttaccaaaa
 S  S  T  I  G  V  G  E  D  L  P  A  D  Y  D  E  W  L  P  K
cttgatcctatccatcggaggagagctggcattttgctgcatccgacgtcgttccgaggg
 L  D  P  I  H  R  R  R  A  G  I  L  L  H  P  T  S  F  R  G
ccttacggtattggagatctcggagaggaagcttttcgcttcattgattggcttcatgac
 P  Y  G  I  G  D  L  G  E  E  A  F  R  F  I  D  W  L  H  D
gctggttgctctgtttggcaggtccttccccttgtgcctccaggaagaaaggctaatgaa
 A  G  C  S  V  W  Q  V  L  P  L  V  P  P  G  R  K  A  N  E
gaaggatcaccatactcaggccaggatgcaaattgtggtaatacgctcttaatttctctg
 E  G  S  P  Y  S  G  Q  D  A  N  C  G  N  T  L  L  I  S  L
gaggagcttgtaaaggacggcttgttgatgaaggatgagcttccagaacctgtaatttct
 E  E  L  V  K  D  G  L  L  M  K  D  E  L  P  E  P  V  I  S
gatcgagtgaactttgatgctgttgctaagctaaaggatcccttggtggttaaggctgca
 D  R  V  N  F  D  A  V  A  K  L  K  D  P  L  V  V  K  A  A
gagaggcttattcggagtggcagtgagcttaaaaaccagcttgaagatttctgcaaggac
 E  R  L  I  R  S  G  S  E  L  K  N  Q  L  E  D  F  C  K  D
cctcaaatatcaggttggcttgaagatgcagcttattttgctgctattgatgatacatta
 P  Q  I  S  G  W  L  E  D  A  A  Y  F  A  A  I  D  D  T  L
aataccttgaattggtatgcttggcccgaacctttaaaaaaccgccatctttcagccttg
 N  T  L  N  W  Y  A  W  P  E  P  L  K  N  R  H  L  S  A  L
gaggaaatttatcaaagcaaaaaggattttatagacattttcatcgcccaacagttcttg
 E  E  I  Y  Q  S  K  K  D  F  I  D  I  F  I  A  Q  Q  F  L
ttccagaggcaatggcagaaagtgcgcaactatgcacaggagaagggaatcagtataatg
 F  Q  R  Q  W  Q  K  V  R  N  Y  A  Q  E  K  G  I  S  I  M
ggagacatgcctatttatgtaggttatcacagtgctgacgtttgggcaaataagaaatat
 G  D  M  P  I  Y  V  G  Y  H  S  A  D  V  W  A  N  K  K  Y
tttttgttgaataggaaaggctttcctcttctagtcagtggtgttcctcctgatgccttc
 F  L  L  N  R  K  G  F  P  L  L  V  S  G  V  P  P  D  A  F
agtgctactggtcaattgtggggaagccctctctatgattggaaaagcatggagaaagat
 S  A  T  G  Q  L  W  G  S  P  L  Y  D  W  K  S  M  E  K  D
ggatattcatggtgggtacgccgcttacaacgagctcaagatctgtatgatgaatttaga
 G  Y  S  W  W  V  R  R  L  Q  R  A  Q  D  L  Y  D  E  F  R
attgaccatttttagaggttttgctggcttttgggctgttccttctgatgcaaaaactgcg
 I  D  H  F  R  G  F  A  G  F  W  A  V  P  S  D  A  K  T  A
atgatgggaaactggaaggctggacctgggaaatccttatttgatgccatctctagagct
 M  M  G  N  W  K  A  G  P  G  K  S  L  F  D  A  I  S  R  A
gttggaaagatcagcatcatagcagaagatttgggagtcattactgaggatgtagtgcag
 V  G  K  I  S  I  I  A  E  D  L  G  V  I  T  E  D  V  V  Q
cttaggaaagatattggtgctcctggaatggctgtccttcagtttggatttggaggtgac
 L  R  K  D  I  G  A  P  G  M  A  V  L  Q  F  G  F  G  G  D
gctgataaccctcatttacctcataaccatgaagccaatcaagttgtatacaccggaact
 A  D  N  P  H  L  P  H  N  H  E  A  N  Q  V  V  Y  T  G  T
catgataatgacacgacccgaggttggtgggacattttgaagcaagaggagaaatcaaat
 H  D  N  D  T  T  R  G  W  W  D  I  L  K  Q  E  E  K  S  N
gtcctgaagtatctttcaattactgaagaggatgatatgccatgggcgctcatccaagct
 V  L  K  Y  L  S  I  T  E  E  D  D  M  P  W  A  L  I  Q  A
gtgtgttcatcagtggcccaaactgcagttatacccctgcaagatattcttggactgggg
 V  C  S  S  V  A  Q  T  A  V  I  P  L  Q  D  I  L  G  L  G
aattctgccaggatgaacgtccctgctactcagtttggaaactggggctggagggtacct
 N  S  A  R  M  N  V  P  A  T  Q  F  G  N  W  G  W  R  V  P
agttccttaagtttcaatcagatggagaaagaagcaacaagactaagggatttgctttca
 S  S  L  S  F  N  Q  M  E  K  E  A  T  R  L  R  D  L  L  S
atgtatgggcgggtgtag
 M  Y  G  R  V  -
```

**Figure 3.3** Nucleotide and deduced amino acid sequences of *medpeI*. The bold letters indicate start and stop codons. The underlined letters indicate predicted signal peptide using Chlorop v1.1.

### 3.1.2 Cloning of *atdpeI* gene from *Arabidopsis thaliana*

#### 3.1.2.1 *atdpeI* gene amplification and preparation

The *atdpeI* gene amplification product was found in single band on 1% agarose gel in Figure 3.4 lane1. The size of PCR product was 1.7 kb as expected for *atdpeI* gene. The PCR product was cleaned and ligated into pET151/D-TOPO® vector.

#### 3.1.2.2 Transformation and colony selection

The PCR product and linear pET151/D-TOPO® vector were ligated. The recombinant plasmid was transformed into competent cell of *E.coli* BL21 Star™(DE3). The *E.coli* BL21 Star™(DE3) containing recombinant plasmid was selected on LB-agar plate contain 50 μg/ml carbenicillin and incubated overnight at 37°C. The culture was subjected to plasmid extraction and checked for plasmid on agarose gel electrophoresis (Figure 3.4 lane 2). Lane 3 showed one band at 7.4 kb from the pET151/D-TOPO® vector cut with *Bam*HI. Restriction map of recombinant plasmid (pEatdpe1) was shown in Figure 3.5.

#### 3.1.2.3 Nucleotide sequencing

To confirm whether the inserted fragment was *atdpeI* gene, the recombinant plasmid was subjected to DNA sequencing using the primer of T7 promoter and T7 reverse which enable sequencing through the 5'-terminus and 3'-terminus of the *atdpeI* inserted gene in the plasmid. The nucleotide sequence of *atdpeI* and predicted signal peptide sequence were shown in Figure 3.6. The 576 amino acid residues was deduced from the *atdpeI* which had an open reading frame of 1731 bp.

The 45 amino acid residues at N-terminal was predicted to be signal peptide by using Chlorop v1.1. Expressed AtDPE1 protein sequence contain only mature enzyme and 6 Histidine residues at N-terminal. (Figure 3.7 (B))

### 3.1.3 Amino acid alignment and phylogenetic analysis

The deduced amino acid sequences from MeDPE1 and AtDPE1 were aligned with enzymes in GH77 family (Figure 3.8). The result of the alignment was shown in Table 3.1. MeDPE1 and AtDPE1 deduced amino acid sequence shared 81.5% similarity and 71.3% identity (Table 3.1). Amino acid sequence alignment between AtDPE1, MeDPE1, StDPE1 and TaMalQ showed conserve sequence, active site and 250s loop when compare from previous report on active site of TaMalQ (Figure 3.8). Three catalytic side-chains are two aspartate (Asp) and one glutamate (Glu) shown in bold letter in Figure 3.8. Phylogenetic tree analysis of plant DPE sequences (DPE1 and DPE2) and bacterial amylomaltase sequence using ClustalX (Figure 3.9) showed three groups: DPE1, DPE2 and amylomaltase. Amylomaltase group was located between DPE1 and DPE2 and closer to DPE1 group than DPE2 group.

### 3.1.4 Expression of recombinant MeDPE1 and AtDPE1

Recombinant *E.coli* cells containing expression vector inserted with *medpe1* and *atdpeI* gene were cultivated at 37°C in Auto Induction Media (AIM) containing glucose and lactose. Cell growth was monitored by optical density at 600 nm. Cells were grown until $OD_{600}$ reached 0.4 (about 4 hours) temperature was then changed to 16°C for protein expression. The enzyme activities were detected after growing at 16°C for 18 hours as intracellular enzyme inside the recombinant *E.coli* cells.

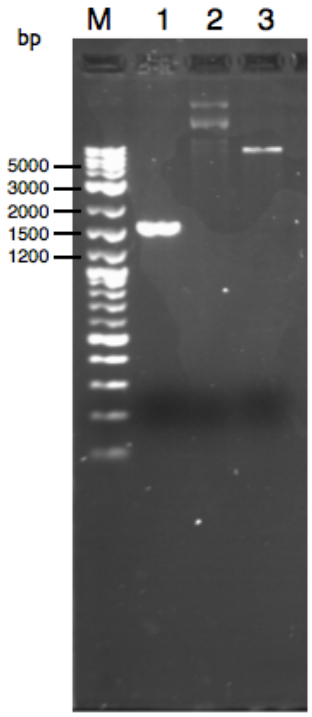


**Figure 3.4** : Agarose gel electrophoresis of PCR product and recombinant plasmids of *atdpeI* gene (Lane M, 2-Log DNA Ladder; Lane 1,PCR product of *atdpeI*; Lane 2, pET151/D-TOPO® with insert; Lane 3, pET151/D-TOPO® with insert cut with *Bam*HI.)

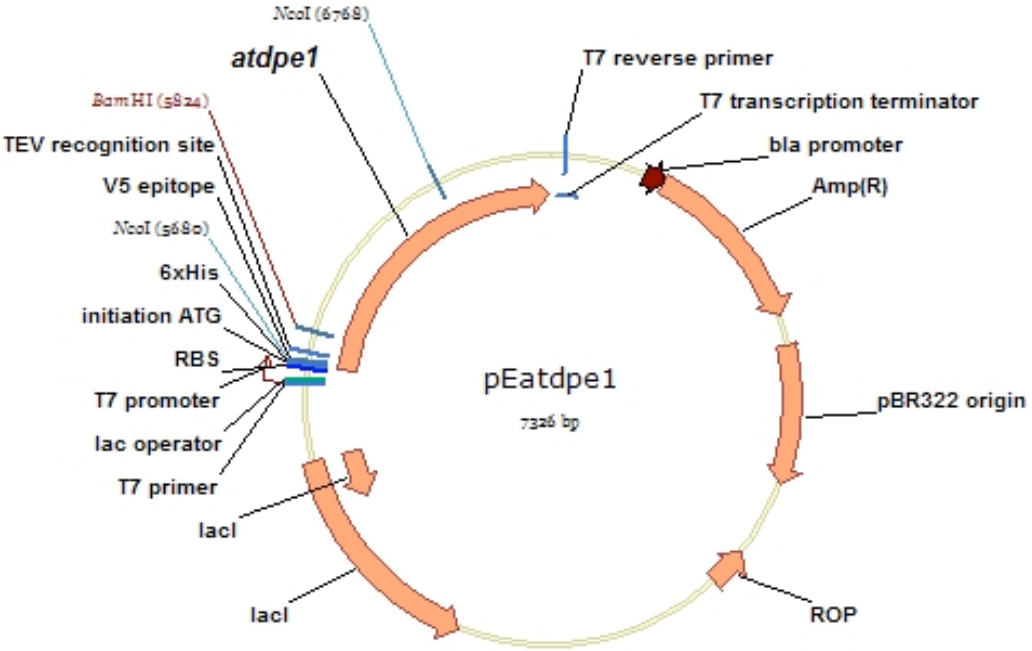


**Figure 3.5** : Restriction map plasmids of pEatdpe1 (pET151/D-TOPO® vector inserted with *atdpeI* gene).

**atg**tcgattctacttaggccgtcgtcctctccttcactctgttcttctctcaagcttttc
 M S I L L R P S S S P S L C S S L K L F
cgattatcctctccggattctttaatcgacgcagctgtcctcaggaacaggacaaagccg
 R L S S P D S L I D A A V L R N R T K P
tcgcagtcgtttcgaatggaggtcgtttcgagtaattccacgtgtctttctagtattagc
 S Q S F R M E V V S S N S T C L S S I S
gtcggtgaagattttccatcagaatatgagcagtggctaccggttccggatccagagagc
 V G E D F P S E Y E Q W L P V P D P E S
aggagaagagctggcgttttgctacacccgacgtcgtttcgtggtcctcatggcattggt
 R R R A G V L L H P T S F R G P H G I G
gatctcggagaagaagccttccggttcatcgattggcttcattctactggttgctccgtt
 D L G E E A F R F I D W L H S T G C S V
tggcaggttcttcctcttgttcctccagacgaaggaggatctccttatgcaggacaggat
 W Q V L P L V P P D E G G S P Y A G Q D
gcaaattgtgggaacacattgttgatttctctagatgagcttgtgaaagacggcttgtta
 A N C G N T L L I S L D E L V K D G L L
atcaaggatgagctcccacaaccaattgatgctgactctgtgaactatcagactgccaac
 I K D E L P Q P I D A D S V N Y Q T A N
aagttaaagagtcccttgattacgaaggcagcaaagaggcttattgatggcaatggtgaa
 K L K S P L I T K A A K R L I D G N G E
ctgaagagcaaactgctagatttccgtaacgacccctctatatcatgttggcttgaagat
 L K S K L L D F R N D P S I S C W L E D
gctgcttattttgcagctattgacaatactttaaatgcatacagttggtttgagtggcct
 A A Y F A A I D N T L N A Y S W F E W P
gaaccacttaaaaaccgtcatctttctgccttggaagctatatatgaaagccaaaaggag
 E P L K N R H L S A L E A I Y E S Q K E
tttatagacttgttcattgctaagcaatttttgttccaaaggcagtggcagaaagttcgt
 F I D L F I A K Q F L F Q R Q W Q K V R
gagtatgcacggcggcaaggagttgatataatgggagatatgcccatttatgtaggatat
 E Y A R R Q G V D I M G D M P I Y V G Y
cacagtgcagacgtttgggcaaataagaaacatttcttactgaacaagaaaggctttcct
 H S A D V W A N K K H F L L N K K G F P
cttcttgttagcggtgttcctcctgacttgttcagtgaaactggtcaactgtggggcagc
 L L V S G V P P D L F S E T G Q L W G S
cctctttatgactggaaagcaatggagagtgaccaatattcttggtgggttaatcgaata
 P L Y D W K A M E S D Q Y S W W V N R I
agacgcgcacaggacttgtatgacgaatgcaggattgatcacttcagaggatttgcaggg
 R R A Q D L Y D E C R I D H F R G F A G
ttttgggcggtccccttctgaagcgaaagttgccatggttggacgatggaaggtaggacct
 F W A V P S E A K V A M V G R W K V G P
ggaaagtcattatttgatgccatttccaaaggcgttgggaagatcaaaatcatagctgaa
 G K S L F D A I S K G V G K I K I I A E
gatttgggagttattactaaagatgtagttgagctgaggaaatctatcggagcacctgga
 D L G V I T K D V V E L R K S I G A P G
atggccgtcctccaatttgctttggaggaggcgccgataacccacatttacctcacaat
 M A V L Q F A F G G G A D N P H L P H N
catgaagtaaaccaagttgtatactctggaactcatgacaacgacactattcgaggctgg
 H E V N Q V V Y S G T H D N D T I R G W
tgggacactctggaccaagaagaaaagtctaaggcaatgaaatacctgtcgatagctgga
 W D T L D Q E E K S K A M K Y L S I A G
gaagacgatatatcatggtcagtcatccaagctgcattctcttcaaccgctcaaaccgca
 E D D I S W S V I Q A A F S S T A Q T A
atcataccgatgcaagacattctaggacttggaagttctgccaggatgaacactccagcc
 I I P M Q D I L G L G S S A R M N T P A
actgaggtggggaattggggttggaggattccaagttcaacgagctttgataatcttgaa
 T E V G N W G W R I P S S T S F D N L E
actgaatctgacagactcagagatcttttgtcattgtacggacggctt**tga**
 T E S D R L R D L L S L Y G R L -

**Figure 3.6** Nucleotide and deduced amino acid sequences of *atdpeI* gene. The bold letters indicate start and stop codons. The underlined letters indicate predicted signal peptide using Chlorop v1.1.

(A) Deduced amino acid of MeDPE1 expressed in *E.coli* DH5α

MDPSSRSAAGTIWEFEAVVSLSSTIGVGEDLPADYDEWLPKLDPIHRRRAGILL
HPTSFRGPYGIGDLGEEAFRFIDWLHDAGCSVWQVLPLVPPGRKANEEGSPYS
GQDANCGNTLLISLEELVKDGLLMKDELPEPVISDRVNFDAVAKLKDPLVVKA
AERLIRSGSELKNQLEDFCKDPQISGWLEDAAYFAAIDDTLNTLNWYAWPEPL
KNRHLSALEEIYQSKKDFIDIFIAQQFLFQRQWQKVRNYAQEKGISIMGDMPIY
VGYHSADVWANKKYFLLNRKGFPLLVSGVPPDAFSATGQLWGSPLYDWKSM
EKDGYSWWRRLQRAQDLYDEFRIDHFRGFAGFWAVPSDAKTAMMGNWKAG
PGKSLFDAISRAVGKISIIAEDLGVITEDVVQLRKDIGAPGMAVLQFGFGGDAD
NPHLPHNHEANQVVYTGTHDNDTTRGWWDILKQEEKSNVLKYLSITEEDDM
PWALIQAVCSSVAQTAVIPLQDILGLGNSARMNVPATQFGNWGWRVPSSLSFN
QMEKEATRLRDLLSMYGRVVD**HHHHHH**

| **Analysis** | **Entire Protein** |
|---|---|
| Length | 553 amino acid |
| Molecular Weight | 62304.45 |

(B) Deduced amino acid of AtDPE1 expressed in *E.*coli BL21 Star™(DE3)

M**HHHHHH**GKPIPNPLLGLDSTENLYFQGIDPFHMSSISVGEDFPSEYEQWLPV
PDPESRRRAGVLLHPTSFRGPHGIGDLGEEAFRFIDWLHSTGCSVWQVLPLVP
PDEGGSPYAGQDANCGNTLLISLDELVKDGLLIKDELPQPIDADSVNYQTANK
LKSPLITKAAKRLIDGNGELKSKLLDFRNDPSISCWLEDAAYFAAIDNTLNAYS
WFEWPEPLKNRHLSALEAIYESQKEFIDLFIAKQFLFQRQWQKVREYARRQG
VDIMGDMPIYVGYHSADVWANKKHFLLNKKGFPLLVSGVPPDLFSETGQLW
GSPLYDWKAMESDQYSWWVNRIRRAQDLYDECRIDHFRGFAGFWAVPSEAK
VAMVGRWKVGPGKSLFDAISKGVGKIKIIAEDLGVITKDVVELRKSIGAPGMA
VLQFAFGGGADNPHLPHNHEVNQVVYSGTHDNDTIRGWWDTLDQEEKSKA
MKYLSIAGEDDISWSVIQAAFSSTAQTAIIPMQDILGLGSSARMNTPATEVGNW
GWRIPSSTSFDNLETESDRLRDLLSLYGRL

| **Analysis** | **Entire Protein** |
|---|---|
| Length | 554 amino acid |
| Molecular Weight | 62261.33 |

**Figure 3.7** Deduced amino acid of MeDPE1 (A) and AtDPE1 (B) expressed in *E.coli*. The bold letters indicate 6 histidine residues. The underlined letters indicate the start of mature enzymes.

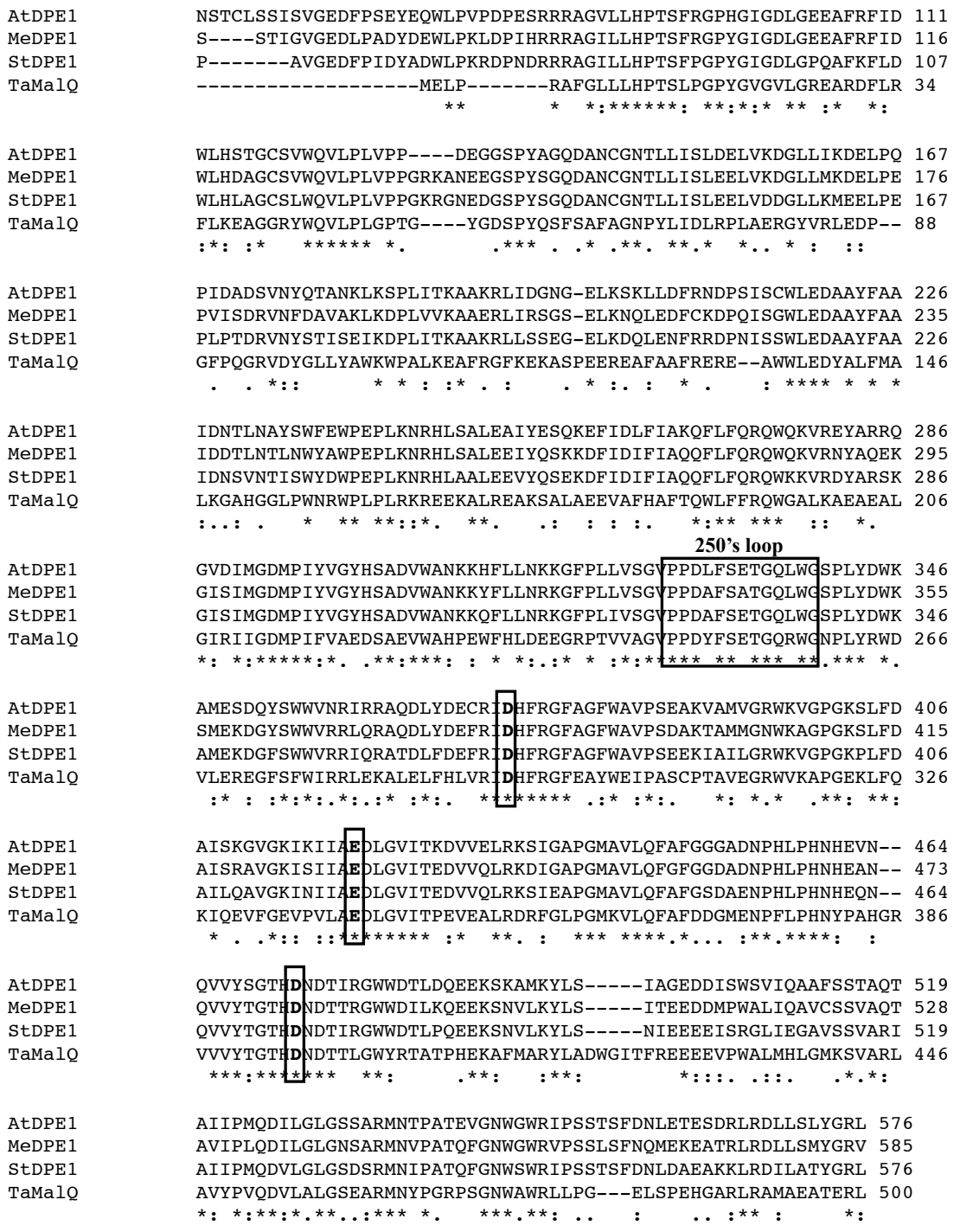


**Figure 3.8** Sequence alignment of amylomaltase and plant D-enzyme (*Arabidopsis*, cassava and potato) generated with CLUSTAL 2.1 multiple sequence alignment. Three catalytic side-chains are marked in bold letter and box. The 250s loop are boxed in black and label. The Access accession number used were as follow : AAK59831.1 (*Arabidopsis thaliana,* AtDPE1), cassava4.1_008552m.g (*Manihot esculenta* Crantz, MeDPE1), Q06801 (*Solanum tuberosum,* StDPE1), BAA33728.1 (*Thermus aquaticus* ATCC 33923, TaMalQ).

**Table 3.1** Scores of deduced amino acid sequence similarity of DPE1 from *Arabidopsis thaliana* and *Manihot esculenta* Crantz compared with other GH77 family by pairwise sequence alignment (http://www.ebi.ac.uk/Tools/psa/emboss_needle/).

| **%identity [%similarity]** | AtDPE1 | CrDPE1 | StDPE1 | TaDPE1 | MeDPE1 | OsDPE1 | AtDPE2 | StDPE2 | MalM | TaMAlQ |
|---|---|---|---|---|---|---|---|---|---|---|
| AtDPE1 | 100 | 44.1 | 59.0 | 60.0 | 71.3 | 60.3 | 16.6 | 16.2 | 35.5 | 35.4 |
| CrDPE1 | [59.3] | 100 | 44.4 | 46.4 | 46.5 | 45.6 | 17.3 | 14.0 | 33.9 | 36.5 |
| StDPE1 | [81.4] | [58.9] | 100 | 61.6 | 70.9 | 60.1 | 16.9 | 16.3 | 40.0 | 37.5 |
| TaDPE1 | [73.9] | [61.4] | [76.4] | 100 | 62.1 | 78.7 | 16.9 | 15.3 | 36.4 | 36.0 |
| MeDPE1 | [81.5] | [60.2] | [83.4] | [78.1] | 100 | 58.4 | 16.4 | 14.9 | 37.5 | 36.8 |
| OsDPE1 | [74.8] | [60.4] | [71.5] | [86.1] | [73.0] | 100 | 16.5 | 14.4 | 35.4 | 35.8 |
| AtDPE2 | [27.9] | [27.4] | [28.1] | [28.8] | [27.6] | [27.6] | 100 | 49.7 | 20.3 | 18.3 |
| StDPE2 | [26.8] | [22.2] | [25.3] | [25.4] | [26.6] | [24.7] | [56.0] | 100 | 16.5 | 14.7 |
| MalM | [50.1] | [46.2] | [52.8] | [51.2] | [51.8] | [50.4] | [32.8] | [25.4] | 100 | 44.4 |
| TaMalQ | [48.7] | [50.8] | [51.5] | [50.0] | [50.4] | [48.0] | [29.1] | [24.0] | [58.9] | 100 |

Accession numbers used were as follow : AAK59831.1 (*Arabidopsis thaliana,* AtDPE1), AAG29839 (*Chlamydomonas reinhardtii,* CrDPE1), Q06801 (*Solanum tuberosum,* StDPE1), DQ068045 (*Triticum aestivum*, TaDPE1), cassava4.1_008552m.g (*Manihot esculenta* Crantz, MeDPE1), NM_001066877 (*Oryza sativa*, OsDPE1), NP_181616 (*Arabidopsis thaliana*, AtDPE2), AAR99599 (*Solanum tuberosum,* StDPE2), NP_213497 (*Aquifex aeolicus* VF5, MalM), BAA33728.1 (*Thermus aquaticus* ATCC 33923, TaMalQ)

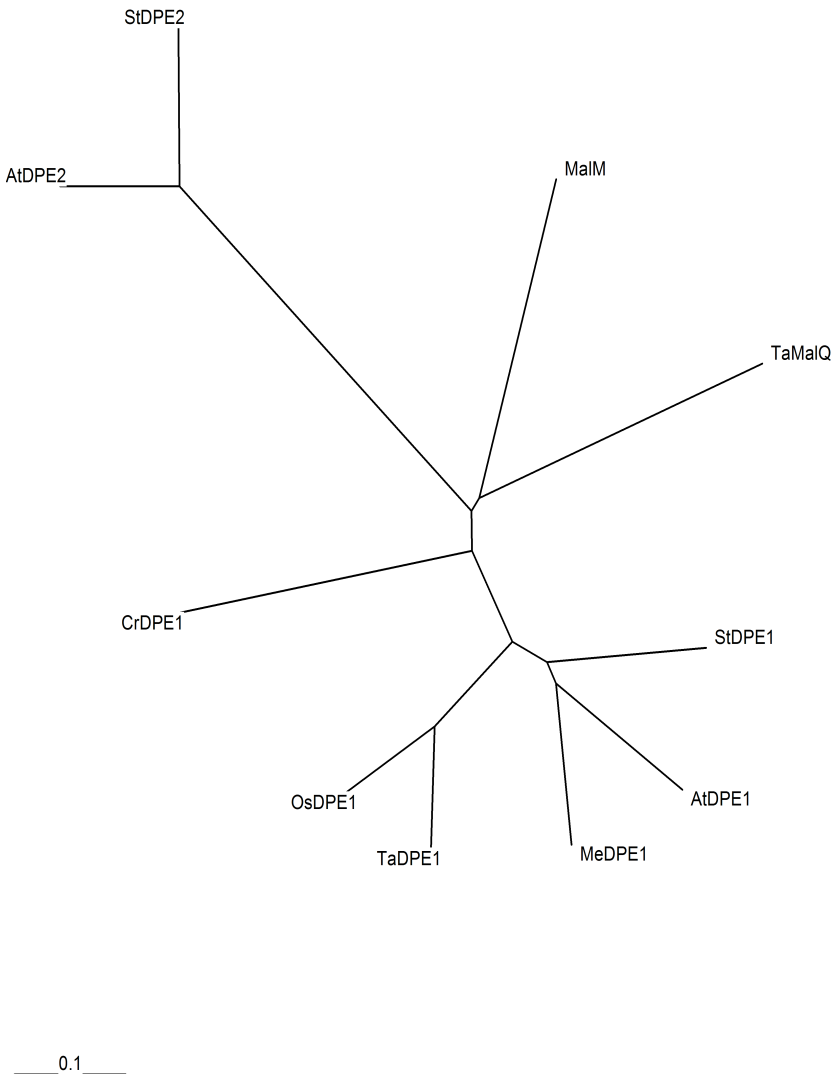


**Figure 3.9** Phylogenetic analysis of GH77 family (DPE1, DPE2 and MalQ). Tree construction was performed by the neighbor-joining method and bootstrap analysis was performed with ClustalX base on amino acid similarities. Accession numbers used were as follow : AAK59831.1 (*Arabidopsis thaliana,* AtDPE1), AAG29839 (*Chlamydomonas reinhardtii,* CrDPE1), Q06801 (*Solanum tuberosum,* StDPE1), DQ068045 (*Triticum aestivum*, TaDPE1), cassava4.1_008552m.g (*Manihot esculenta* Crantz, MeDPE1), NM_001066877 (*Oryza sativa*, OsDPE1), NP_181616 (*Arabidopsis thaliana*, AtDPE2), AAR99599 (*Solanum tuberosum,* StDPE2), NP_213497 (*Aquifex aeolicus* VF5, MalM), BAA33728.1 (*Thermus aquaticus* ATCC 33923, TaMalQ)

## 3.2 Purification of recombinant MeDPE1 and AtDPE1

### 3.2.1 Column chromatography of recombinant DPE1

The recombinant MeDPE1 and AtDPE1 enzymes were produced as intracellular enzymes. They were extracted from the recombinant *E.coli* cells by breaking the cells with cell lysis machine and centrifugation. The supernatant contained the released enzymes as assayed by hexokinase-G6P dehydrogenase method as described in section 2.8.2. Purification of the recombinant enzymes employed two columns chromatographies on affinity chromatography using HiTrap IMAC FF column and size exclusion chromatography using HiLoad 26/60 sephadex 75 prep grade. The gel filtration chromatogram of purified MeDPE1 (Figure 3.10 A) and AtDPE1 (Figure 3.10 B) showed single peak and the molecular weights were determined using molecular weight calibration curve (Figure 3.11). The molecular weights of the recombinant MeDPE1 and AtDPE1 were 117.03 kDa and 123.17 kDa, respectively.

### 3.2.2 Determination of the molecular weight on SDS-PAGE

Both enzymes showed major band on SDS-PAGE (Figure 3.12) with molecular weight at 61 kDa for MeDPE1 (Figure 3.13 A) and 64 kDa for AtDPE1 with slight contaminated band around 70 kDa (Figure 3.13 B).

### 3.2.3 Detection of DPE1 activity by native PAGE

The activity of recombinant DPE1 was investigated on native-PAGE containing 0.3% (w/v) glycogen. DPE1 catalyzed the transfer of glucan unit from maltodextrin to the glycogen. Dark band on yellow background was detected when

the gel was stained with iodine The position was corresponding to protein band on protein staining (Figure 3.14).

**(A)**

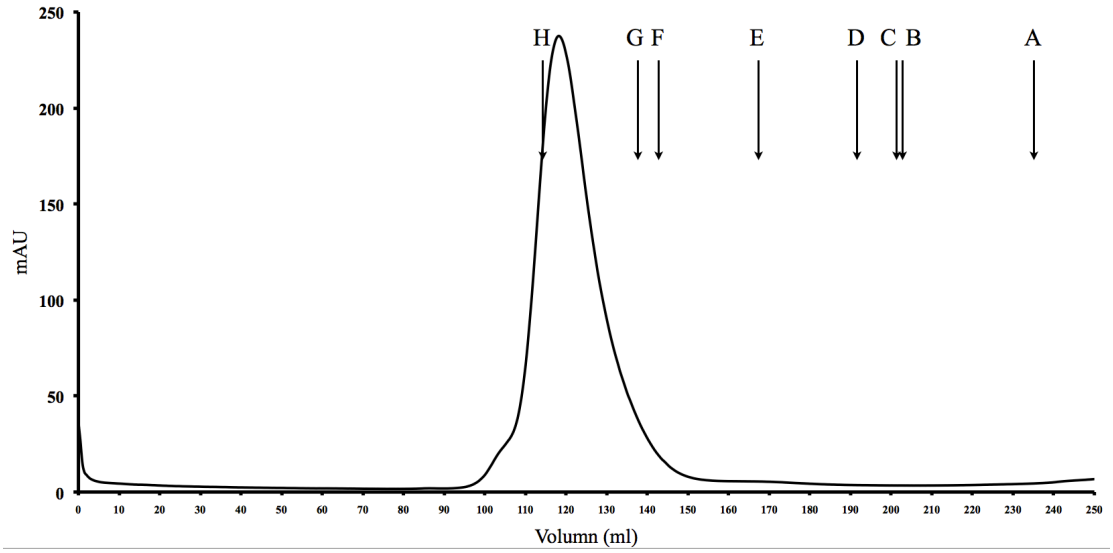


**(B)**

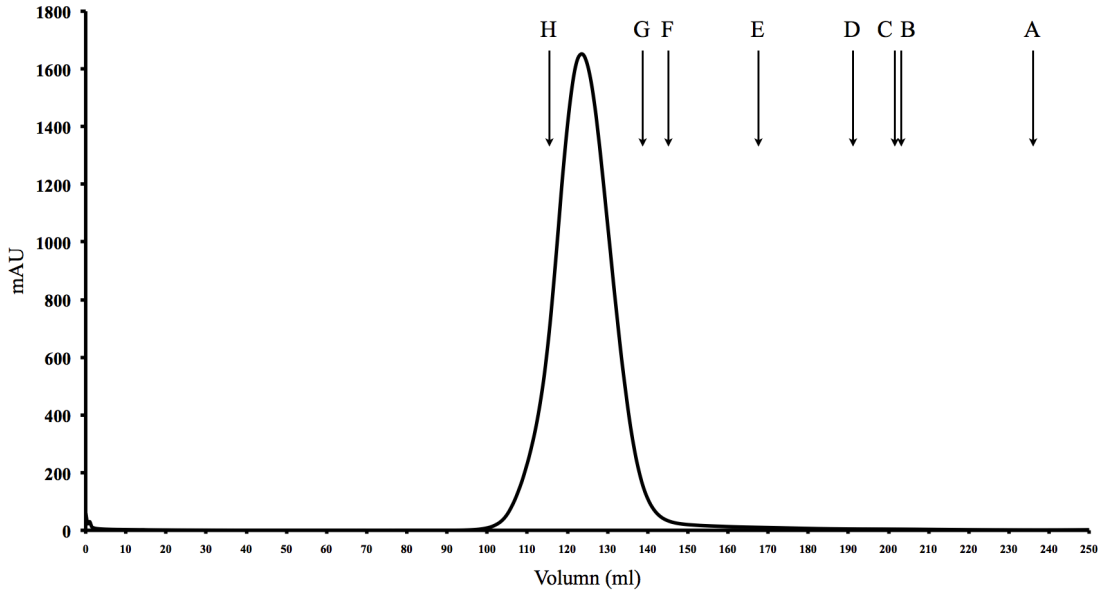


**Figure 3.10** Chromatogram of MeDPE1(A) and AtDPE1 (B) separation on gel filtration (HiLoad 26/60 seperdex 75 prep grade). A-H were standard molecular weight; Aprotinin (A) (6.5 kDa), Cytochrome C (B) (12.4 kDa), RNAse A (C) (13.7 kDa), Myoglobin (D) (17.6 kDa), Carbonic anhydrase (E) (29.0 kDa), HPLF+7 monomer (F) (56.8 kDa), BSA (G) (66.0 kDa) and ADH (H) (150.0 kDa).

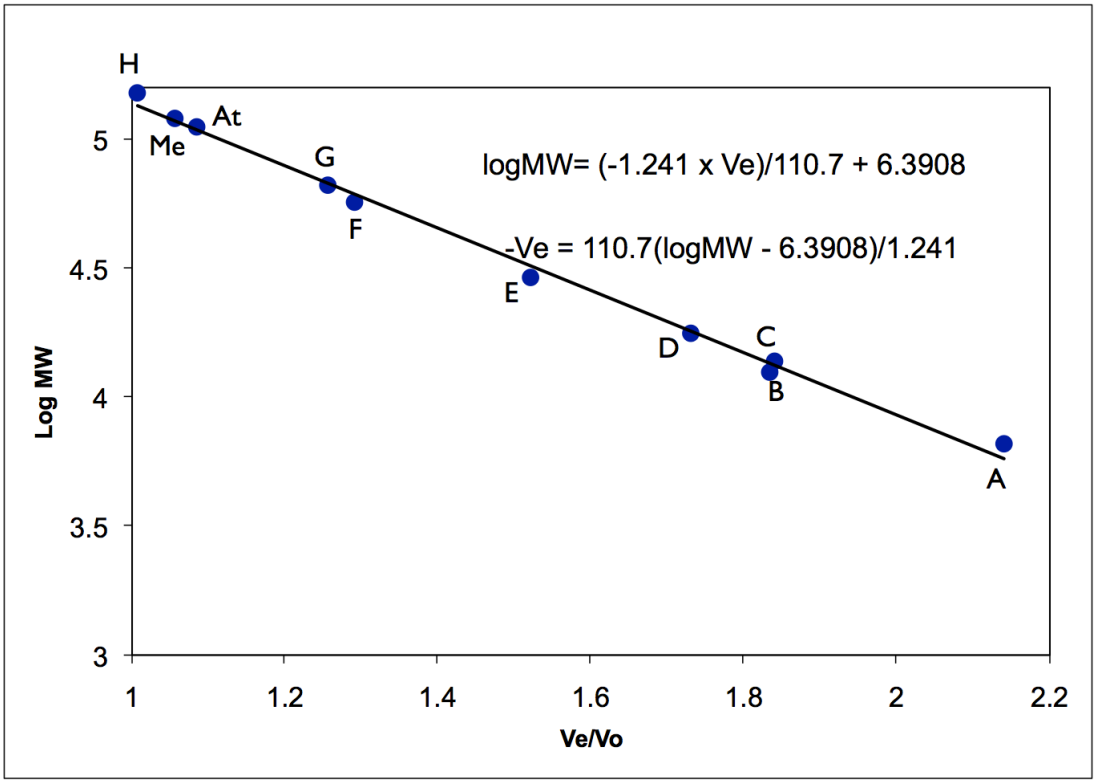


**Figure 3.11** Molecular weight calibration curve from chromatography on gel filtration HiLoad 26/60 seperdex 75 prep grade column; Aprotinin (A) (6.5 kDa), Cytochrome C (B) (12.4 kDa), RNAse A (C) (13.7 kDa), Myoglobin (D) (17.6 kDa), Carbonic anhydrase (E) (29.0 kDa), HPLF+7 monomer (F) (56.8 kDa), BSA (G) (66.0 kDa) and ADH (H) (150.0 kDa). MeDPE1 (Me) and AtDPE1 (At).

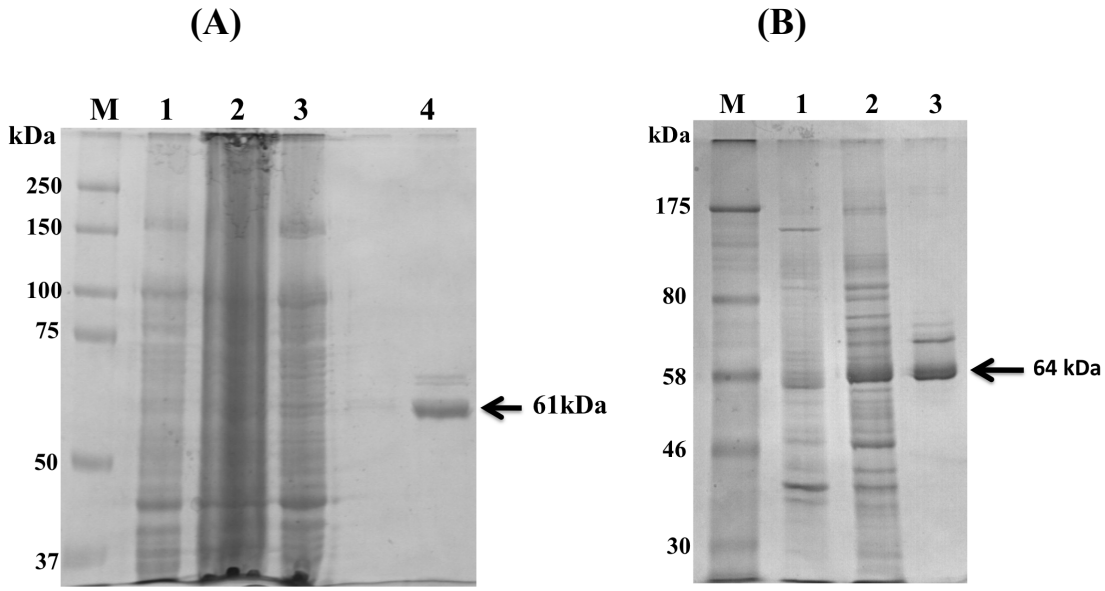


**Figure 3.12** SDS-PAGE of the recombinant MeDPE1(A) and AtDPE1(B) from each purification step; standard protein markers (M), whole recombinant MeDPE1 cell (lane1(A)), whole recombinant MeDPE1 (lane2(A)), Crude enzyme MeDPE1 (lane3(A)), purified MeDPE1 from gel filtration (lane4(A)), whole recombinant AtDPE1 cell (lane1(B)), crude enzyme AtDPE1 (lane2(B)) and purified AtDPE1 from gel filtration (Lane 3(B)).

**(A)**

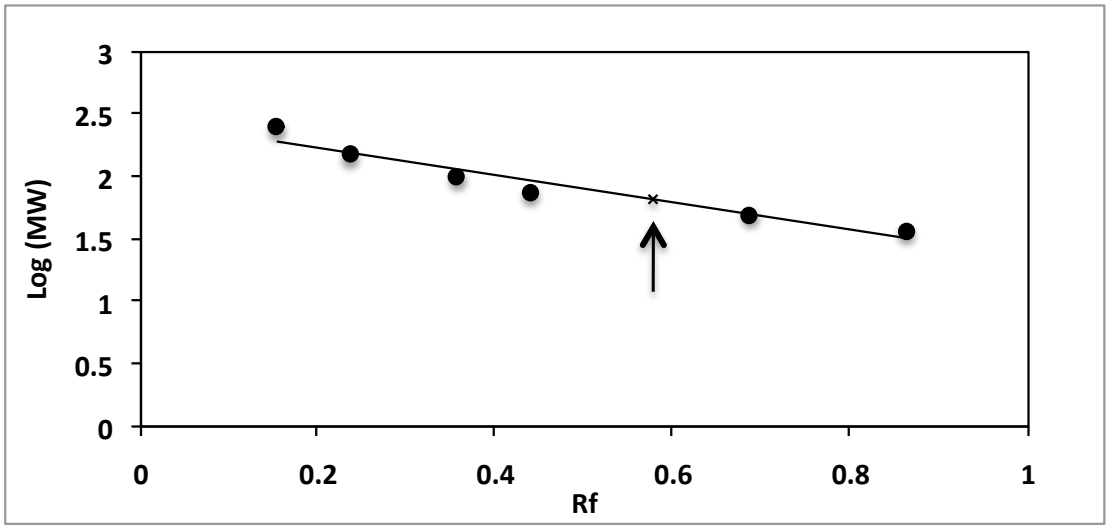


**(B)**

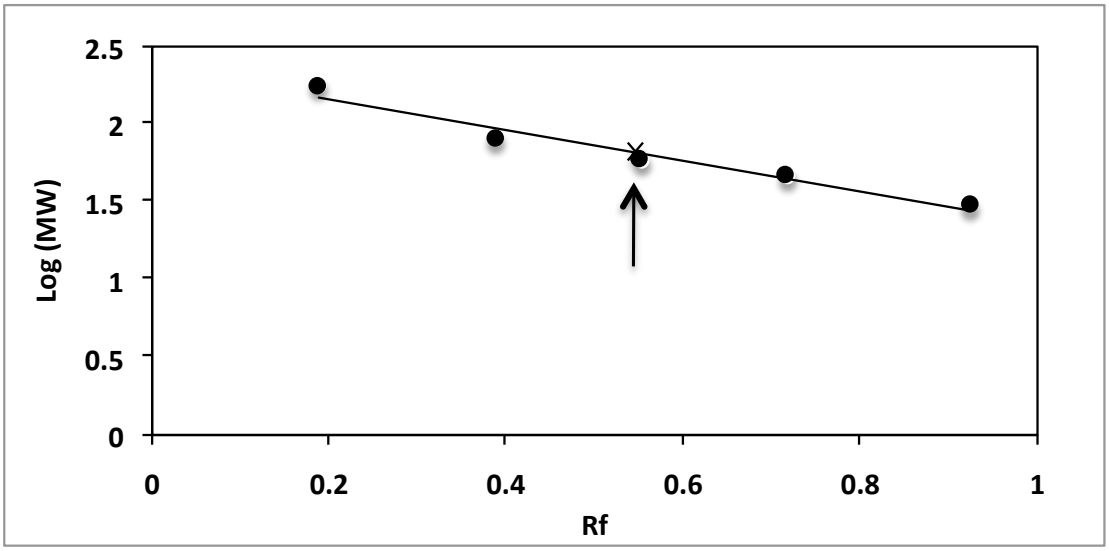


**Figure 3.13** Molecular weight calibration curve obtained from SDS-PAGE of the recombinant MeDPE1(A) and AtDPE1(B).
Arrow indicates the position of Purified MeDPE1 and AtDPE1 respectively.

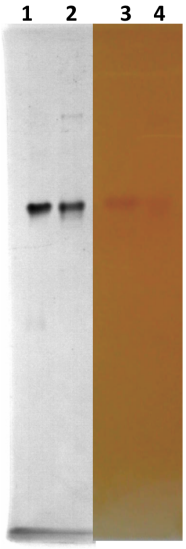


**Figure 3.14** Non-denaturing PAGE (Glycogen native PAGE) of purified recombinant MeDPE1 and AtDPE1 (Lane 1, 2) MeDPE1, AtDPE1 in coomassie stain (Lane 3, 4) MeDPE1 and AtDPE1 in iodine staining.

### 3.2.4 Purification efficiency of recombinant AtDPE1 and MeDPE1

Table 3.2 showed the calculated specific activity, purification fold and %yield during purification processes. After successive chromatographic on Ni column and gel filtration, the fold of purification of MeDPE1 and AtDPE1 were 75 and 30 respectively. The %yield of MeDPE1 was 71.1% while the yield of AtDPE1 was 35.1%

**Table 3.2** Purification table of recombinant DPE1 (MeDPE1 and AtDPE1).

| Purification Step | Total Volume (ml) | protein concentration (mg/ml) | Total Protein (mg protein) | Total activity (Unit) [1] | Specific activity (Unit/ mg protein) | Yield (%) | Purification fold |
|---|---|---|---|---|---|---|---|
| Crude enzyme (MeDPE1) | 37 | 34.4 | 1272.8 | 1838.3 | 1.44 | 100 | 1 |
| Ni-column,Gel filtration (MeDPE1) | 0.31 | 38.7 | 12.07 | 1307.5 | 108.29 | 71.1 | 75 |
| Crude enzyme (AtDPE1) | 45 | 240 | 10800 | 27000 | 2.5 | 100 | 1 |
| Ni-column,Gel filtration (AtDPE1) | 1.65 | 77 | 127.05 | 9484.3 | 74.65 | 35.1 | 30 |

[1] One unit of activity was defined as the amount of enzyme which produce 1 μmol of glucose per minute at 37°C.

## 3.3 Biochemical characterizations of recombinant MeDPE1 and AtDPE1

Since DPE1 has been classified principally on its disproportionating activity, all characteristics studied was base on the disproportionating activity with maltotriose as substrate.

### 3.3.1 Optimum pH

Both recombinant enzymes showed highest disproportionating activity at pH range 6-8 at 37°C in 0.1 M MOPS and phosphate buffer. Small decrease in activity was observed when Tris-HCl buffer was used. At pH 3-4, disproportionating activity were not observed in both enzymes and activities decreased at pH 9-10. (Figures 3.15A and 3.15B).

### 3.3.2 Optimum Temperature

Both recombinant enzymes showed highest disproportionating activity at temperature range 35-40°C and activity decreased when temperature was higher than 45°C (Figure 3.16).

### 3.3.3 Temperature stability

Effect of temperature on the stability of enzymes was studied by incubating the enzymes at 25°C and 37°C in MOPS buffer pH 7.0 up to 16 hours. Samples were taken at intervals and assayed disproportionating activity were assayed with maltotriose. The activity at zero time was taken as 100% relative activity. Activities of both MeDPE1 and AtDPE1 were more stable at 25°C. Sharp drop in activities were observed for MeDPE1 during the first 3 hours (to 35-50%) at both temperatures whereas activity of AtDPE1 decrease to 50-60%. After 3 hours incubations, the activity of both enzymes remained stable up to 16 hours (Figure 3.17)

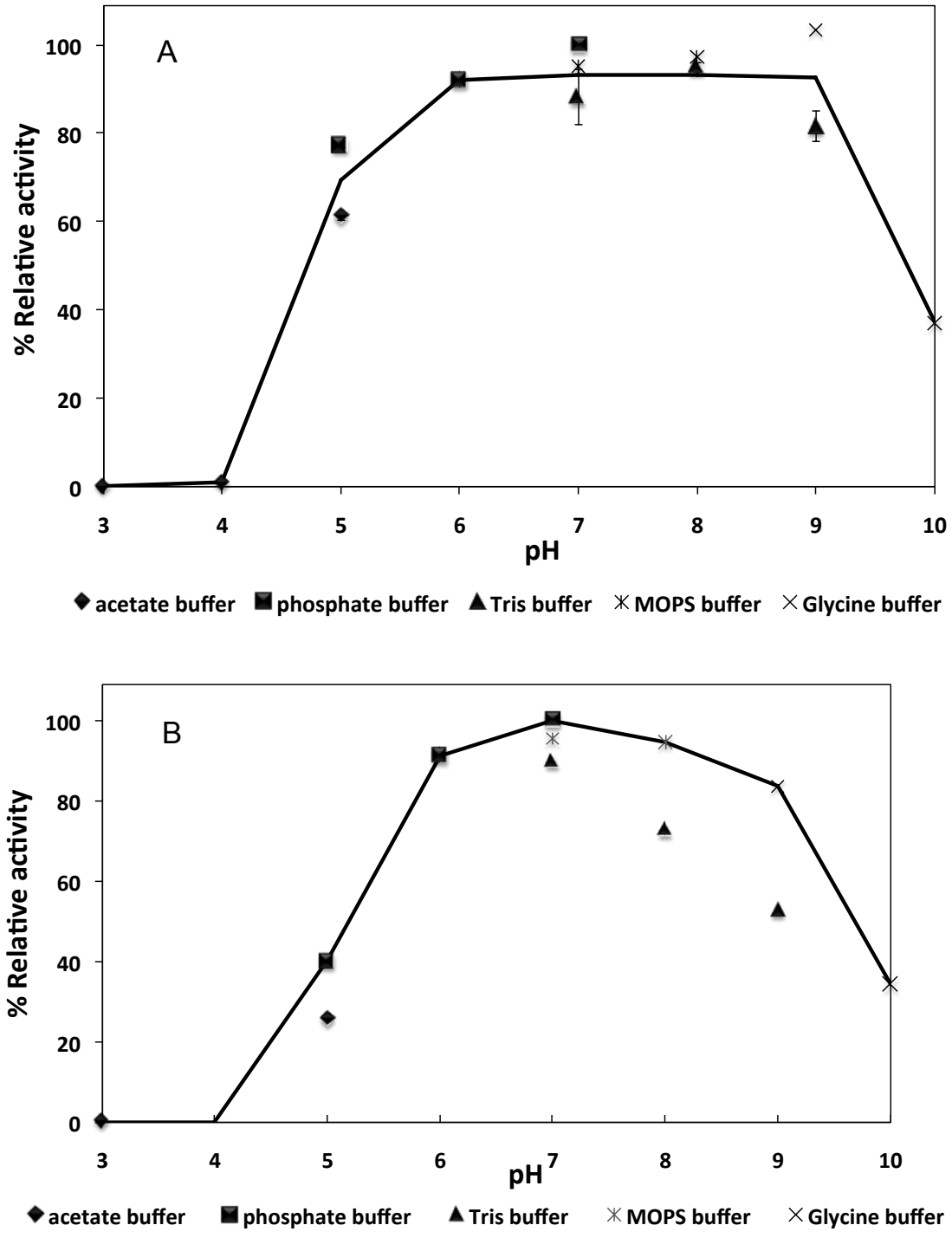


**Figure3.15** Optimum pH for disproportionation activity of purified MeDPE1 (A) and AtDPE1 (B)

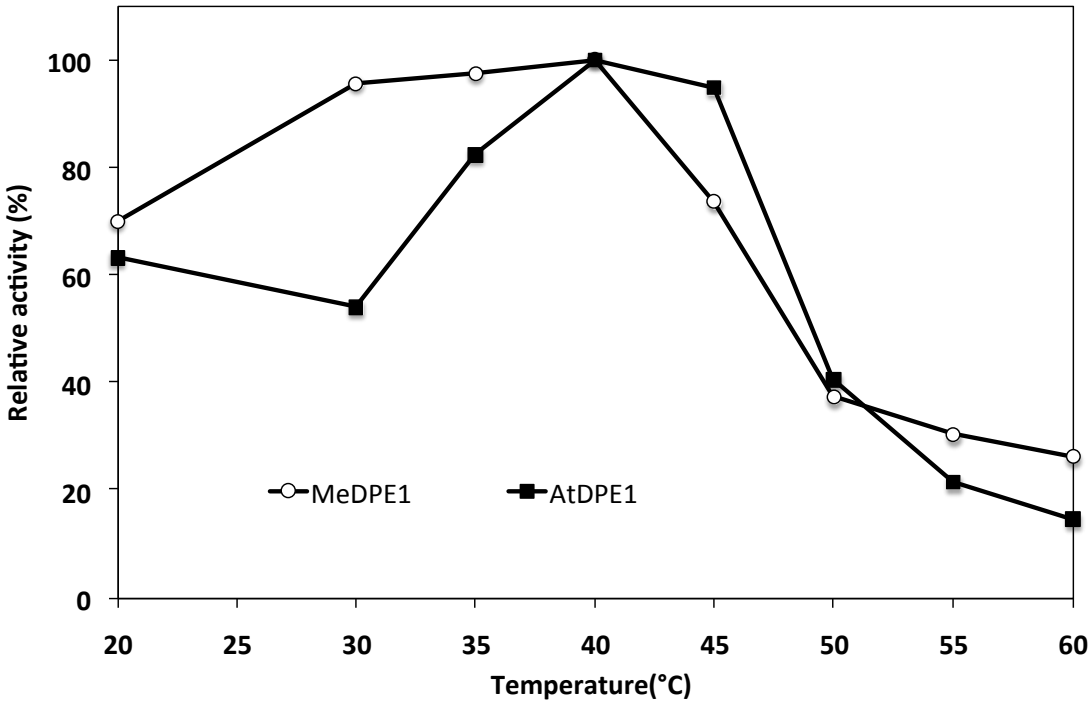


**Figure 3.16** Optimum temperature for disproportionation activity of MeDPE1 and AtDPE1

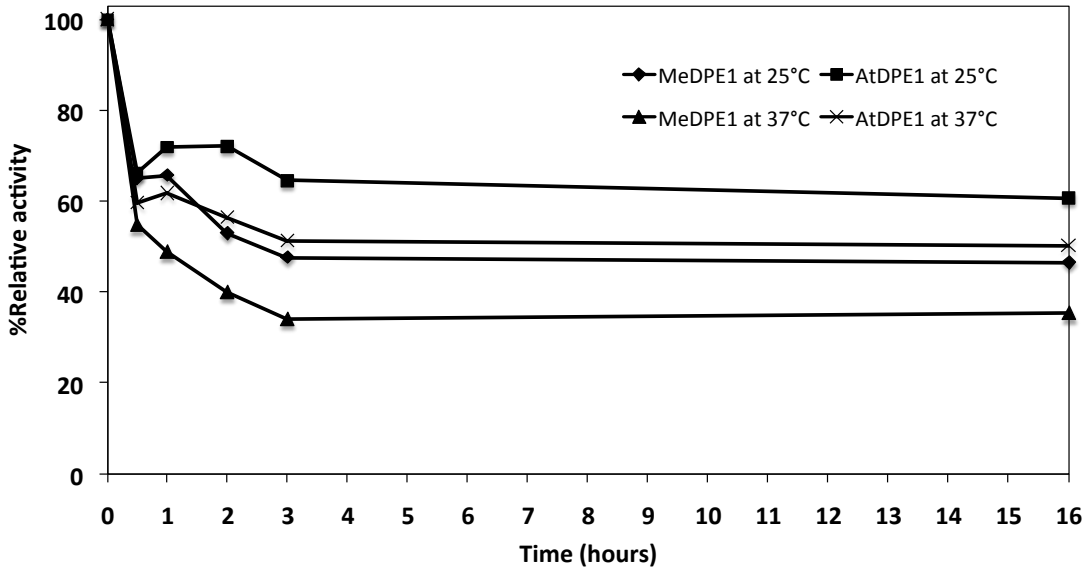


**Figure 3.17** Temperature stability of recombinant AtDPE1 and MEDPE1.

### 3.3.4 Determination of kinetic parameters

Kinetic parameters was determined for recombinant MeDPE1 and AtDPE1 using maltotriose as substrate and the glucose released was measured by using hexokinase-G6P dehydrogenase method, at 1 minute after add maltotriose at difference concentration. Lineweaver-Burk plot was prepared (Figure 3.18) and kinetic parameters was calculated as that shown in Table 3.3. The $K_m$ of AtDPE1 for maltotriose was 29.9 mM and MeDPE1 was 39.7 mM. The $k_{cat}/K_m$ of AtDPE1 was greater than MeDPE1.

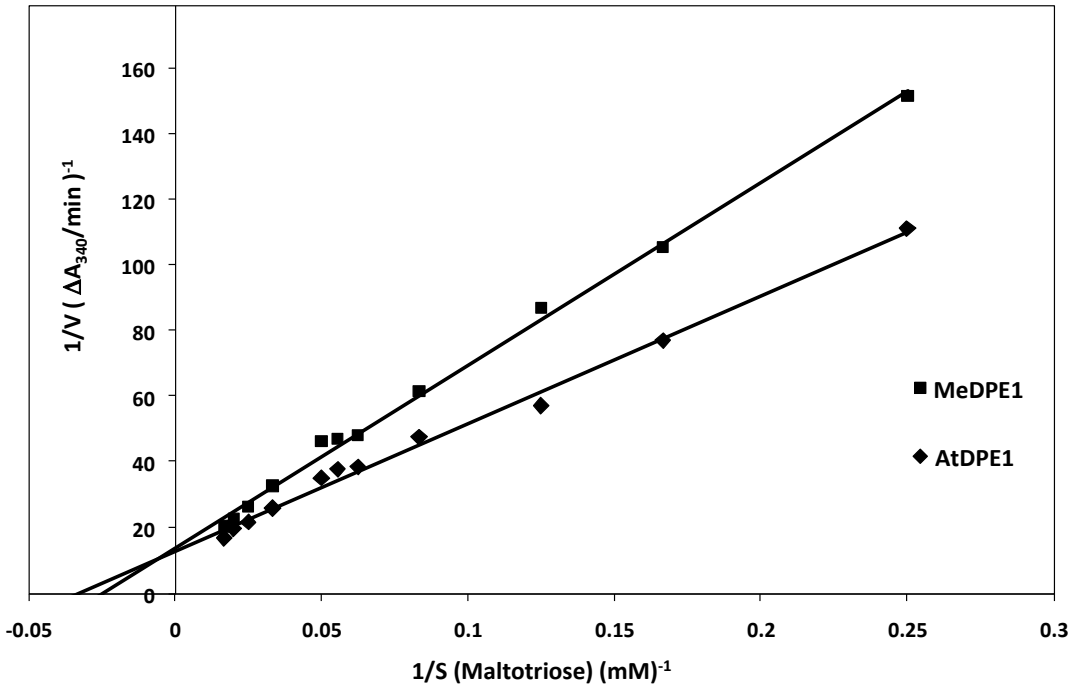


**Figure 3.18** Lineweaver-Burk plot of recombinant AtDPE1 and MeDPE1 with maltotriose as substrate. Glucose released was measured by hexokinase-G6P dehydrogenase method.

**Table 3.3** Kinetic parameter of recombinant AtDPE1 and MeDPE1 on maltotriose as substrate.

| | $K_m$ (maltotriose) mM | $V_{max}$ nmol glucose $min^{-1}$µg $protein^{-1}$ | $k_{cat}$ $min^{-1}$ | $k_{cat}/K_m$ $mM^{-1}min^{-1}$ |
|---|---|---|---|---|
| AtDPE1 | 29.9 | 59.1 | 36796 | 1231 |
| MeDPE1 | 39.7 | 54.9 | 34171 | 861 |

## 3.4 Oligosaccharide products of MeDPE1 and AtDPE1.

### 3.4.1 HPAEC-PAD analysis

Products from incubations of maltotriose with recombinant enzymes (MeDPE1, AtDPE1) were analyzed by HPAEC-PAD (Figure 3.19) in comparison with AtDPE2 and amylomaltase. Glucose, maltose ($Glc_2$), maltotriose ($Glc_3$), maltotetraose ($Glc_4$), maltopentaose ($Glc_5$), maltohexaose ($Glc_6$), malheptaose ($Glc_7$) and longer oligosaccharide were observed in amylomaltase reaction. For AtDPE2, no new peak was observed in addition to the maltotriose ($Glc_3$). For MeDPE1 reaction, peaks of glucose, maltotriose ($Glc_3$), maltopentaose ($Glc_5$) and malheptaose ($Glc_7$) were observed. Although in AtDPE1 reaction, maltotriose peak diminished but no significant product.

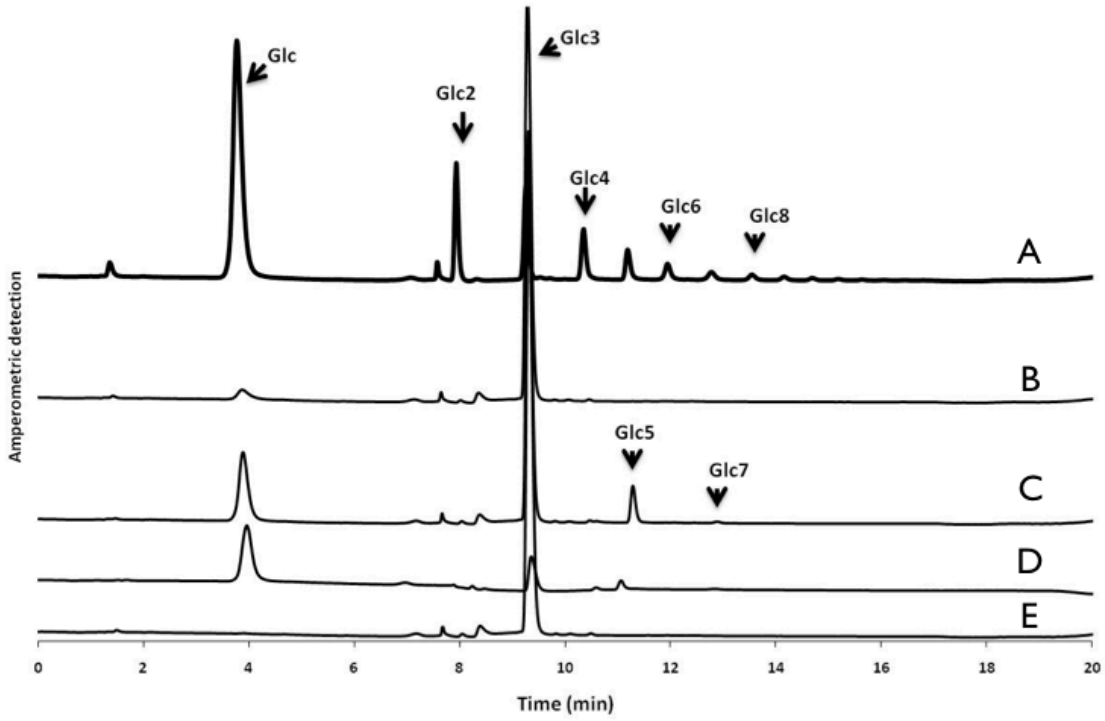


**Figure 3.19** Oligosaccharide patterns of 4-α-glucanotransferase. Disproportionating reaction using maltotriose analyzed by HPAEC-PAD. amylomaltase from *E.coli* (A), DPE2 from *Arabidopsis* (B), DPE1 from Cassava (C), DPE1 from *Arabidopsis* (D), No enzyme (E).

**3.5 Determination of acceptor specificity on oligosaccharide array.**

Oligosaccharide array which contains many types of oligosaccharide acceptors on a membrane (appendix I) was used to monitor acceptor specificity of recombinant MeDPE1 and AtDPE1. Glycogen labeled with radioisotope $^{14}$C-glucose at the non-reducing end was used as donor for the transfer maltosyl unit to acceptor on oligosaccharide array. Detection of $^{14}$C-glucose that was transferred to the membrane was performed by phosphor Imaging. In the results, AtDPE1 transferred maltosyl unit to membrane type I at block A8 and B8 which contained α-(1→4)-D-glucobiose and α-(1→4)-D-glucopentaose, respectively. AtDPE1 also transferred maltosyl unit to membrane type II on the block G7, H7, G8 and H8 which contained α-(1→4)-D-glucotriose (maltotriose), D-glycosyl-α-(1→6)-D-maltotriasyl-α-(1→6)-D-maltotriose, α-(1→4)-D-glucohexaose (maltohexaose) and α-(1→6),(1→4) -D-glucododecaose, respectively (Figure 3.20). While MeDPE1 did not show similar transfer on the membrane as in AtDPE1 (Figure 3.21).

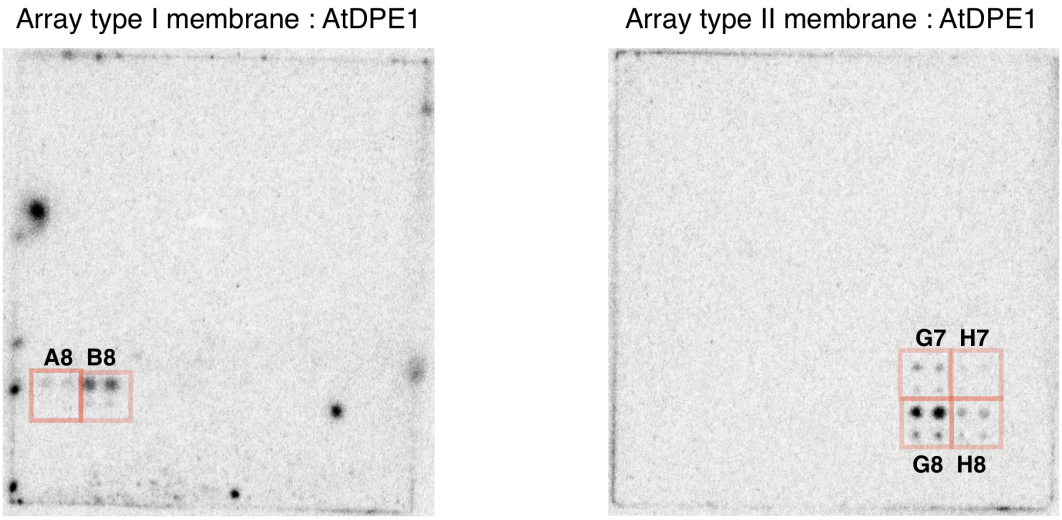


**Figure 3.20** Acceptor specificity of AtDPE1 using oligosaccharide array type I and type II and $^{14}$C-glycogen as donor.

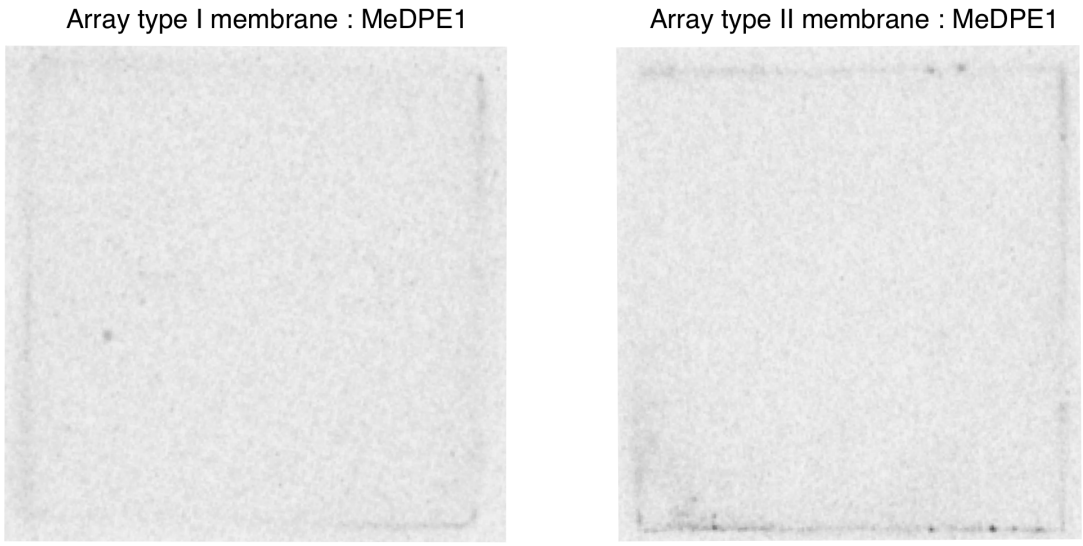


**Figure 3.21** Acceptor specificity of MeDPE1 using oligosaccharide array type I and type II and $^{14}$C-glycogen as donor.

### 3.6 Large ring cyclodextrins production

The production of large ring cyclodextrins (LR-CDs) or cycloamyloses from amylose by recombinant AtDPE1 and MeDPE1 were studied. Large ring cyclodextrins were detected by degree of polymerization (DP) using HPAEC-PAD and MALDI-TOF-MS analysis techniques. The products formed were fractionated into 3 molecular weight groups by membrane filtration at different molecular weight cut point. In HPAEC-PAD analysis, large ring cyclodextrins were observed at degree of polymerization starting from 17 and 18 from reaction catalyzed AtDPE1 and MeDPE1, respectively (Figure 3.22 A to F) and some small peaks smaller than DP17. Peaks were compared with standard cycloamylose obtained from amylomaltase (*Thermus aquaticus* ATCC 33923) (appendix J).

In MALDI-TOF-MS analysis, a series of product peaks with molecular mass corresponding to cyclic molecules containing glucose units. The series of peaks started from the mass of 20 glucose units and increase at the increment of a glucosyl unit (162 Da) for each successive peaks. (Figure 3.23) The molecular mass of the products corresponded to cyclic molecules contained glucose ranging from 20 to 34 units.

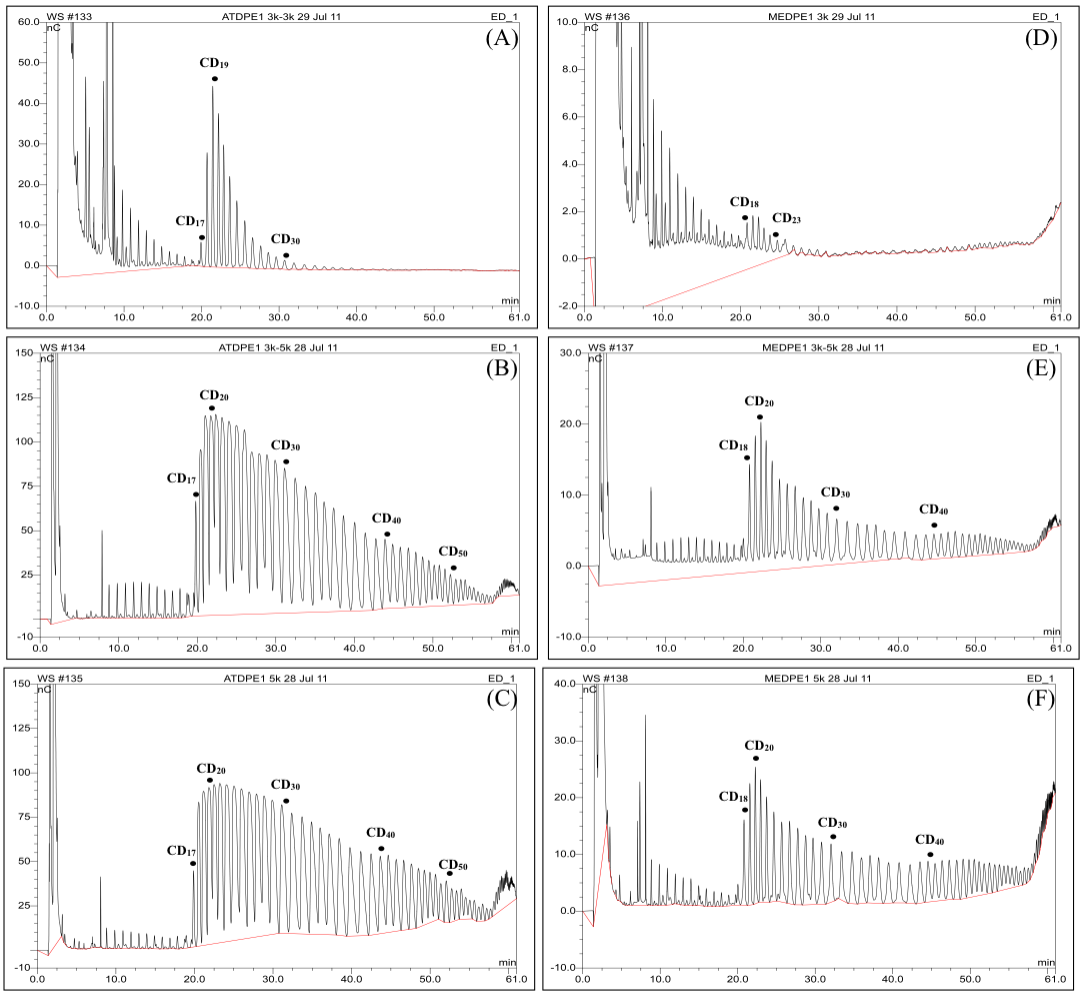


**Figure 3.22** HPAEC-PAD analysis of large-ring cyclodextrin product. AtDPE1(A to C) and MeDPE1(D to F) fraction1(MWCO3000):A, D, fraction2 (MWCO3000 to 5000) : B,E and fraction3(MWCO5000): C, F ;$CD_n$, n is the glucose number of large ring cyclodextrin.

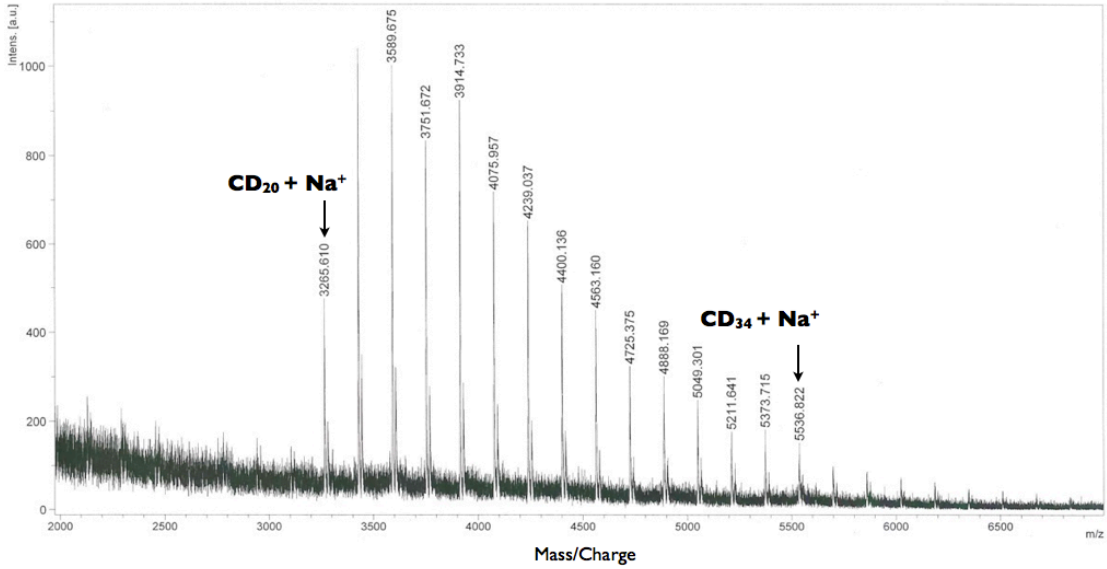


**Figure 3.23** MALDI-TOF-MS analysis of large-ring cyclodextrins product. The theoretical m/z of $(CD)_n+Na^+$ is $162_n + 23$; n is the glucose numbers in the large ring cyclodextrins.

**3.7 Inclusion complex of LR-CDs mixture with polyaniline.**

LR-CDs mixture (partition 2) from section 2.14.1 was mixed with polyaniline (section 2.15). Complexes formed between LR-CDs and polyaniline were retained on centrifugal membrane filter unit with molecular weight cut off 5000. The retained fraction was analyzed by scanning UV-Vis spectrophotometer for absorption at wavelength range 200 - 850 nm, in compare with polyaniline alone and LR-CDs alone (Figure 3.24). LR-CDs alone did not show any significant absorption spectrum. Polyaniline shown absorption around 280 nm. The fraction obtained from mixing polyaniline and LR-CDs showed different absorption spectrum from polyaniline alone, with new absorption peak appeared at 240 nm and reduction in peak height at 280 nm.

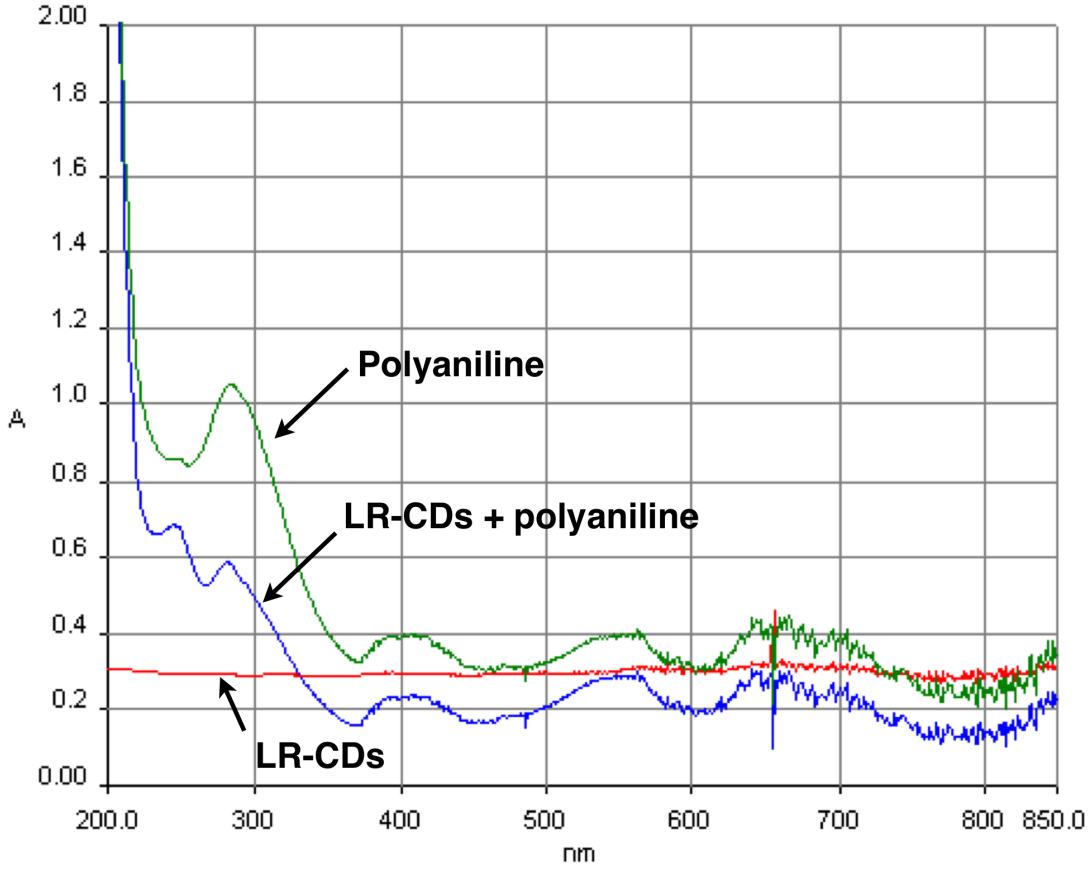


**Figure 3.24** UV-Vis absorption spectrum of LR-CDs complex with polyaniline.

## 3.8 Investigation on the use of 4-α-glucanotransferase in producing useful products.

### 3.8.1 Synthesis and detection of fluoro-oligosaccharide products

#### 3.8.1.1 Small scale production

Deoxyfluoroglucose derivatives (2FGlc (2-deoxy-2-fluoro-D-glucose), 3FGlc (3-deoxy-3-fluoro-D-glucose), 4FGlc (4-deoxy-4-fluoro-D-glucose) and 6FGlc (6-deoxy-6-fluoro-D-glucose) ) were used as acceptors for transferring glucan from glycogen donor by using 4-α-glucanotransferases. Each reaction mixture was analyzed by TLC technique. MeDPE1 reaction mixture showed small spots of product on reaction mixture using acceptors 2FGlc, 3FGlc and 6FGlc (Figure 3.25). The $R_f$ values of the products were calculated and shown in Table 3.4. Reaction of amylomaltase (Figure 3.25) showed small spots of product in the reaction mixtures using acceptors 2FGlc, 3FGlc and 6FGlc. In TLC analysis of AtDPE2 reaction mixture. Large product spots of reaction mixture using acceptors 2FGlc, 3FGlc and 6FGlc were observed (Figure 3.25). The $R_f$ values showed in Table 3.4 were similar indicating that the products from amylomaltase and AtDPE2 reaction mixtures were the same.

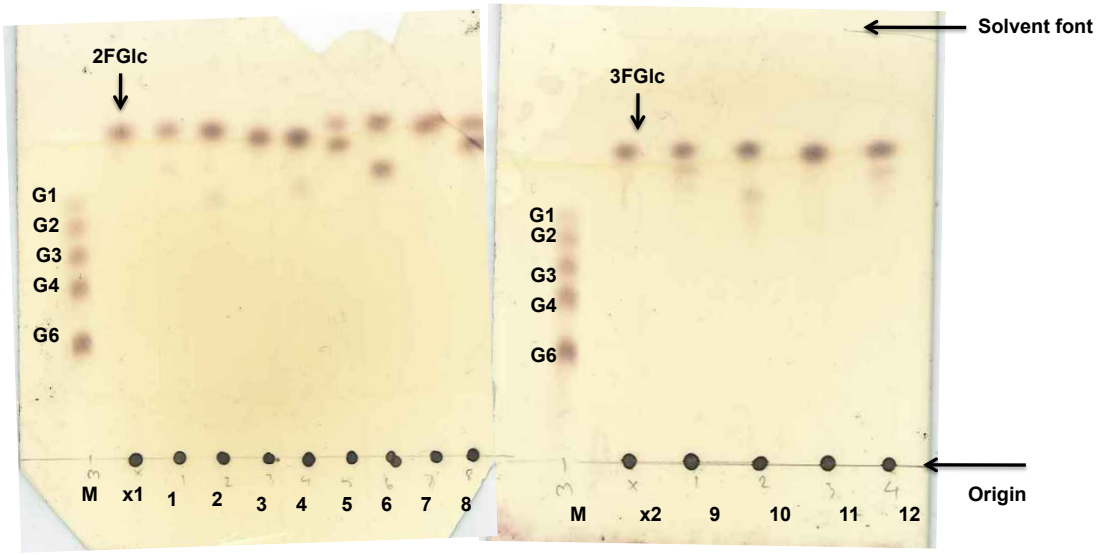


**Figure 3.25** TLC chromatogram of reaction products of MeDPE1, AtDPE2 and Amylomaltase incubated with glycogen donor and deoxyfluoroglucose derivatives. Lane M: Standard sugar from glucose (G1) to maltohexaose (G6). lane x1, 2FGlc/ no enzyme; lane x2, 3FGlc/ no enzyme; lane 1, 2FGlc / MeDPE1; lane 2, 3FGlc/ MeDPE1; lane 3, 4FGlc/MeDPE1; lane 4, 6FGlc/MeDPE1; lane 5, 2FGlc / AtDPE2; lane 6, 3FGlc/AtDPE2; lane 7, 4FGlc/AtDPE2; lane 8, 6FGlc/AtDPE2; lane 9, 2FGlc/ Amy; lane 10, 3FGlc/Amy; lane 11, 4FGlc/Amy; lane 12, 6FGlc/Amy. Arrow indicate spots corresponding to 2FGlc and 3FGlc without enzyme.

**Table 3.4** $R_f$ value from TLC analysis of reaction products of MeDPE1, AtDPE2 and amylomaltase incubated with glycogen donor and deoxyfluoroglucose derivatives acceptor.

| Lane | Product | Rf |
|---|---|---|
| Lane M : standard sugar | G1 (Glucose)<br>G2 (Maltose)<br>G3 (Maltotriose)<br>G4 (Maltotetraose)<br>G6 (Maltohexaose) | 0.54<br>0.49<br>0.43<br>0.36<br>0.25 |
| Lane x1:2FGlc / no enz | 2FGlc | 0.70 |
| Lane 1 : 2FGlc / MeDPE1 | 2FGlc<br>product 1 | 0.70<br>0.61 |
| Lane 2 : 3FGlc / MeDPE1 | 3FGlc<br>product 2 | 0.70<br>0.55 |
| Lane 3 : 4FGlc / MeDPE1 | 4FGlc | 0.69 |
| Lane 4 : 6FGlc / MeDPE1 | 6FGlc<br>product 3 | 0.69<br>0.58 |
| Lane 5 : 2FGlc / AtDPE2 | 2FGlc<br>product 4 | 0.70<br>0.66 |
| Lane 6 : 3FGlc / AtDPE2 | 3FGlc<br>product 5 | 0.70<br>0.61 |
| Lane 7 : 4FGlc / AtDPE2 | 4FGlc | 0.70 |
| Lane 8 : 6FGlc / AtDPE2 | 6FGlc<br>product 6 | 0.70<br>0.67 |
| Lane x2 :3FGlc / no enz | 3FGlc | 0.70 |
| Lane 9 : 2FGlc / Amy | 2FGlc<br>product 7 | 0.70<br>0.66 |
| Lane 10 : 3FGlc / Amy | 3FGlc<br>product 8 | 0.70<br>0.61 |
| Lane 11 : 4FGlc / Amy | 4FGlc | 0.70 |
| Lane 12 : 6FGlc / Amy | 6FGlc<br>product 9 | 0.70<br>0.67 |

### 3.8.1.2 Large scale preparation and product isolation

AtDPE2 was used for the study on large scale preparation of fluoromaltose derivatives because it produced spot on TLC plate with very high intensity compare to MeDPE1 and amylomaltase. Glycogen and precipitated proteins were removed from products in fluoro oligosaccharide reaction mixture of AtDPE2 using ultrafiltration (Centricon (MWCO 30,000)) followed by gel filtration chromatography (TSK-HW40S) to separate oligosaccharide. The gel filtration chromatograms of deoxyfluoroglucose derivatives for acceptors 2FGlc (2-deoxy-2-fluoro-D-glucose), 3FGlc (3-deoxy-3-fluoro-D-glucose) and 6FGlc (6-deoxy-6-fluoro-D-glucose) were shown in Figure 3.26, 3.27 and 3.28 respectively. Two major peaks appeared in all gel filtration profiles. The fractions in TLC analysis of each gel filtration peak was performed and shown as the inset in each gel filtration profiles. AtDPE2 seems to transfer only one glucosyl residue to each acceptor. The first peak containing the interesting products was pooled and further analyzed.

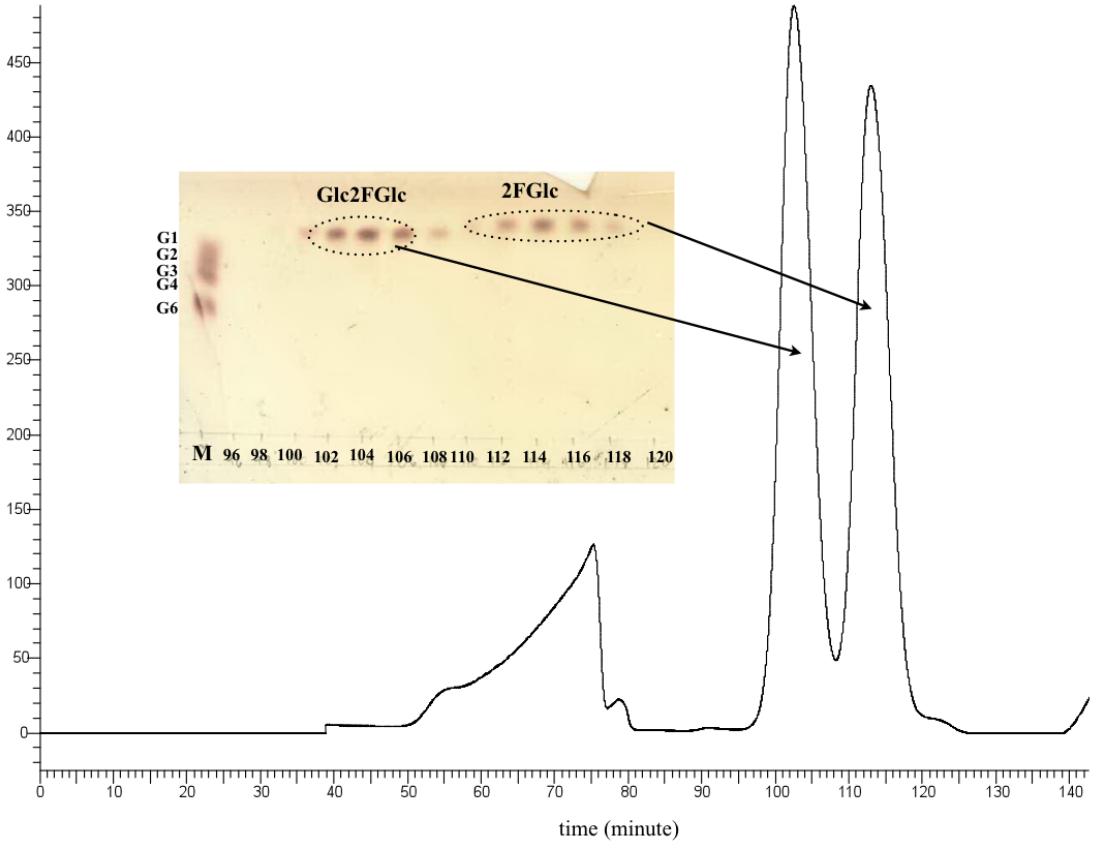


**Figure 3.26** Gel filtration profile (TSK-HW40S column) of reaction products of 2-deoxy-2-fluoro-D-glucose and glycogen with AtDPE2. The column height 50 cm, flow rate 0.5 ml/min, MQ-water as mobile phase. M, Standard sugar (G1) and maltodextrin (G2, G3, G4 and G6); Number in TLC plate indicated time fraction in gel filtration; 2FGlc, 2-deoxy-2-fluoro-D-glucose; Glc2FGlc, expect to product

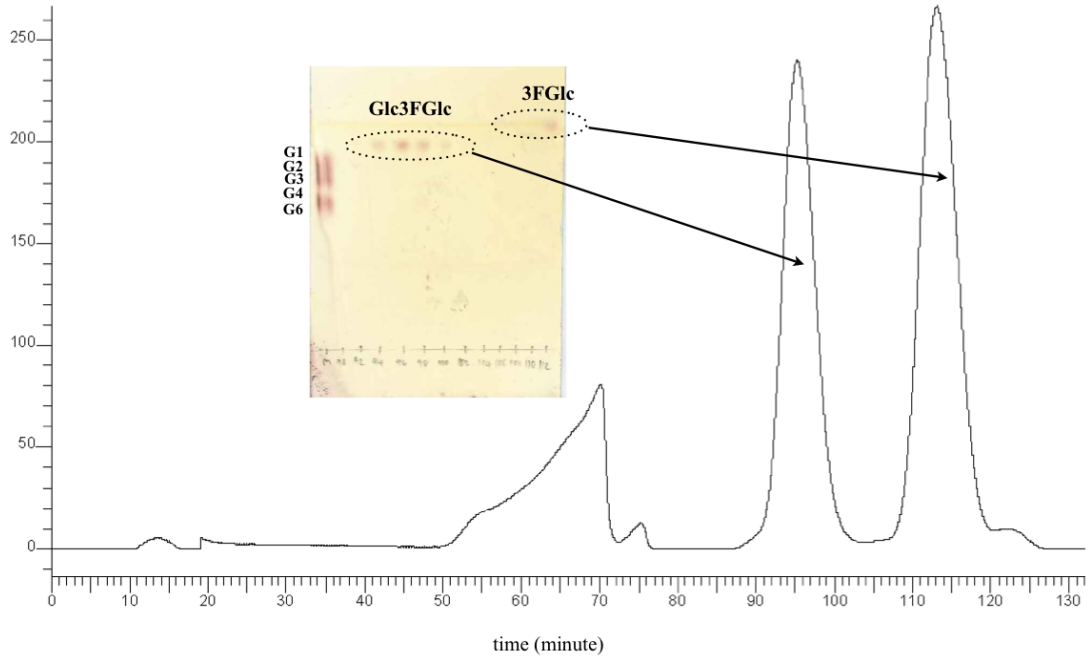


**Figure 3.27** Gel filtration profile (TSK-HW40S column) of reaction products of 3-deoxy-3-fluoro-D-glucose and glycogen with AtDPE2. The column height 50 cm, flow rate 0.5 ml/min, MQ-water was used as mobile phase. M, Standard sugars (G1) and maltodextrin (G2, G3, G4 and G6); Number in TLC plate indicated time fraction in gel filtration; 3FGlc, 3-deoxy-3-fluoro-D-glucose; Glc3FGlc, expect to product.

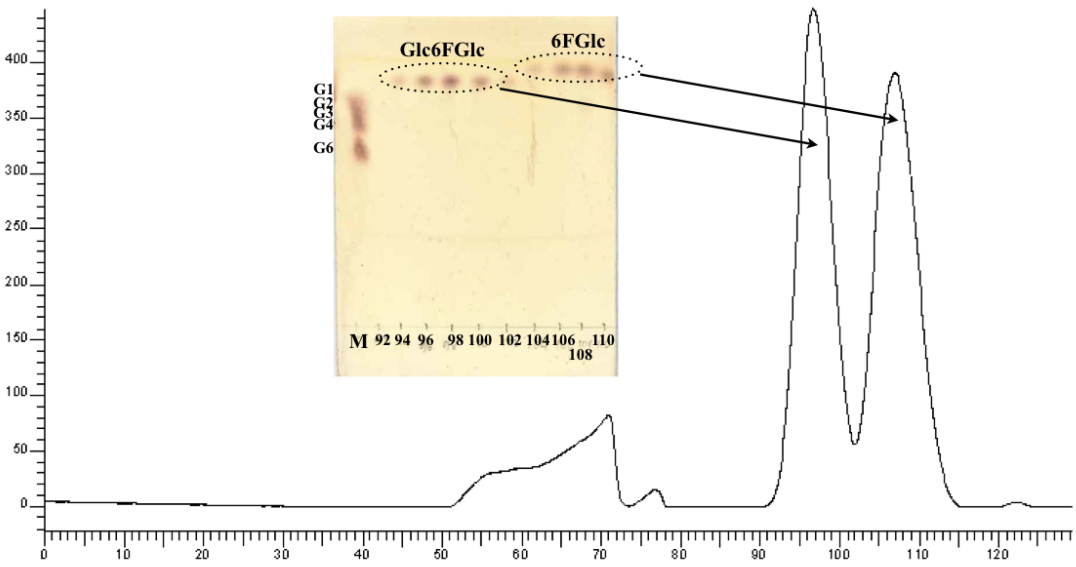


**Figure 3.28** Gel filtration profile (TSK-HW40S column) of reaction products of 6-deoxy-6-fluoro-D-glucose and glycogen with AtDPE2, The column height 50 cm, flow rate 0.5 ml/min, MQ-water as mobile phase. M, Standard sugar (G1) and maltodextrin (G2, G3, G4 and G6); Number in TLC plate indicate fraction time in gel filtration; 6FGlc, 6-deoxy-6-fluoro-D-glucose; Glc6FGlc, expect to product.

### 3.8.2 Characterization of deoxyfluoromaltose derivatives

#### 3.8.2.1 Optical rotation and high resolution mass spectrometry

The purified deoxyfluoromaltose derivatives from the first peak of each gel filtration profile were analyzed for optical rotations and molecular weight and their % yield calculated (Table 3.5). The purified product was scaled up in mg quantities of deoxyfluoromaltose. The molecular weight of each product corresponded to the size of fluoromaltose derivatives shown in Figure 3.29.

**Table 3.5** Calculated %yield, optical rotations and observed sodium ion adduct masses for Glc2FGlc, Glc3FGlc and Glc6FGlc by High resolution MS.

| Product | %yield (weight) | Optical rotations | High resolution mass spectrometry | | |
|---|---|---|---|---|---|
| | | $[\alpha]_D^{20°C}$ | $[M+Na]^+$ calculated | $[M+Na]^+$ observed | Error (ppm) |
| Glc2FGlc | 36.5 (8.6 mg) | +125.6 (c0.16,$H_2O$) | 367.1011 | 367.1010 | -0.262 |
| Glc3FGlc | 34.6 (8.5 mg) | +131.25 (c0.16,$H_2O$) | 367.1011 | 367.1009 | -0.425 |
| Glc6FGlc | 35.3 (8.8 mg) | +132.5 (c0.16,$H_2O$) | 367.1011 | 367.1009 | -0.562 |

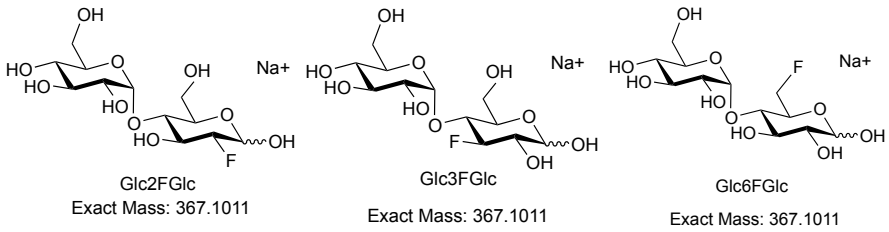


**Figure 3.29** Structures of deoxyfluoromaltose derivatives (Glc2FGlc (2-deoxy-2-fluoromaltose), Glc3FGlc (3-deoxy-3-fluoromaltose) and Glc6FGlc (6-deoxy-6-fluoromaltose)) and their calculated molecular weights.

### 3.8.2.2 Nuclear Magnetic Resonance (NMR)

The purified deoxyfluoromaltose derivatives from gel filtration were also analyzed by $^{19}$F-NMR and $^{1}$H-NMR to elucidate their structures. The $^{19}$F-NMR pattern of Glc2FGlc (2-deoxy-2-fluoromaltose) (Figure 3.30(A)), Glc3FGlc (3-deoxy-3-fluoromaltose) (Figure 3.32(A)) and Glc6FGlc (6-deoxy-6-fluoromaltose) (Figure 3.34(A)) showed two peaks of β-anomer and α-anomer of products. The $^{1}$H-NMR results of Glc2FGlc (2-deoxy-2-fluoromaltose)(Figure 3.30(B)), Glc3FGlc (3-deoxy-3-fluoromaltose)(Figure 3.32(B)) and Glc6FGlc (6-deoxy-6-fluoromaltose) (Figure 3.34(B)) confirmed the structure of deoxyfluoromaltose derivatives. Comparison of $^{19}$F-NMR of fluoromaltose derivative with fluroglucose derivatives showed spectrum change. (Figures 3.31, 3.33 and 3.35)

A

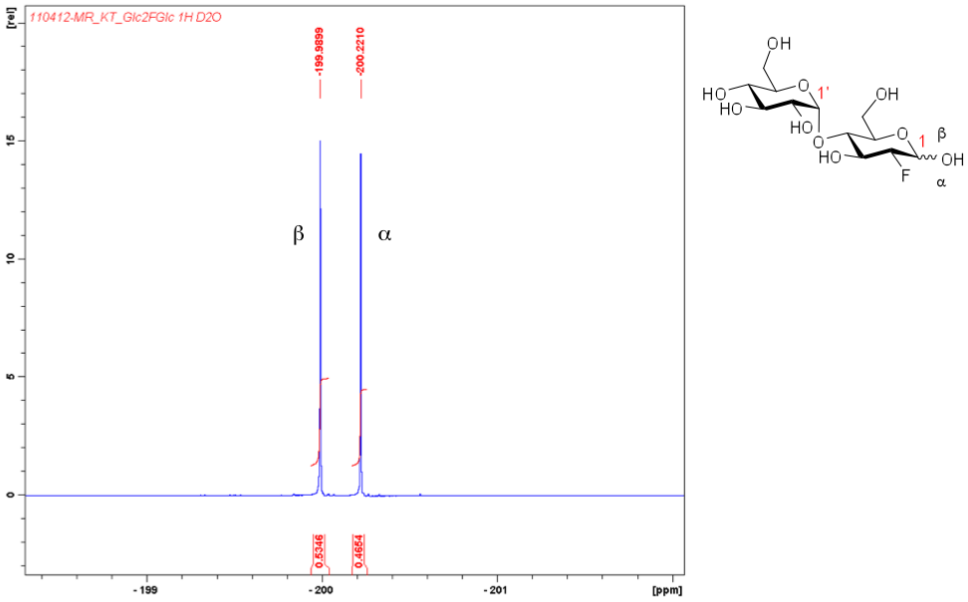


B

**$^{19}$F NMR Spectrum (ppm): -200.0 (0.53F, β-anomer), -200.2 (0.47F, α-anomer).**

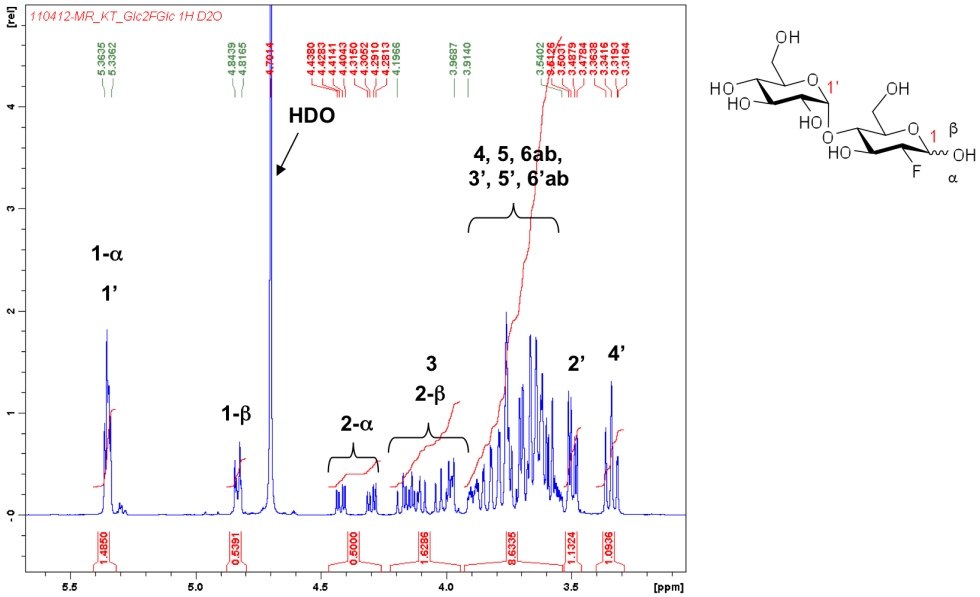


**$^{1}$H NMR Spectrum (ppm): 5.36-5.34 (1.5H, m, H1', H1-α), 4.84-4.82 (0.5H, m, H1-β), 4.35 (0.5H, ddd, $J_{2,F}$ = 49.3 Hz, $J_{2,3}$ = 9.43 Hz, $J_{2,1}$ = 4.0 Hz, H2-α), 4.20-3.97 (1.5H, m, H2-β, H3), 3.91-3.54 (8H, m, H4, H5, H6ab, H3', H5', H6'ab), 3.50 (1H, dd, $J_{2',3'}$ = 10.0 Hz, $J_{2',1'}$ = 3.90 Hz, H2'), 3.34 (1H, dd, $J_{4',5'}$ = $J_{3',4'}$ = 9.4 Hz, H4').**

**Figure 3.30** The $^{19}$F-NMR (A) and $^{1}$H-NMR (B) spectrum of the product Glc2FGlc (2-deoxy-2-fluoromaltose)

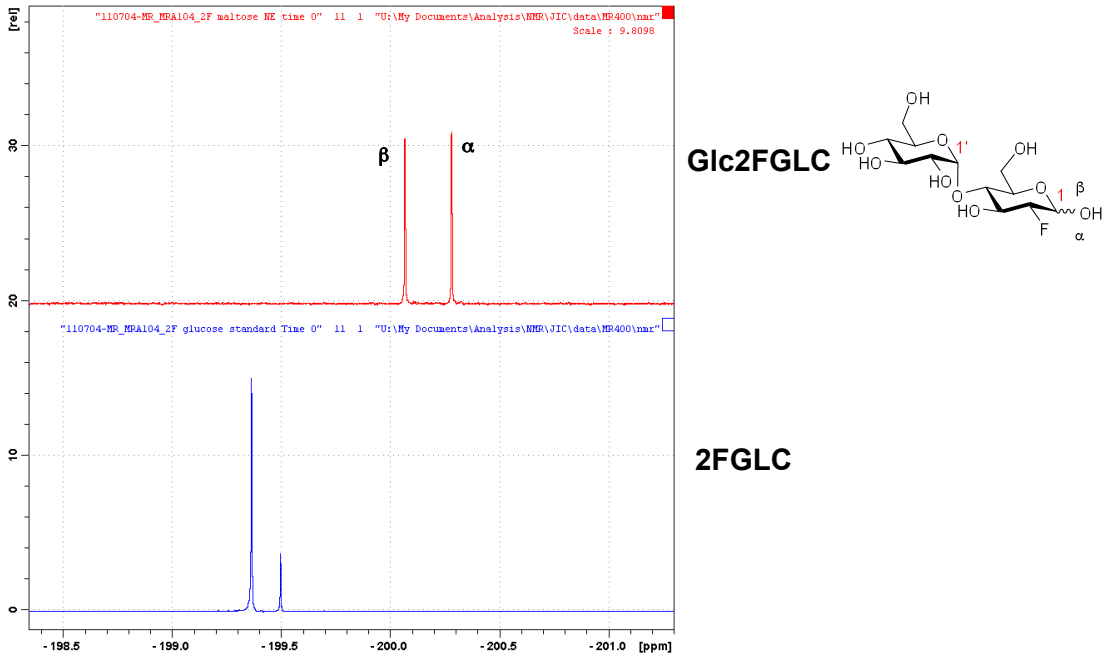


**Figure 3.31** Comparison of $^{19}$F-NMR spectrum of the product Glc2FGlc (2-deoxy-2-fluoromaltose) and 2FGlc (2-deoxy-2-fluoro-D-glucose)

A

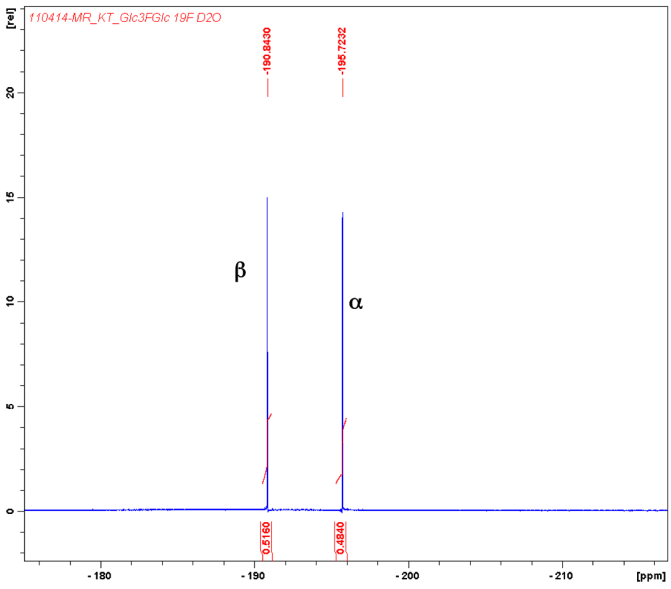


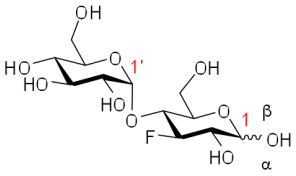


B

**$^{19}$F NMR Spectrum (ppm): -190.8 (0.52F, β-anomer), -195.7 (0.48F, α-anomer).**

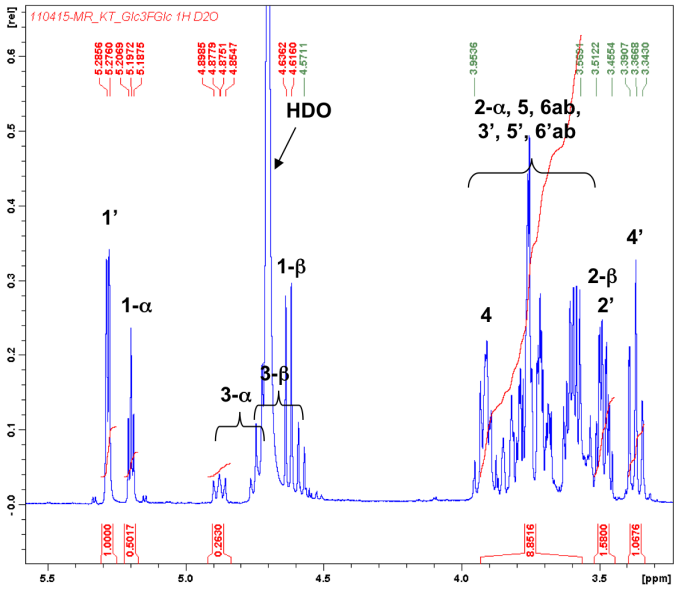


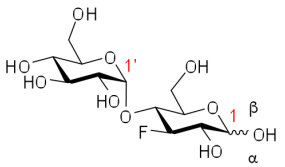


**$^{1}$H NMR Spectrum (ppm): 5.28 (1H, d, $J_{1',2'}$ = 4.03 Hz, H1'), 5.20 (0.5H, dd, $J_{1,2}$ = $J^{1}_{1\alpha,F}$ = 3.88 Hz, H1-α), 4.81 (0.5H, ddd, $J_{2,3}$ = 8.20 Hz, $J_{3,4}$ = 9.32 Hz, $J_{3,F}$ = 53.29 Hz, H3-α), 4.66 (0.5H, ddd, $J_{2,3}$ = $J_{3,4}$ = 8.76 Hz, $J_{3,F}$ = 52.56 Hz, H3-β), 4.62 (0.5H, d, $J_{1\beta,2}$ = 8.08 Hz, H1-β), 3.95-3.57 (8.5H, H2-α, H4, H5, H6ab, H3', H5', H6'ab), 3.51-3.46 (1.5H, H2-β, H2'), 3.37 (1H, dd, $J_{3',4'}$ = $J_{4',5'}$ = 9.23 Hz, H4').**

**Figure 3.32** The $^{19}$F-NMR (A) and $^{1}$H-NMR (B) spectrum of the product Glc3FGlc (3-deoxy-3-fluoromaltose)

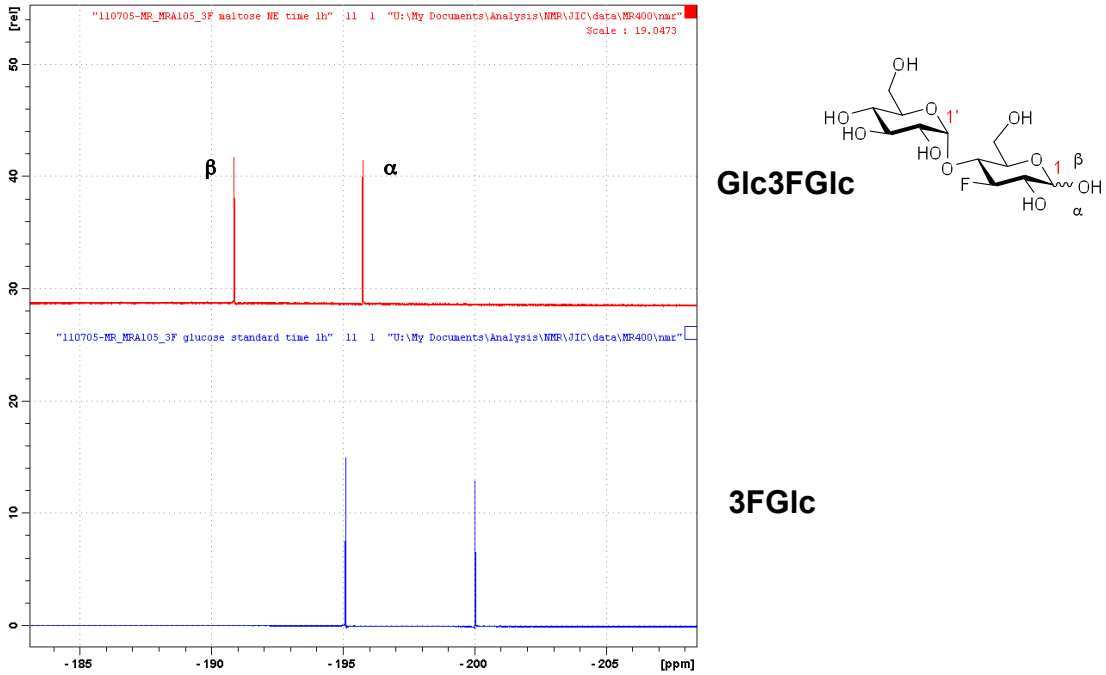


**Figure 3.33** Comparison of $^{19}$F-NMR spectrum of the product Glc3FGlc (3-deoxy-3-fluoromaltose) and 3FGlc (3-deoxy-3-fluoro-D-glucose)

A

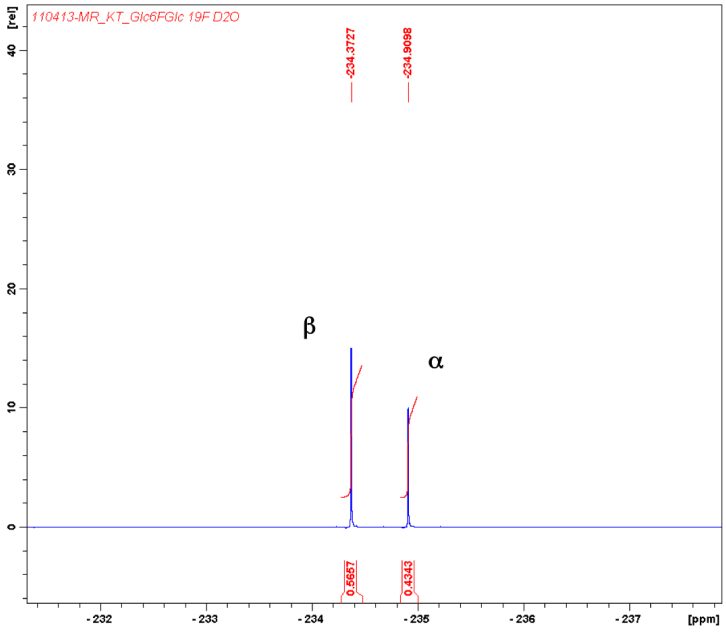


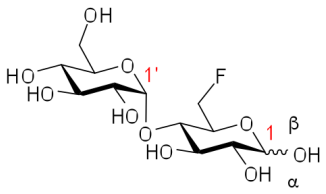


**$^{19}$F NMR Spectrum (ppm): -234.4 (0.57F, β-anomer), -234.9 (0.43F, α-anomer).**

B

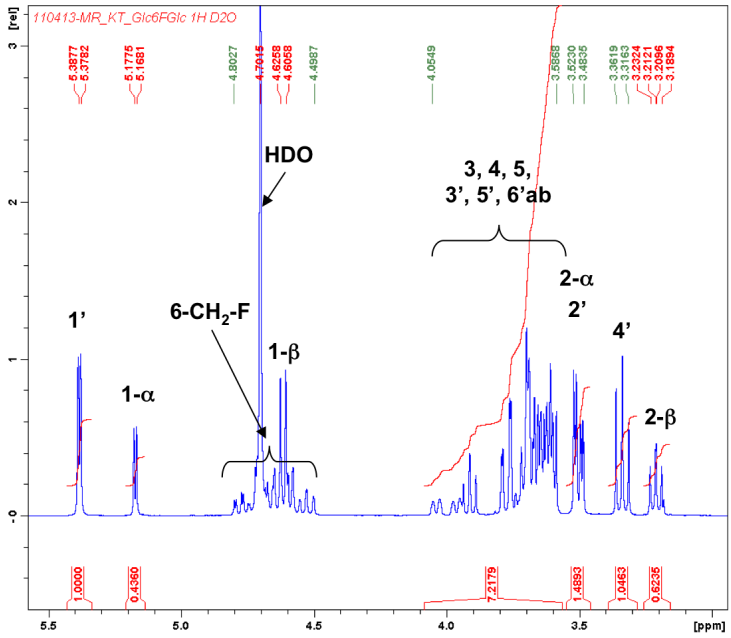


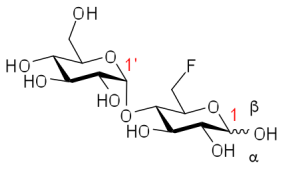


**$^{1}$H NMR Spectrum (ppm): 5.38 (1H, d, $J_{1',2'}$ = 3.8 Hz, H1'), 5.17 (0.4H, d, $J_{1,2}$ = 3.8 Hz, H1-α), 4.80-4.50 (2H, m, $H_2$6), 4.62 (0.6H, d, $J_{1,2}$ = 8.0 Hz, H1-β), 4.05-3.59 (7H, m, H3, H4, H5, H3', H5', H6'ab), 3.52-3.48 (1.4H, m, H2-α, H2'), 3.34 (1H, dd, $J_{4',5'}$ = $J_{3',4'}$ = 9.5 Hz, H4'), 3.21 (0.6H, dd, $J_{1,2}$ = 8.0 Hz, $J_{2,3}$ = 9.1 Hz, H2-β).**

**Figure 3.34** The $^{19}$F-NMR (A) and $^{1}$H-NMR (B) spectrum of the product Glc6FGlc (6-deoxy-6-fluoromaltose)

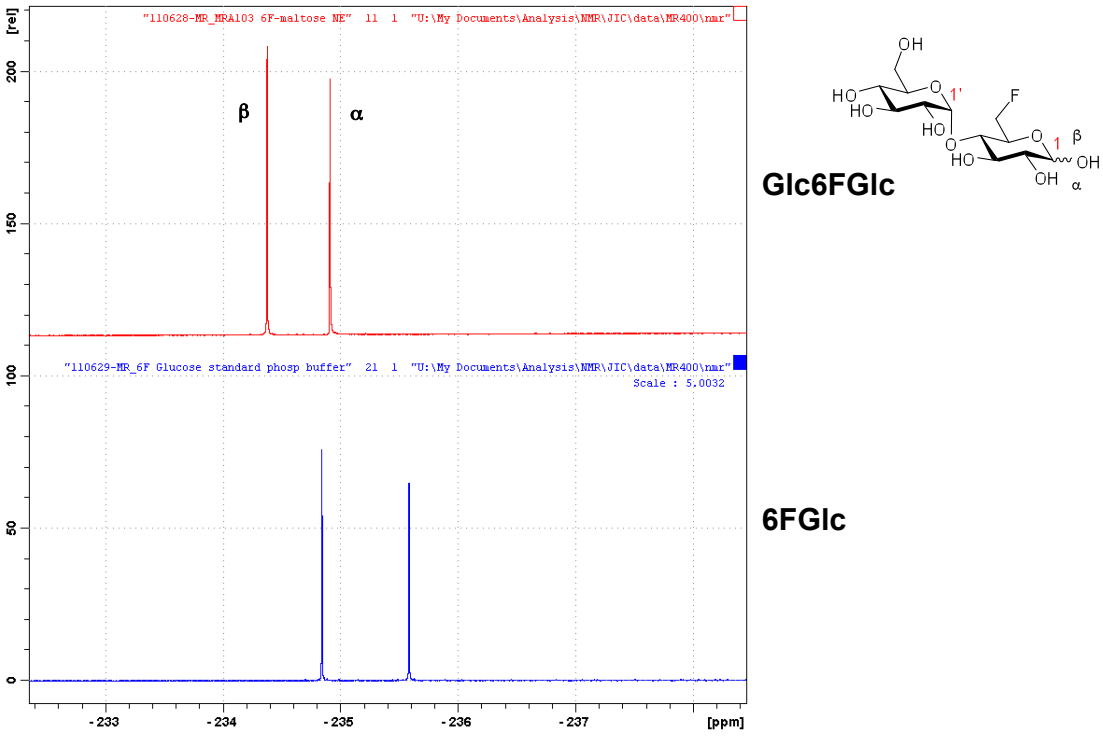


**Figure 3.35** Comparison of $^{19}$F-NMR spectrum of the product Glc6FGlc (6-deoxy-6-fluoromaltose) and 6FGlc (6-deoxy-6-fluoro-D-glucose□

# CHAPTER IV

# DISCUSSION

Starch metabolism is a very important biological precess in plants. It involves the processes from photosynthesis to carbohydrate distribution and storage in non-photosynthetic organs. Many enzymes are engaged in starch synthesis and breakdown. Studies on the functions of the enzymes involved would lead to the understanding of starch metabolism. The role of several enzymes such as starch synthase, starch branching enzymes and starch debranching enzymes have been reported in many plants including cassava (Salehuzzaman *et al.* 1993). Disproportionation enzymes or 4-α-glucanotransferases have been reported in *Arabidopsis* and potatoes (Critchley et al. 2001; Stettler et al. 2009)(Takaha et al. 1993) but it is still not clear of its role in starch metabolism. There has not been any reported on D-enzyme is cassava. Here we report the cloning and expression of D-enzyme from cassava tubers in parallel with D-enzyme from *Arabidopsis*. Since there was reported on the ability of D-enzyme to produce cycloamyloses, we also investigate the use of the transformant enzymes in producing useful products for industrial applications.

## 4.1 Structures of AtDPE1 and MeDPE1

### 4.1.1 DNA sequencing and deduce amino acid sequence

The phylogenetic tree of GH77 family (DPE1, DPE2 and amylomaltase) showed that DPE can be separated in two groups (DPE1 and DPE2) sharing 16% identity. AtDPE1 and MeDPE1 were located in DPE1 group with 71% identity in

amino acid sequence. Amino acid of sequences AtDPE1 and MeDPE1 were close to previous report of DPE1 from potato (StDPE1), sharing identity at 59% and 70.9% respectively. In phylogenetic tree, amylomaltase from *Thermus aquaticus* ATCC 33923 and *Aquifex aeolicus* VF5 were located between the DPE1 and DPE2 groups but closer to DPE1 group. The DPE1 group contained GH77 domain and chloroplast signal peptide at N-terminal. Signal peptide was searched on the deduced amino acid sequence of MeDPE1 and AtDPE1 using ChloroP v1.1. This program can predict signal peptide at N-terminal. The amino acid sequence of mature enzyme was used to prepare gene for cloning and expression because in nature the signal peptide was cut off during its transfer to chloroplast. The recombinant enzymes should be close to wild type. The signal peptide was not present in the structure of DPE1 from potato (PDB ID : 1X1N). The deduced amino acid of MeDPE1 and AtDPE1 contained six histidine residue for purification Ni affinity chromatography.

### 4.1.2 Protein structure

There were previous reports on the structure of enzymes in the GH77 family using X-ray crystallography technique (Table 4.1). The only report on crystal structure of DPE1 was from potato which did not cover the study on explanation of the protein structure or the mechanism of DPE1. The structure of AtDPE1 and MeDPE1 were predicted using structure of DPE1 from potato (StDPE1) as a template (PDB ID : 1X1N). Prediction program “SWISS-MODEL SERVER” (http://swissmodel.expasy.org) was used. The protein structure of enzyme in GH77 family contains domain A inserted with subdomains B1, B2 and B3. The 250s loop inserted

in domainA is a unique function of this GH77 family. Domain A was a core domain TIM barrel $(\beta/\alpha)_8$ core structure which was commonly found in α-amylase family. Comparison of the structure of amylomaltase, StDPE1, predicted AtDPE1 and predicted MeDPE1 did not show major difference. We compared the predicted structure to amylomaltase to predict the active site and mechanism of this enzyme.

### 4.1.3 Active sites

The active site of amylomaltase was reported (Przylas et al. 2000). Three catalytic amino acid residues (Asp293, Glu340 and Asp395) played an important catalytic role in transglycosylation mechanism. The active sites of AtDPE1 and MeDPE1 were defined using alignment based on deduced amino acid sequence and predicted protein structure. The three active sites (two Asp and one Glu residues) of MeDPE1 and AtDPE1 were shown in Figure 3.8. This active site should play an important role in disproportionating activity via covalent intermediate that commonly found in the α-amylase family (Figure 4.1).

**Table 4.1** Previous reports on protein crystal structure of GH77 family

| Organism | PDB ID | Substrate |
|---|---|---|
| **Amylomaltase** | | |
| *Aquifex aeolicus* VF5 | 1TZ7 | w/o substrate |
| *Thermus aquaticus* ATCC 33923 * | 1CWY<br>1ESW | w/o substrate<br>complex with acarbose |
| *Thermus brockiamus* | 2X1I | w/o substrate |
| *Thermus Thermophilus* TB8 | 2OWX<br>2OWC<br>2OWW | w/o substrate<br>complex with acarbose<br>acarbose and 4-deoxyglucose |
| **DPE1** | | |
| *Solanum tuberosum (Potato)* | 1X1N | w/o substrate |

* First protein crystal have been published.

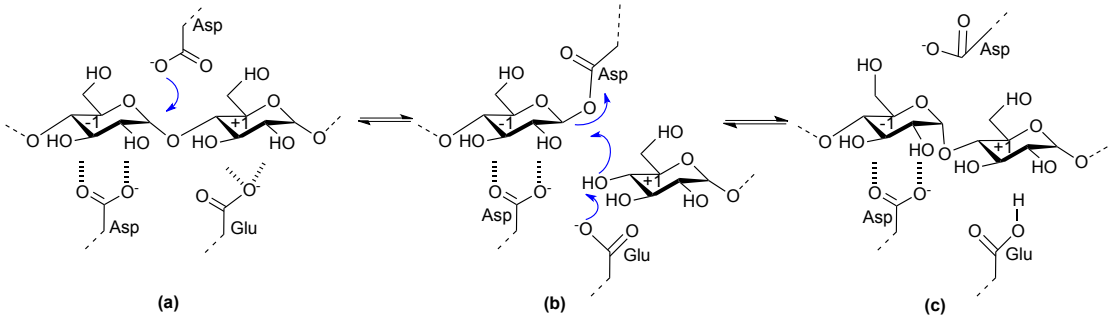


**Figure 4.1** Scheme for the mechanism of the disproportionating activity of DPE1. The reaction proceeded via a covalent intermediate (b). glucose -1 and +1 position were in the cleavage site at non reducing end and reducing end, respectively).

**4.2 Protein expression and purification**

MeDPE1 was expressed in *E.coli* DH5α using expression vector pTrcHis2C containing a *trc* promoter. Inducing with lactose at 16°C, the enzyme was found as soluble enzyme inside the cells (intracellular enzyme). While expression at 37°C was observed as inclusion body. When MeDPE1 was expressed in expression vector containing T7 promoter (pET21-D vector), inclusion body was formed both at 16 and 37°C. AtDPE1 was expressed in *E.coli* BL21(DE3) star™ using expression vector pET151/D-TOPO™ containing a T7 promoter. Enzyme induction was performed using lactose at 16°C to avoid formation of inclusion body. The enzyme was found as soluble enzyme inside the cells (intracellular enzyme). Comparison of protein expression level between AtDPE1 and MeDPE1 showed that expression of AtDPE1 produced five folds higher activity than MeDPE1 because AtDPE1 was expressed as soluble enzyme under T7 promoter. Although protein and enzyme expressed from transformant of *Arabidopsis* were much higher than MeDPE1. The yield and fold of purification were much lower. This may be due to more contaminating protein were presence in the enzyme preparation from *Arabidopsis*. Although high amount of protein (>90%) was removed though the two column chromatographies, high amount of enzyme activity was also lost (~60%). There was reported that DPE1 from potato was expressed using *trc* promoter at 15°C and inclusion body was formed at 37°C (Takaha et al. 1993) and DPE1 from rice was also expressed using *tac* promoter at 18°C (Akdogan et al. 2011). To express this group of enzymes, the strong promoter such as T7 promoter must be avoided because inclusion body was formed.

## 4.3 Characterization of the enzymes

### 4.3.1 Molecular weight

The results from gel filtration chromatography (Figure 3.10) and SDS-PAGE (Figure 3.12) showed that MeDPE1 and AtDPE1 should have the structure of homodimer with subunit molecular weight of 61 kDa for MeDPE1 and 64 kDa for AtDPE1. SDS-PAGE showed appearance of fade contaminated bands but in native gel there was only one band which stained positive on glycogen gel (Figure 3.14). The molecular weight and quaternary structures of other D-enzyme were shown in Table 4.2. DPE1 from potato and pea were also reported to show homodimer structure and size of their subunits were in the same range.

**Table 4.2** Molecular weight of 4-α-glucanotransferases.

| Organism | Molecular weight in each subunit | subunit | References |
|---|---|---|---|
| DPE1 | | | |
| Cassava | 61 kDa | 2 | This study |
| *Arabidopsis* | 64 kDa | 2 | This study |
| Potato | 65 kDa | 2 | (Takaha et al. 1993) |
| Pea (*Pisum sativum* L.) | 50 kDa | 2 | (Kakefuda et al. 1989) |
| Wheat endosperm | 54 kDa | 1 | (Bresolin et al. 2006) |
| Amylomaltase | | | |
| *Thermus aquaticus* ATCC 33923 | 57 kDa | 1 | (Terada et al. 1999; Przylas et al. 2000; Przylas et al. 2000) |
| *Thermotoga maritima* | 53 kDa | 1 | (Liebl et al. 1992) |

### 4.3.2 Disproportionating reactions

Recombinant MeDPE1 and AtDPE1 were shown to catalyzed the transfer maltosyl unit from maltotriose to another maltotriose to produce maltopentaose and glucose in early stage of the reaction. At longer incubation time. Oligosaccharides with DP from 5,7,9,11, n+2 should be formed resulting from addition of maltosyl units on the available oligosaccharides. The activity of these recombinant AtDPE1 and MeDPE1 were performed using maltotriose ($Glc_3$) as sole substrate and the oligosaccharide products detected by HPAEC-PAD (Figure 3.19) or by monitoring the released of glucose in the reaction same as previous reported of DPE1 from potato (Takaha et al. 1993). When we used maltotriose as substrate, the oligosaccharide patterns were totally different in DPE1, DPE2 and amylomaltase. DPE1 transferred maltosyl unit from maltotriose. In HPAEC-PAD result, AtDPE1 seemed to be more active than MeDPE1 because maltotriose decreased significantly. However, the glucose maltopentaose and maltoheptaose peaks were lower than observed for MeDPE1. It was speculated that these primary products could act as new substrate resulting in formation of longer oligosaccharides not detected in the HPAEC-PAD profiles. Amylomaltase can transfer glucosyl unit from maltotriose. This DPE1 property was unique in GH77 family because amylomaltase and DPE2 transferred glucosyl unit while DPE1 transferred maltosyl unit rather than glucosyl unit. DPE2 required longer oligosaccharide such as glycogen to act as donor (Akdogan et al. 2011). DPE1 can also transfer maltodextrin (donor) to glycogen (acceptor) to form longer chain act as amylose at the non-reducing end of glycogen. The longer chain

(amylose) can be observed by using iodine staining on activity gel (Figure 3.14) same as previously reported on DPE1 from *Triticum aestivum* (Bresolin et al. 2006) and *Chlamydomonas reinhardtii* (Colleoni *et al.* 1999) that showed activity in glycogen staining with iodine. Glycogen in the gel did not bind iodine in its molecule well because it contained high degree of branching with shorter oligosaccharides resulting in yellow background on the gel. When the gel was incubated with DPE1 and maltodextrins, the enzyme transferred maltodextrins to the branches of glycogen. The longer oligosaccharides produced in the branches can form helices which can bind $I_2$ inside at the DPE1 band, producing dark band on yellow background of glycogen.

### 4.3.3 Effect of pH and temperatures

The pH optimum of both enzymes were at 6-8 at 37°C in 0.1 M MOPS and phosphate buffer. In Tris-HCl buffer, there was small decrease in activity on the DPE1 activity at pH 7, 8 and 9. At pH 3-4, disproportionating activity was not observed and activities decrease at pH 9-10. The optimum pH of the DPE1 from other plants had been reported (Table 4.3). The optimum pH's of plant DPE1 were observed in the neutral range of 6.5-8 while bacterial amylomaltase showed optimum pH at acidic or alkaline pH. This may be due to the nature of plants which have more sophisticated physiological system and usually prefer less hashed condition. Bacteria were unicellular organisms which can withstand more acidic or alkaline conditions, thus their enzymes work well in these pH's compared to higher organism like plants. The optimum temperature of AtDPE1 and MeDPE1 were at 35-40°C. The DPE1 from rice was reported to have optimum temperature at 30°C. MeDPE1 and AtDPE1 retained activity up to 40-50% at 25°C and 37°C for 16 hours. Cassava is well known from its drought tolerance including hot weather. Thus, its enzymes can withstand high temperature.

**Table 4.3** Optimum pH of 4-α-glucanotransferases.

| Organism | Optimum pH | Buffer | References |
|---|---|---|---|
| DPE1 | | | |
| Cassava | 6-8 | MOPS and phosphate | This study |
| *Arabidopsis* | 6-8 | MOPS and phosphate | This study |
| *Arabidopsis* leaf | 6.6 | sodium acetate | (Lin et al. 1988) |
| Pea (*Pisum sativum* L.) | 7.5-8.0 | - | (Kakefuda et al. 1989) |
| Rice (*Oryza sativa*) | 7.0 | Sodium phosphate | (Akdogan et al. 2011) |
| Amylomaltase | | | |
| *Thermus aquaticus* ATCC 33923 | 5.5-6.0 | - | (Terada et al. 1999) |
| *Thermus thermophilus* HB8 | 5.5-6.0 | - | (Kaper et al. 2007) |
| *Synechocystis sp.* PCC 6803 | 7.0 | 50 mM phosphate | (Lee *et al.* 2009) |
| *Thermus brockianus* | 6.0 | sodium citrate | (Bang et al. 2006) |
| *Thermotoga maritima* | 7.0-8.0 | Phosphate | (Liebl *et al.* 1992) |
| *Thermus aquaticus* YT-1 | 7.5 | - | (Park *et al.* 2007) |

### 4.3.4 Kinetic parameters

Maltotriose was used as substrate from determined kinetic parameter of MeDPE1 and AtDPE1 because of glucose product from reaction was immediately measure by hexokinase-G6P dehydrogenase method. Maltopentaose product can became a acceptor for transfer maltosyl unit from maltotriose to product glucose unit. In kinetic determination of this enzyme we used maltotriose as substrate. The initial velocity was determined to be one minute because incubation at longer time may be interfered by the initial maltopentaose ($Glc_5$) product become new acceptors of the reaction. The $K_m$ of AtDPE1 and MeDPE1 were calculated at 29.9 mM and 39.7 mM maltotriose, respectively. The $k_{cat}/K_m$ values of AtDPE1 were 1231 $min^{-1}$ which was 1.4 fold higher than MeDPE1. The result suggested that maltotriose bound to active site of AtDPE1 better than MeDPE1. AtDPE1 was an enzyme in the leaves which involved in the formation of transitory starch and also breakdown of starch for mobilization to non-photosynthetic organs, while MeDPE1 was a D-enzyme from cassava tubers which was mainly involved in starch synthesis for storage. Therefore, AtDPE1 worked better with small sugar molecules like maltotriose in the temporary sugar storage and sugar mobilization process in the leaves while MeDPE1 may play role in producing oligosaccharides of suitable length for amylose and amylopectin formations in the tubers.

### 4.3.5 Acceptor specificity

Oligosaccharide array was used to monitor the substrate specific of the DPE1. The 81 types of oligosaccharide print on each membrane were used as an acceptor

such as α-L-arabinose, β-D-galactose, β-D-mannose, etc printed on membrane type I. Lactose, β-D-xylobiose, D-galactose, etc printed on membrane type II (appendix I). This method is the fast tool for screening various types of acceptors present on each type of acceptors on the membrane. The advantage of this technique is fast screening of various carbohydrate acceptors in one reaction. The type of acceptor can be matched to the physiological function of each enzyme. In the monitor the product, the sugar donor labelled with radio active was required. Because maltotriose labelled with radioactive was not available commercially, glycogen containing $^{14}$C-glucose at the non-reducing end was used as donor. The $^{14}$C-glucose glycogen was synthesized using PHS2 (cytosolic α-1,4-glucan phosphorylase). This enzyme can transfer $^{14}$C-glucose from $^{14}$C-Glucose-1-phosphate to the non reducing end of glucose chain in glycogen(Lu et al. 2006). On the membrane incubated with AtDPE1, signals were detected at blocks A8 and B8 on membrane type I and G7, H7, G8 and H8 on membrane type II . All of these were glucose connected with α-1,4-glucan. However, On the membrane incubated with MeDPE1, no signal was detected. Normally, to detect signal using phosphor Imaging required only 2-3 hours but in our experiment the spot with high intensity observed for AtDPE1 was detected at 10 days incubation. The results indicated that AtDPE1 was specific to glucose linked by α-1,4 glucosidic bond e.g. maltotriose, maltopentaose and not specific to other sugars. DPE1 in nature seemed to be involved in only the transfer of glucans via α-1,4 glycosidic bond to acceptor glucose unit. Glycogen may be too bulky compared to amyloses and amylopectins, the carbohydrates the two enzymes encountered in nature ,thus weak

signals detected on the membrane. AtDPE1 may also be more active in the transfer process than MeDPE1 as observed in the kinetic results.

### 4.3.6 Cycloamylose production

It was found that enzymes in GH77 family can catalyze intramolecular transglycosylation reaction (cyclization) to produce large ring cyclodextrins, giving better yield of large ring cyclodextrins than using cyclodextrin glycosyltransferase (CGTases, EC 2.4.1.19) (Takaha et al. 1996). In GH77 family, 4-α-glucanotransferase can be classified into two groups based on the source of enzymes and report on cycloamylose production. The first group was amylomaltase from bacteria *Thermus aquaticus* ATCC 33923 (Terada et al. 1999), *Synechocystis* sp. PCC 6803 (Lee *et al.* 2009) which produced large ring cyclodextrins with DP ≥ 22, *Pyrococcus kodakaraensis* KOD1 (Tachibana *et al.* 2000) can produce large ring cyclodextrins with DP ≥ 16. Second group was DPE1 from plants, the potato DPE1 produced large ring cyclodextrins with DP ≥ 17 (Takaha et al. 1996). In this report production of LR-CDs by with AtDPE1 and MeDPE1 with amylose as starting material were investigated. The reaction mixture were treated with glucoamylase (Exo-1,4-α-glucosidase) which can eliminate remaining amylose but can not hydrolyses the cycloamylose. Fractionation of cycloamylose products was performed with ultrafiltration technique which separated the remaining amylose substrate and small oligosaccharides which can interfere in the detection of cycloamyloses. From HPAEC-PAD analysis, products with minimum degree of polymerization at 17 and 18 to larger cycloamyloses were observed from reaction mixture of AtDPE1 and

MeDPE1, respectively. This corresponded to previous report on production of LR-CDs by DPE1 from potato (Takaha et al. 1996). Analysis by MALDI-TOF-MS showed the mass of cycloamyloses corresponding to previous report on mass of cycloamyloses (Endo 2011). Quantitative analysis can not be done on MALDI-TOF-MS because the technique depended on the ionization properties of cycloamyloses. Large molecules produced lower ionization than small molecules and MALDI-TOF-MS can not ionize large oligosaccharides (DP > 34) while HPAEC-PAD can detect cycloamyloses with DP ≥ 50. Cycloamylose production by MeDPE1 and AtDPE1 were performed at room temperature (25°C) while amylomaltase from *Thermus aquaticus* ATCC 33923 was incubated at 70°C (Terada et al. 1999). MeDPE1 and AtDPE1 should be a convenient alternative source of enzymes for cycloamylose productions. The cycloamylose produced in our experiment was primarily tested for complexation with polyaniline (figure 3.24) successfully. The result of inclusion complex between polyaniline with cyclodextrins were also reported (Yuan *et al.* 2003). Therefore, the cycloamyloses produced from MeDPE1 and AtDPE1 should be further tested for inclusion complex formation with chemicals or drug compounds for industrial and medical applications.

**4.4 Production of useful oligosaccharides from 4-α-glucanotransferases**

There were many reports on the use of 4-α-glucanotransferases in producing useful products from their transglycosylation reactions (Tachibana et al. 2000) Since, there were many recombinant enzymes at hand, experiments were performed to investigate some useful products which could be obtained. In section 3.6, the

production of cycloamyloses were already investigated. The transglycosylation activity of 4-α-glucanotransferases enzyme (amylomaltase from *E.coli,* MeDPE1 and AtDPE2) was performed using glycogen as donor and deoxyfluoroglucose derivatives (2-deoxy-2-fluoro-D-glucose (2FGlc), 3-deoxy-3-fluoro-D-glucose (3FGlc), 4-deoxy-4-fluoro-D-glucose (4FGlc) and 6-deoxy-6-fluoro-D-glucose(6FGlc)) as acceptor to produce deoxyfluoroglucose derivatives. Figure 4.2 showed proposed reaction of glycogen and 2FGlc, the product was a longer oligosaccharide containing deoxyfluoroglucose at the reducing end. Glycogen was chosen as donor because it contained many non-reducing ends and more soluble in water than soluble starch. After the reaction glycogen was removed by ultrafiltration technique (Amicon centrifugal filters (30 kDa cut off)). Glucose cannot transfer to 4' position of 4-deoxy-4-fluoro-D-glucose since it was occupied by fluorine group. TLC analysis revealed that reactions with MeDPE1 and amylomaltase showed products with less intensity compared to AtDPE2 reaction mixture. AtDPE1 showed reaction pattern same as MeDPE1 (data not shown). AtDPE2 seemed to add only one glucosyl residue to the acceptor and then reaction stopped. AtDPE2 was able to use glycogen as substrate because it had two starch binding domains at the N-terminal (Steichen et al. 2008). In physiological condition AtDPE2 transfers glucose unit to arabinogalactan (similar to glycogen) (Weise et al. 2011). Since, it showed higher transglycosylation products on TLC, AtDPE2 reaction mixture was chosen for large scale preparation. Gel filtration chromatography technique using TSK-HW40S column was successful used to separate fluoro-oligosaccharide products from deoxyfluoroglucose derivatives.

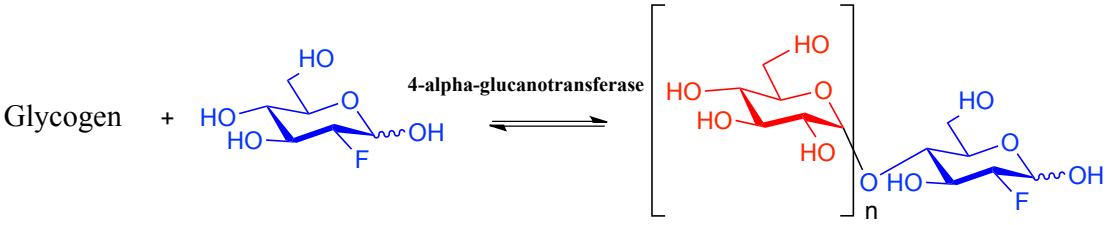


**Figure 4.2** Scheme for the reaction of transglycosylation activity of 4-α-glucanotransferase using glycogen as donor and 2-deoxy-2-fluoro-D-glucose as acceptor.

To detect the presence of anomeric mixtures in hemiacetal forms are more complicated. It is difficult to use mass spectrometry detection. One way to monitor the carbohydrate is using radioisotope labeling (e.g. $^{3}H$, $^{14}C$, $^{18}F$) combined with autoradiograph and stable isotope (e.g. $^{2}H$, $^{13}C$, $^{15}N$) combined with NMR and Mass spectrometry or using sugar with chromophore/fluorophore detectable by UV/VIS or fluorimetric detection (Roscher *et al.* 2000). Derivatisation of sugar substrate with fluorine-19 and the use of $^{19}F$ NMR spectroscopy offers another attractive possibility to enhance the tractability of sugars in biological systems. Fluorine NMR offers a simple and powerful tool for monitoring enzyme mediated transformations (Andre *et al.* 2001). In NMR spectroscopy, $^{19}F$ NMR provides a highly sensitive probe with no background signal. Line broadening and chemical shift are highly sensitive to changes in solvent, environment and conformation (Belle *et al.* 2009). Fluorinated analogues of carbohydrate substrates are useful tools in mapping the interaction with the active site and enzymatic mechanism of carbohydrate processing enzymes (Withers Stephen *et al.* 1988). Fluorine has often been considered a useful analog for hydroxyl groups because it is the same size, highly electronegative and contains non-bonded electron pairs similar to oxygen.

The fluoro-oligosaccharide products obtained in our experiment was confirmed as deoxyfluoromaltose using high resolution mass spectrometry, $^{19}F$-NMR and $^{1}H$-NMR technique. The deoxyfluoromaltose derivatives can be used as substrate for easy monitoring of enzyme mechanism by $^{19}F$-NMR technique. One of the

application of the fluoromaltose derivatives was monitoring the reaction mixture using $^{19}$F-NMR. The substrate for primary test was performed using the fluoromaltose derivatives as substrate for trehalose synthase which can convert maltose (two glucose units connected with α-1, 4 glucosidic bond) to trehalose (two glucose units connected with α, α-1, 1 glucosidic bond). The products were followed by $^{19}$F-NMR technique. When 2Fmaltose was used as substrate, specific conversion to trehalose was observed with α-anomer of maltose. When 3Fmaltose was used as substrate, hydrolysis of 3Fmaltose to glucose was observed. Reaction with 6Fmaltose showed the hydrolysis to glucose and conversion to trehalose (unpublished data).

**4.5 Possible roles of MeDPE1 and AtDPE1**

The functions of DPE1 in vivo were reported in two aspects. Firstly DPE1 was reported to be involved in degradation of transitory starch at night (Critchley et al. 2001). It was proposed that DPE1 used maltotriose from degradation of starch by β-amylase to produce maltopentaose ($Glc_5$) which can be substrate for β-amylase again. In this experiment, MeDPE1 and AtDPE1 were shown to transfer of maltosyl group from maltotriose ($Glc_3$) and released glucose which was monitored by hexokinase-G6P dehydrogenase method. From HPAEC-PAD analysis on the oligosaccharide patterns, MeDPE1 produced oligosaccharides with degree of polymerization (DP) in the increasing order of n+2 i.e. 1, 3, 5. This degree of polymerization was totally different from amylomaltase reaction which showed the degree of polymerization (DP) in the increasing order of one glucose unit i.e.1, 2, 3, 4, 5, 6, 7, 8. While DPE2 can not catalyze the reaction when only maltotriose in the reaction mixture. This

result corresponded to that reported in the wild type of DPE1 from *Arabidopsis* leaf (Lin *et al.* 1988), amylomaltase from *Thermus aquaticus* ATCC 33923(Terada et al. 1999) and DPE2 from rice (Akdogan et al. 2011). Secondly, Colleoni *et al* preposed that DPE1 from *Chlamydomonas reinhardtii* could be involved in amylopectin structure and starch biosynthesis (Colleoni et al. 1999). DPE1 transferred maltosyl unit from oligosaccharides to glycogen or amylopectin. In the experiment on native gel electrophoresis (Figure 3.14), MeDPE1 and AtDPE1 showed the transfer of glucan unit from maltodextrin to glycogen which was detected as blue band on yellow background when stained with iodine solution. This result indicated that both enzymes can transfer glucan to glycogen to produce longer glycogen chain detected by iodine stain. The result on native gel corresponded to previous report on native gel of crude enzyme of DPE1 from *Arabidopsis thaliana* which showed dark band when stained with iodine (Critchley et al. 2001). DPE1 from *Chlamydomonas reinhardtii* also showed dark band of DPE1 activity (Colleoni et al. 1999). In vivo, both enzymes may transfer oligosaccharides to amylopectin in starch synthesis pathway.However, AtDPE1 and MeDPE1 exhibited both similar and different characteristics.

From the overall results, it could be concluded that AtDPE1 and MeDPE1 were from the same family. Although their biochemical properties were quite similar there were some characteristics indicated that they may have different functions according to the organs they were originated from AtDPE1, which originated in leaves, may play wider roles, involved in both transitory starch synthesis and transitory starch breakdown for carbohydrate mobilization to non-photosynthetic

organs. On the other hand, MeDPE1 originated from storage organs (cassava tubers) was probably involved mainly in starch biosynthesis. The cloning and expression of MeDPE1 was the first report on cassava DPE1. This work together with previous report on starch branching enzymes, starch synthase and future study on other starch metabolizing enzymes such as debranching enzymes (isoamylase and pullulanase) would lead to the understanding of starch metabolism in cassava. In addition, the possible use of the recombinant enzymes in production of cycloamyloses for industrial applications is also promising.

# CHAPTER V

# CONCLUSION

1. The DPE1 genes from *Arabidopsis thalana* (*atdpe1*) and *Manihot esculenta* Crant (*medpe1*) were cloned, expressed and characterized.
2. Deduced amino acids of both enzyme showed 2 Asp and 1 Glu as catalytic residues same as amylomaltase from *Thermus aquaticus* ATCC 33923.
3. The *atdpeI* and *medpeI* genes were successfully and expressed in *E.coli* as intracellular His-tagged AtDPE1 and MeDPE1.
4. Ni-affinity column followed by gel filtration chromatography were used to purify AtDPE1 and MeDPE1.
5. Purified recombinant AtDPE1 and MeDPE1 were found to be homodimer The molecular weights of the subunits were 64 kDa and 61 kDa, respectively.
6. Both recombinant enzymes can transfer glucan from maltodextrin to glycogen on native PAGE and showed single band on iodine staining. Both enzymes showed optimum pH at 6-8 in MOPS and phosphate buffer and optimum temperature at 37-40°C and activity were retained at 40-50% at 37°C for 16 hours.
7. The recombinant MeDPE1 and AtDPE1 demonstrated a disproportionating activity with maltotriose as sole substrate by transfer maltosyl unit from one maltotriose to another to produce maltopentaose and glucose.

8. Oligosaccharide array technique was used to screen specific acceptor of AtDPE1 and MeDPE1. Acceptor specificity of AtDPE1 were maltotriose, maltohexaose and α-(1→6),(1→4)-D-glucododecaose.
9. Cycloamyloses with degree of polymerization in the ≥17 and ≥18 can be produced from amylose incubated with recombinant AtDPE1 and MeDPE1, respectively and detected by HPAEC-PAD and MALDI-TOF-MS.
10. In transglycosylation reaction, glycogen can be used as donor to transfer glucan to fluoroglucose derivatives. Fluoromaltose derivatives can be produced by MeDPE1, AtDPE2 and amylomaltase but large scale preparation was better with AtDPE2. The product was purified by ultrafiltration (Centricon (MWCO 30,000)) and gel filtration (TSK-HW40S) technique.
11. The structure of fluoromaltose derivatives were confirmed by $^{19}$F-NMR, $^{1}$H-NMR and high resolution mass spectrometry techniques.

# REFERENCES

Akdogan, G., Kubota, J., Kubo, A., Takaha, T. and Kitamura, S. (2011). Expression and characterization of rice disproportionating Enzymes. Journal of Applied Glycoscience 58(3): 99-105.

Andre, C., Spangenberg, P., Gentil, E. and Rabiller, C. (2001). In situ $^{19}F$ NMR spectroscopy study of enzymatic transglycosylation reactions using alpha-D-aldohexopyranosyl fluorides as donors and acceptors. Tetrahedron: Asymmetry 12(5): 779-783.

Attanasio, G., Cinquanta, L., Albanese, D. and Matteo, M. D. (2004). Effects of drying temperatures on physico-chemical properties of dried and rehydrated chestnuts (*Castanea sativa*). Food Chemistry 88(4): 583-590.

Bang, B. Y., *et al*. (2006). Cloning and overexpression of 4-alpha-glucanotransferase from *Thermus brockianus* (TBGT) in *E. coli.* Journal of Microbiology and Biotechnology 16(11): 1809-1813.

Barends, T. R. M., Bultema, J. B., Kaper, T., van der Maarel, M. J. E. C., Dijkhuizen, L. and Dijkstra, B. W. (2007). Three-way stabilization of the covalent intermediate in amylomaltase, an alpha-amylase-like transglycosylase. Journal of Biological Chemistry 282(23): 17242-17249.

Belle, C., Béguin, C., Hamman, S. and Pierre, J.-L. (2009). $^{19}F$ NMR: An underused efficient probe for paramagnetic metal centers in bioinorganic solution chemistry. Coordination Chemistry Reviews 253(7-8): 963-976.

Bresolin, N. S., *et al*. (2006). Characterisation of disproportionating enzyme from wheat endosperm. Planta 224(1): 20-31.

Cantarel, B. L., Coutinho, P. M., Rancurel, C., Bernard, T., Lombard, V. and Henrissat, B. (2009). The Carbohydrate-Active EnZymes database (CAZy): an expert resource for glycogenomics. Nucleic Acids Res 37(Database issue): D233-238.

Colleoni, C., *et al*. (1999). Biochemical characterization of the *Chlamydomonas reinhardtii* alpha-1,4 glucanotransferase supports a direct function in amylopectin biosynthesis. Plant Physiology 120(4): 1005-1014.

Critchley, J. H., Zeeman, S. C., Takaha, T., Smith, A. M. and Smith, S. M. (2001). A critical role for disproportionating enzyme in starch breakdown is revealed by a knock-out mutation in *Arabidopsis*. Plant Journal 26(1): 89-100.

Deckert, G., *et al*. (1998). The complete genome of the hyperthermophilic bacterium *Aquifex aeolicus*. Nature 392(6674): 353-358.

Endo, T. (2011). Large-ring cyclodextrins. Trends in Glycoscience and Glycotechnology 23(130): 79-92.

Gessler, K., *et al*. (1999). V-Amylose at atomic resolution: X-ray structure of a cycloamylose with 26 glucose residues (cyclomaltohexaicosaose). Proceedings of the National Academy of Sciences 96(8): 4246-4251.

Harata, K., Akasaka, H., Endo, T., Nagase, H. and Ueda, H. (2002). X-ray structure of the delta-cyclodextrin complex with cycloundecanone. Chem Commun (Camb)(17): 1968-1969.

Henrissat, B. (1991). A classification of glycosyl hydrolases based on amino acid sequence similarities. Biochemical Journal 280(2): 309-316.

Ivanov, P. M. (2010). Conformations of some large-ring cyclodextrins derived from conformational search with molecular dynamics simulations and principal component analysis. The Journal of Physical Chemistry B 114(8): 2650-2659.

Jacob, J., *et al*. (1999). Band-flip and kink as novel structural motifs in alpha-(1, 4)-D-glucose oligosaccharides. Crystal structures of cyclodeca- and cyclotetradecaamylose. Carbohydrate Research 322(3-4): 228-246.

Joint Genome Institute. Phytozome v6.0. [online]. 2010. Available from : http://www.phytozome.net [2010, April 10]

Jones, G. and Whelan, W. J. (1969). The action pattern of D-enzyme, a transmaltodextrinylase from potato. Carbohydrate Research 9(4): 483-490.

Kakefuda, G. and Duke, S. H. (1989). Characterization of Pea Chloroplast D-Enzyme (4-alpha-D-Glucanotransferase). Plant Physiol 91(1): 136-143.

Kaper, T., *et al*. (2007). Identification of acceptor substrate binding subsites +2 and +3 in the amylomaltase from *Thermus thermophilus* HB8. Biochemistry 46(17): 5261-5269.

Lee, B.-H., Oh, D.-K. and Yoo, S.-H. (2009). Characterization of 4-(alpha) -glucanotransferase from *Synechocystis* sp. PCC 6803 and its application to various corn starches. New Biotechnology 26(1-2): 29-36.

Liebl, W., Feil, R., Gabelsberger, J., Kellermann, J. and Schleifer, K.-H. (1992). Purification and characterization of a novel thermostable 4-α-glucanotransferase of *Thermotoga maritima* cloned in *Escherichia coli*. European Journal of Biochemistry 207(1): 81-88.

Lin, T.-P., Spilatro, S. R. and Preiss, J. (1988). Subcellular localization and characterization of amylases in *Arabidopsis* Leaf. Plant Physiology 86(1): 251-259.

Lin, T. P. and Preiss, J. (1988). Characterization of D-enzyme (4-alpha-Glucanotransferase) in *Arabidopsis* Leaf. Plant Physiol 86(1): 260-265.

Lin, X., *et al*. (1999). Sequence and analysis of chromosome 2 of the plant *Arabidopsis thaliana*. Nature 402(6763): 761-768.

Lloyd, J. R., Blennow, A., Burhenne, K. and Kossmann, J. (2004). Repression of a novel isoform of disproportionating enzyme (stDPE2) in potato leads to inhibition of starch degradation in leaves but not tubers stored at low temperature. Plant Physiology 134(4): 1347-1354.

Lu, Y. and Sharkey, T. (2004). The role of amylomaltase in maltose metabolism in the cytosol of photosynthetic cells. Planta 218(3): 466-473.

Lu, Y., Steichen, J. M., Yao, J. and Sharkey, T. D. (2006). The role of cytosolic alpha-glucan phosphorylase in maltose metabolism and the comparison of amylomaltase in *Arabidopsis* and *Escherichia coli*. Plant Physiology 142(3): 878-889.

Machida, S., Ogawa, S., Xiaohua, S., Takaha, T., Fujii, K. and Hayashi, K. (2000). Cycloamylose as an efficient artificial chaperone for protein refolding. FEBS Letters 486(2): 131-135.

Miyazawa, I., Ueda, H., Nagase, H., Endo, T., Kobayashi, S. and Nagai, T. (1995). Physicochemical properties and inclusion complex formation of delta-cyclodextrin. European Journal of Pharmaceutical Sciences 3(3).

Muhrbeck, P. and Eliasson, A. C. (1987). Influence of pH and ionic strength on the viscoelastic properties of starch gels, A comparison of potato and cassava starches. Carbohydrate Polymers 7(4): 291-300.

Nassar, N. and Ortiz, R. (2010). Breeding cassava to feed the poor. Sci Am 302(5): 78-82, 84.

Park, J.-H., *et al*. (2007). The action mode of *Thermus aquaticus* YT-1 4-alpha-glucanotransferase and its chimeric enzymes introduced with starch-binding domain on amylose and amylopectin. Carbohydrate Polymers 67(2): 164-173.

Plou, F. J., Segura, A. G. d. and Ballesteros, A. (2007). Application of glycosidases and transglycosidases in the synthesis of oligosaccharides industrial enzymes. J. Polaina and A. P. MacCabe, Springer Netherlands**:** 141-157.

Przylas, I., Terada, Y., Fujii, K., Takaha, T., Saenger, W. and Sträter, N. (2000). X-ray structure of acarbose bound to amylomaltase from *Thermus aquaticus*. European Journal of Biochemistry 267(23): 6903-6913.

Przylas, I., *et al*. (2000). Crystal structure of amylomaltase from *Thermus aquaticus*, a glycosyltransferase catalysing the production of large cyclic glucans. Journal of Molecular Biology 296(3): 873-886.

Roscher, A., Kruger, N. J. and Ratcliffe, R. G. (2000). Strategies for metabolic flux analysis in plants using isotope labelling. Journal of Biotechnology 77(1): 81-102.

Salehuzzaman, S. N. I. M., Jacobsen, E. and Visser, R. G. F. (1993). Isolation and characterization of a cDNA encoding granule-bound starch synthase in cassava (*Manihot esculenta* Crantz) and its antisense expression in potato. Plant molecular biology 23(5): 947-962.

Steichen, J. M., Petty, R. V. and Sharkey, T. D. (2008). Domain characterization of a 4-alpha-glucanotransferase essential for maltose metabolism in photosynthetic leaves. Journal of Biological Chemistry 283(30): 20797-20804.

Stettler, M., Eicke, S., Mettler, T., Messerli, G. l., Hortensteiner, S. and Zeeman, S. C. (2009). Blocking the Metabolism of Starch Breakdown Products in *Arabidopsis* Leaves Triggers Chloroplast Degradation. Molecular Plant 2(6): 1233-1246.

Strokopytov, B., *et al*. (1996). Structure of Cyclodextrin Glycosyltransferase Complexed with a Maltononaose Inhibitor at 2.6 Å Resolution. Implications for Product Specificity. Biochemistry 35(13): 4241-4249.

Suganuma, T., Setoguchi, S., Fujimoto, S. and Nagahama, T. (1991). Analysis of the characteristic action of D-enzyme from sweet potato in terms of subsite theory. Carbohydrate Research 212(0): 201-212.

Tachibana, Y., Takaha, T., Fujiwara, S., Takagi, M. and Imanaka, T. (2000). Acceptor specificity of 4-alpha-glucanotransferase from *Pyrococcus kodakaraensis* KOD1, and synthesis of cycloamylose. Journal of Bioscience and Bioengineering 90(4): 406-409.

TAIR, Gene locus AT5G64860. T. A. I. R. [online]. (2011). Available from :'http://www.arabidopsis.org/servlets/TairObject?accession=Locus:2177714&showAllNote=true.[2011, 20 February]

Takaha, T., Critchley, J., Okada, S. and Smith, S. M. (1998). Normal starch content and composition in tubers of antisense potato plants lacking D-enzyme (4-alpha-glucanotransferase). Planta 205(3): 445-451.

Takaha, T. and Smith, S. M. (1999). The functions of 4-alpha-glucanotransferases and their use for the production of cyclic glucans. Biotechnology and Genetic Engineering Reviews 16: 257-280.

Takaha, T., Yanase, M., Okada, S. and Smith, S. M. (1993). Disproportionating enzyme (4-α-glucanotransferase; EC 2.4.1.25) of potato. Purification, molecular cloning, and potential role in starch metabolism. Journal of Biological Chemistry 268(2): 1391-1396.

Takaha, T., Yanase, M., Takata, H., Okada, S. and Smith, S. M. (1996). Potato D-enzyme catalyzes the cyclization of amylose to produce cycloamylose, a novel cyclic glucan. Journal of Biological Chemistry 271(6): 2902-2908.

Takaha, T., Yanase, M., Takata, H., Okada, S. and Smith, S. M. (1998). Cyclic glucans produced by the intramolecular transglycosylation activity of potato D-enzyme on amylopectin. Biochemical and Biophysical Research Communications 247(2): 493-497.

Terada, Y., Fujii, K., Takaha, T. and Okada, S. (1999). *Thermus aquaticus* ATCC 33923 amylomaltase gene cloning and expression and enzyme characterization: production of cycloamylose. Applied and Environmental Microbiology 65(3): 910-915.

Terada, Y., Sanbe, H., Takaha, T., Kitahata, S., Koizumi, K. and Okada, S. (2001). Comparative study of the cyclization reactions of three bacterial cyclomaltodextrin glucanotransferases. Applied and Environmental Microbiology 67(4): 1453-1460.

Terada, Y., Yanase, M., Takata, H., Takaha, T. and Okada, S. (1997). Cyclodextrins are not the major cyclic alpha-1,4-glucans produced by the initial action of cyclodextrin glucanotransferase on amylose. Journal of Biological Chemistry 272(25): 15729-15733.

Tomono, K., *et al*. (2002). Interaction between cycloamylose and various drugs. Journal of Inclusion Phenomena and Macrocyclic Chemistry 44(1): 267-270.

Wattebled, F., *et al*. (2003). STA11, a *Chlamydomonas reinhardtii* locus required for normal starch granule biogenesis, encodes disproportionating enzyme. further evidence for a function of alpha-1,4 glucanotransferases during starch granule biosynthesis in green algae. Plant Physiology 132(1): 137-145.

Weise, S. E., van Wijk, K. J. and Sharkey, T. D. (2011). The role of transitory starch in C3, CAM, and C4 metabolism and opportunities for engineering leaf starch accumulation. Journal of Experimental Botany 62(9): 3109-3118.

Withers Stephen, G., Street Ian, P. and Percival Michael, D. (1988). Fluorinated carbohydrates as probes of enzyme specificity and mechanism. Fluorinated Carbohydrates, American Chemical Society. 374: 59-77.

Yanase, M., Takata, H., Takaha, T., Kuriki, T., Smith, S. M. and Okada, S. (2002). Cyclization reaction catalyzed by glycogen debranching enzyme (EC 2.4.1.25/EC 3.2.1.33) and its potential for cycloamylose production. Applied and Environmental Microbiology 68(9): 4233-4239.

Yuan, G.-L., Kuramoto, N. and Takeishi, M. (2003). Preparation of inclusion complex between polyaniline and β-cyclodextrin in aqueous solution. Polymers for Advanced Technologies 14(6): 428-432.

Zeeman, S. C., Smith, S. M. and Smith, A. M. (2004). The breakdown of starch in leaves. New Phytologist 163(2): 247-261.

Zeeman, S. C., Smith, S. M. and Smith, A. M. (2007). The diurnal metabolism of leaf starch. Biochemical Journal 401(1): 13-28.

Zheng, M., Endo, T. and Zimmermann, W. (2002). Synthesis of large-ring cyclodextrins by cyclodextrin glucanotransferases from bacterial isolates. Journal of Inclusion Phenomena 44(1-4): 387-390.

# APPENDICES

# Appendix A

## Preparation for SDS-polyacrylamide gel electrophoresis

### 1. Stock reagents

#### 2 M Tris-HCl pH 8.8

| | | |
|---|---|---|
| Tris(hydroxymethyl)-aminomethane | 24.2 | g |

Adjusted pH to 8.8 with 1 N HCl and adjusted volume to 100 ml with distilled water

#### 1 M Tris-HCl pH 6.8

| | | |
|---|---|---|
| Tris(hydroxymethyl)-aminomethane | 12.1 | g |

Adjusted pH to 6.8 with 1 N HCl and adjusted volume to 100 ml with distilled water

#### 10% (w/v) SDS

| | | |
|---|---|---|
| Sodium dodecyl sulfate | 10 | g |

Adjusted volume to 100 ml with distilled water

#### 50% (v/v) Glycerol

| | | |
|---|---|---|
| 100% Glycerol | 50 | ml |

Added 50 ml distilled water

**1% (w/v) Bromophenol blue**

Bromophenol blue 100 mg

Brought to 10 ml with distilled water and stir until dissolved. Filtration was performed to remove aggregated dye.

**2. Working Solutions**

**Solution A**

**30% Acrylamide, 0.8% bis-acrylamide, 100 ml**

| | | |
|---|---|---|
| Acrylamide | 29.2 | g |
| N,N'-methylene-bis-acrylamide | 0.8 | g |

Adjusted volume to 100 ml with distilled water

**Solution B**

**4x Seperating Gel Buffer**

| | | |
|---|---|---|
| 2 M Tris-HCl pH 8.8 | 75 | ml |
| 10% SDS | 4 | ml |
| Distilled water | 21 | ml |

**Solution C**

**4x Stacking Gel Buffer**

| | | |
|---|---|---|
| 1 M Tris-HCl pH 6.8 | 50 | ml |
| 10% SDS | 4 | ml |
| Distilled water | 46 | ml |

**10% Ammonium persulfate**

| | | |
|---|---|---|
| Ammonium persulfate | 0.5 | g |
| Distilled water | 5 | ml |

**Electrophoresis Buffer**

| | | |
|---|---|---|
| Tris(hydroxymethyl)-aminomethane | 3 | g |
| Glycine | 14.4 | g |
| Sodium dodecyl sulfate | 1 | g |

Adjusted volume to 1 liter with distilled water

**5x Sample buffer**

| | | |
|---|---|---|
| 1 M Tris-HCl pH 6.8 | 0.6 | ml |
| 50% Glycerol | 5 | ml |
| 10% SDS | 2 | ml |
| 2-Mercaptoethanol | 0.5 | ml |
| 1% Bromophenol blue | 1 | ml |
| Distilled water | 0.9 | ml |

**Coomassie Gel Stain**

| | | |
|---|---|---|
| Coomassie Blue R-250 | 1 | g |
| Methanol | 450 | ml |
| Distilled water | 450 | ml |
| Glacial acetic acid | 100 | ml |

**Coomassie Gel Destain**

| | | |
|---|---|---|
| Methanol | 100 | ml |
| Glacial acetic acid | 100 | ml |
| Distilled water | 800 | ml |

# Appendix B

## Preparation for native-polyacrylamide gel electrophoresis

### 1) Stock reagents

**2 M Tris-HCl pH 8.8**

Tris(hydroxymethyl)-aminomethane 24.2 g

Adjusted pH to 8.8 with 1 N HCl and adjusted volume to 100 ml with distilled water

**1 M Tris-HCl pH 6.8**

Tris(hydroxymethyl)-aminomethane 12.1 g

Adjusted pH to 6.8 with 1 N HCl and adjusted volume to 100 ml with distilled water

**50% (v/v) Glycerol**

100% Glycerol

Add 50 ml distilled water

**1% (w/v) Bromophenol blue**

Bromophenol blue 100 mg

Brought to 10 ml with distilled water and stir until dissolved.

Filtration was performed to remove aggregated dye.

**2) Working Solutions**

**Solution A**

**30% Acrylamide, 0.8% bis-acrylamide, 100 ml**

| | | |
|---|---|---|
| Acrylamide | 29.2 | g |
| N,N'-methylene-bis-acrylamide | 0.8 | g |

Adjusted volume to 100 ml with distilled water

**Solution B**

**4x Seperating Gel Buffer**

| | | |
|---|---|---|
| 2 M Tris-HCl pH 8.8 | 75 | ml |
| Distilled water | 25 | ml |

**Solution C**

**4x Stacking Gel Buffer**

| | | |
|---|---|---|
| 1 M Tris-HCl pH 6.8 | 50 | ml |
| Distilled water | 50 | ml |

**10% Ammonium persulfate**

| | | |
|---|---|---|
| Ammonium persulfate | 0.5 | g |
| Distilled water | 5 | ml |

**1% Glycogen**

| | | |
|---|---|---|
| Glycogen from oyster | 0.05 | ml |
| Distilled water | 5 | ml |

**Electrophoresis Buffer**

| | | |
|---|---|---|
| Tris(hydroxymethyl)-aminomethane | 3 | g |
| Glycine | 14.4 | g |

Adjusted volume to 1 liter with distilled water

**5x Sample buffer**

| | | |
|---|---|---|
| 1 M Tris-HCl pH 6.8 | 3.1 | ml |
| 50% Glycerol | 5 | ml |
| 1% Bromophenol blue | 0.5 | ml |
| Distilled water | 1.4 | ml |

# Appendix C

## Map and feature of pTrcHis2C

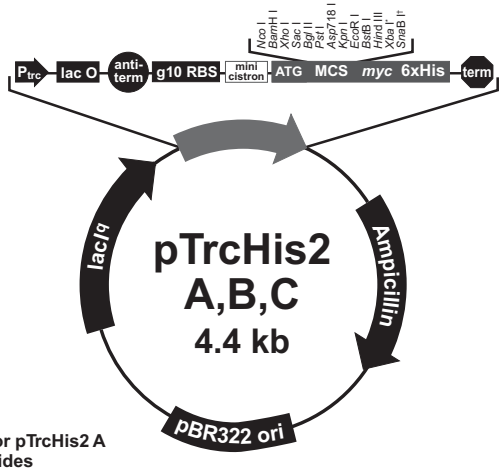


**Comments for pTrcHis2 A**
**4406 nucleotides**

*trc* promotor region: bases 190-382
-35 region: bases 193-198
-10 region: bases 216-221
lac operator (*lac*O): bases 228-248
*rrn*B antitermination signal: bases 264-333
gene 10 region: bases 346-354
Ribosome binding site: bases 369-373
pTrcHis forward priming site: bases 370-390
Minicistron ORF: bases 383-409
Reinitiation RBS: bases 398-403
Expression ATG: bases 413-415
Multiple cloning site: bases 411-464
*myc* epitope: bases 471-503
Polyhistidine tag: bases 516-533
*myc*His reverse priming site: bases 508-527
*rrn*B T1 and T2 transcriptional terminators: bases 639-796
Ampicillin resistance ORF: bases 1076-1936
pBR322 origin: bases 2081-2754
*Lac* Repressor (*lacI*$^{q}$) ORF: bases 3408-4367

* *Xba* I is only found in pTrcHis2 B

† *Sna*B I is only found in pTrcHis2 C

**Multiple Cloning Site of pTrcHis2 C**

Below is the multiple cloning site for pTrcHis2 C. Restriction sites are labeled to indicate cleavage site. The boxed sequence is the variable region that facilitates in frame cloning with the C-terminal peptide. This variable region is located between the *Hin*d III site and the *myc* epitope. The multiple cloning site has been confirmed by sequencing and functional testing.

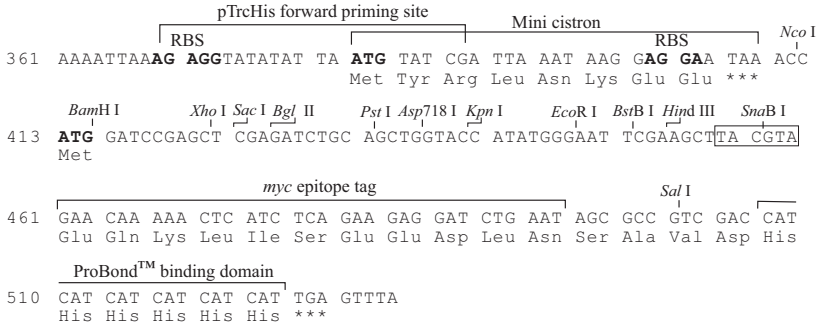

# Appendix D

## Map and feature of pET151/D-TOPO®

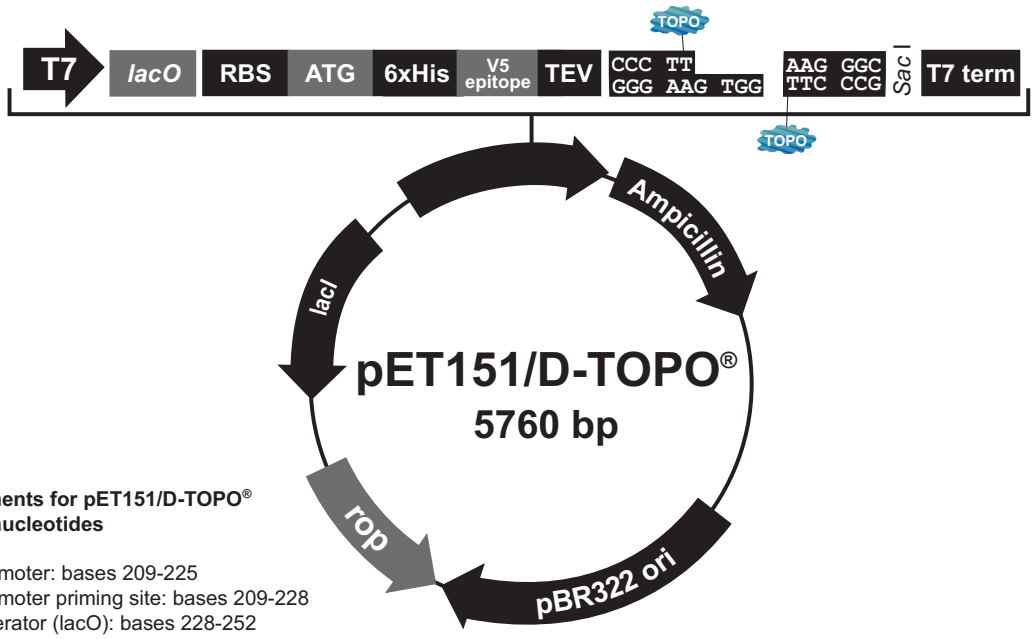


**Comments for pET151/D-TOPO®**
**5760 nucleotides**

T7 promoter: bases 209-225
T7 promoter priming site: bases 209-228
lac operator (lacO): bases 228-252
Ribosome binding site (RBS): bases 282-289
Initiation ATG: bases 297-299
Polyhistidine (6xHis) region: bases 300-317
V5 epitope: bases 318-359
TEV recognition site: bases 360-380
TOPO® cloning site (directional): bases 387-400
T7 reverse priming site: bases 455-474
T7 transcription termination region: bases 416-544
*bla* promoter: bases 849-947
Ampicillin (*bla*) resistance gene: bases 948-1808
pBR322 origin: bases 1953-2626
*ROP* ORF: bases 2997-3188 (complementary strand)
*lacI* ORF: bases 4500-5612 (complementary strand)

## TOPO® Cloning Site of pET151/D-TOPO®

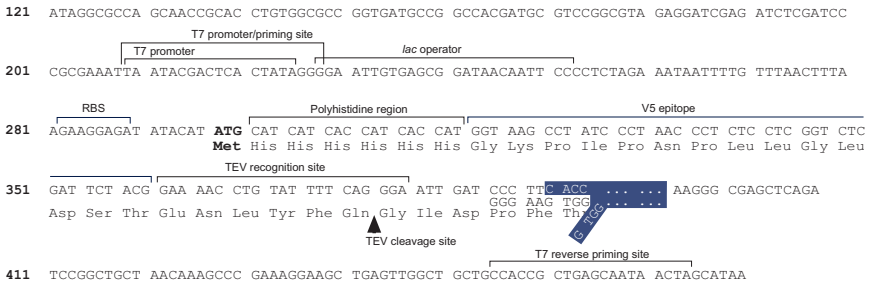

# `Appendix E

**Preparation of Hexokinase-G6P dehydrogenase assay cocktail and standard glucose**

**1) Hexokinase assay cocktail**

Make up fresh

| Reagent | One plate (20ml)* | 5 ml |
|---|---|---|
| 200mM HEPES pH 7.9 | 2.75 ml | 0.6875 ml |
| 200mM $MgCl_2$ | 0.1 ml | 0.025 ml |
| Water | 17.14 ml | 4.285 ml |
| ATP | 6.7 mg | 1.675 mg |
| NAD | 5.8 mg | 1.45 mg |
| Hexokinase | 44 µl | 11 µl |

2) Add 2µl of glucose-6-phosphate dehydrogenase (G6PDH) (1:5 dilution with distilled water) To each reaction assay after start absorbent (Abs1) was recorded.

* add 40 µl of G6PDH in kinetic determination.

**Standard glucose**

REAGENTS: (add distilled water to make total volume of 10 µl)

Glucose 0 – 100 nmol ( ADD WATER TO 10 µl)

10 mM Glucose Stock: 10 µl = 100 nmol per well

10 mM Glucose Stock: 8 µl = 80 nmol per well

10 mM Glucose Stock: 6 µl = 60 nmol per well

10 mM Glucose Stock: 5 µl = 50 nmol per well

10 mM Glucose Stock: 4 µl = 40 nmol per well

10 mM Glucose Stock: 3 µl = 30 nmol per well

10 mM Glucose Stock: 2 µl = 20 nmol per well

10 mM Glucose Stock: 1 µl = 10 nmol per well

## Appendix E (continue)

**Standard curve of glucose determination by hexokinase-G6P dehydrogenase assay method**

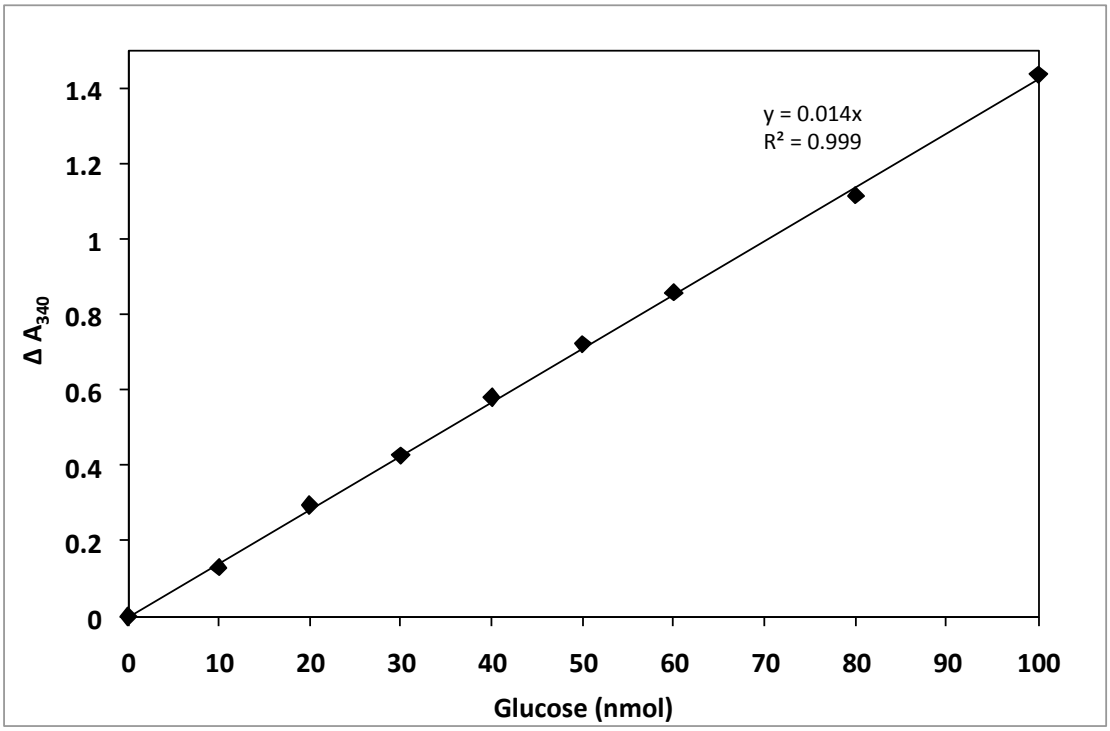


**Assay glucose by combined reaction of hexokinase and glucose-6-phosphate dehydrogenase and follow change in absorption of NADH at $OD_{340}$**

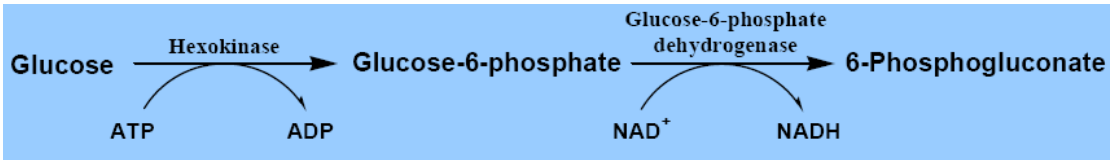

# Appendix F

## Bacterial media culture

### LB (Luria-Bertani) Medium and Plates

1.0% Tryptone

0.5% Yeast Extract

1.0% NaCl

1.5% agar (Agar plate)

For 1 liter, dissolve 10 g tryptone, 5 g yeast extract, and 10 g NaCl (add 15 g/L agar for agar plate) in 1000 ml with deionized water.

### Auto Induction Media (AIM) formula (g/l)

| | | |
|---|---|---|
| Tryptone | 10 | g |
| Yeast extract | 5 | g |
| $(NH_4)_2SO_4$ | 3.3 | g |
| $KH_2PO_4$ | 6.8 | g |
| $Na_2HPO_4$ | 7.1 | g |
| Glucose | 0.5 | g |
| α-Lactose | 2.0 | g |
| $MgSO_4$ | 0.15 | g |

Add 1000 ml with deionized water. The medium was sterilized by autoclaving at 15 $lb/in^2$ for 15 minutes.

# Appendix G

## Lysis solution

50mM Tris-HCl pH 8.0, 0.5M NaCl, 30mM Immidazole, 0.3 mg/ml DTT, 50 µg/ml lysozyme, 1 tablet of protease inhibitor cocktail from Roche and 12.5 µg/µl DNase

## Buffer for purification protein

Buffer A (washing buffer)

- 0.5 M NaCl and 30 mM Immidazole in 50 mM Tris-HCl pH 8.0

Buffer B (elute buffer)

- 0.5 M NaCl and 500 mM Immidazole in 50 mM Tris pH 8.0

GF buffer (Gel filtration buffer)

-100 mM NaCl in 50 mM HEPES pH 7.5

# Appendix H

## Glycogen solution (25mg/ml)

Dissolve 250 mg of Glycogen from oyster Type II in 10 ml MQ-Water and dialysed 4 times against MQ-water with dialysis membranes (500 MWCO).

## Orcinol solution

Dissolve 360 mg of 3,5-dihydroxytoluene in 150 ml ethanol and 10 ml of water. Put solution on ice and add 20 ml of conc. sulfuric acid.

# Appendix I

## Oligosaccharide array type I

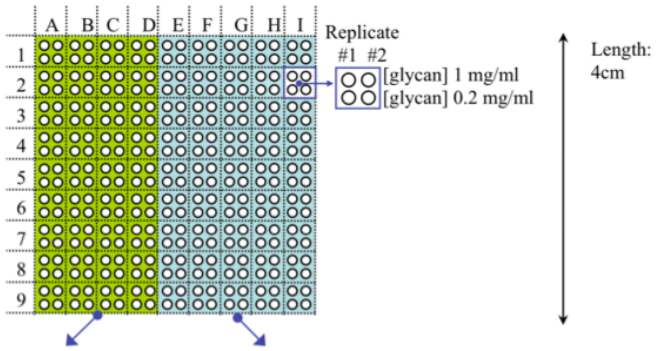


| | Epitope displayed in BSA-conjugate |
|---|---|
| A1 | α-(1→4)-D-heptagalacturonate (DE 0%) |
| B1 | α-(1→4)-D-pentagalacturonate (DE 0%) |
| C1 | β-D-galactose |
| D1 | β-(1→4)-D-galactotetraose |
| A2 | α-L-arabinose |
| B2 | α-(1→5)-L-arabinobiose |
| C2 | α-(1→5)-L-arabinotriose |
| D2 | α-(1→5)-L-arabinotetraose |
| A3 | α-(1→5)-L-arabinopentaose |
| B3 | α-(1→5)-L-arabinohexaose |
| C3 | α-(1→5)-L-arabinoheptaose |
| D3 | β-(1→4)-D-glucopentaose |
| A4 | β-D-mannose |
| B4 | β-(1→4)-D-mannotriose |
| C4 | β-(1→4)-D-mannotetraose |
| D4 | β-(1→4)-D-mannopentaose |
| A5 | β-D-xylose |
| B5 | β-(1→4)-D-xylotriose |
| C5 | β-(1→4)-D-xylotetraose |
| D5 | β-(1→4)-D-xylopentaose |
| A6 | Conjugate of Xyloglucan heptamer XXX(G)- |
| B6 | Conjugate of Xyloglucan octamer XXL(G)- |
| C6 | Conjugate of Xyloglucan nonamer XLL(G)- |
| D6 | $6^{1}$-α-D-galactosyl-β-(1→4)-D-mannobiose |
| A7 | (1→3),(1→4)-β-D-glucotriose [G4G3G(G)-] |
| B7 | (1→3),(1→4)-β-D-glucotetraose [G3G4G4G(G)-] |
| C7 | (1→3),(1→4)-β-D-glucopentaose [G3G4G3G4G(G)-] |
| D7 | $6^{3}$,$6^{4}$-*di*galactosyl-β-(1→4)-D-mannotetraose |
| A8 | α-(1→4)-D-glucobiose |
| B8 | α-(1→4)-D-glucopentaose |
| C8 | α -(1→6)-D-glycosyl-α-(1→4)-D-maltotriose G6G4G |
| D8 | α-(1→6)-D-glycosyl-α-(1→4)-D-maltosyl-maltose G6G4G4G6G4G |
| A9 | β-D-glucose |
| B9 | β-(1→3)-D-glucotriose |
| C9 | β-(1→3)-D-glucotetraose |
| D9 | β-(1→3)-D-glucopentaose |
| | * DE; degree of methyl esterification |

| | |
|---|---|
| E1 | Lime pectin, DE 11% (Danisco #F11) |
| F1 | Lime pectin, DE 43% (Danisco #F43) |
| G1 | Lime pectin DE 0% (Danisco #B00) |
| H1 | Lime pectin, DE 16% (Danisco #P16) |
| I1 | Sugar beet pectin (Danisco #SBP6232) |
| E2 | Pectic galactan #1 (lupin, INRA/Nantes) |
| F2 | Pectic galactan #2 (potato, INRA/Nantes) |
| G2 | Pectic galactan #3 (lupin, Megazyme) |
| H2 | Pectic galactan #4 (tomato, J. Paul Knox) |
| I2 | RGII enriched pectin (red wine) |
| E3 | RGI #1 (soy bean, Megazyme) |
| F3 | RGI #2 (carrot, INRA/Nantes) |
| G3 | RGI #3 (sugar beet, INRA/Nantes) |
| H3 | RGI #4 (Arabidopsis, INRA/Nantes) |
| I3 | Seed mucilage (Arabidopsis, INRA/Nantes) |
| E4 | Arabinan (sugar beet, Megazyme) |
| F4 | Arabinan, de-branched (sugar beet, Megazyme) |
| G4 | (1→5)-alpha-L-arabinan (sugar beet, Megazyme) |
| H4 | RGI #5 (potato, Megazyme) |
| I4 | Xylogalacturonan, XGA (apple, INRA/Nantes) |
| E5 | Xylan (birch wood, Sigma-Aldrich) |
| F5 | Arabinoylan (wheat, Megazyme) |
| G5 | 4-Methoxy-glucoronoarabinoxylan (birch, Sigma-Aldrich) |
| H5 | Xyloglucan, non fucosylated (tamarind seed, Megazyme) |
| I5 | Xyloglucan, fucosylated (pea, INRA/Nantes) |
| E6 | Carboxymethyl-cellulose, CM-cellulose (Avicel) |
| F6 | Hydroxymethyl-cellulose, MeO-cellulose (Avicel) |
| G6 | Hydroxyethyl-cellulose, EtO-cellulose (Avicel) |
| H6 | (1→6),(1→3)-β-D-glucan (laminarin, Sigma-Aldrich) |
| I6 | (1→3)-β-D-glucan (pachyman) |
| E7 | β-glucan #1 (lichenan, icelandic moss, Megazyme) |
| F7 | β-glucan #2 (barley, Megazyme) |
| G7 | β-glucan #3 (oat, Megazyme) |
| H7 | β-glucan #4 (yeast) |
| I7 | (1→6),(1→4)-α-D-glucan (pullulan) |
| E8 | Glucomannan |
| F8 | Galactomannan |
| G8 | Gum guar |
| H8 | Gum Arabic (Sigma-Aldrich) |
| I8 | Locust bean gum (Megazyme) |
| E9 | Xanthan gum (Danisco #R80) |
| F9 | Carrageenan #1 (Danisco #100) |
| G9 | Carrageenan #2 (Danisco #201) |
| H9 | Alginate, sodium salt (Danisco #FD-155) |
| I9 | Sugar beet arabinan (Megazyme) |

# Appendix I (continue)

## Oligosaccharide array type II

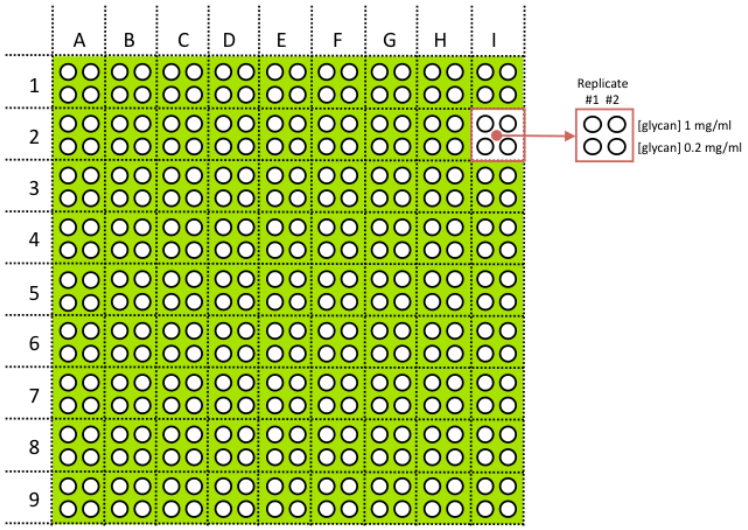


| | Oligosaccharide conjugated to BSA |
|---|---|
| A1 | 6,6‴‘,6‴‘‘-*tri*methyl-α-(1→4)- D-hexagalacturonate (DE 50%) |
| A2 | 6',6'',6‴-trimethyl-α-(1→4)- D-hexagalacturonate (DE 50%) |
| A3 | 6,6‴‘-*di*methyl-α-(1→4)- D-hexagalacturonate (DE 33%) |
| A4 | 6',6'',6‴,6‴‘-tetramethyl-α-(1→4)- D-hexagalacturonate (DE 66%) |
| A5 | 6',6'',6‴‘-trimethyl-α-(1→4)- D-hexagalacturonate (DE 50%) |
| A6 | α-(1→4)-D-pentagalacturonate (DE 0%) |
| A7 | α-(1→4)- D-hexagalacturonate (DE 0%) |
| A8 | α-(1→4)- D-heptagalacturonate, lyase product (DE 0%) |
| A9 | α-(1→4)- D-octagalacturonate, lyase product (DE 0%) |
| B1 | α-(1→5)-L-arabinobiose |
| B2 | α-(1→5)- L-arabinotriose |
| B3 | α-(1→5)- L-arabinotetraose |
| B4 | α-(1→5)- L-arabinopentaose |
| B5 | α-(1→5)- L-arabinohexaose |
| B6 | α-(1→5)- L-arabinoheptaose |
| B7 | α-(1→5)- L-arabinooctaose |
| B8 | β-(1→4)- D-galactotetraose |
| B9 | β-(1→4)- D-galactobiose, feruloylated |
| C1 | β-D-xylobiose |
| C2 | β-(1→4)-D-xylotriose |
| C3 | β-(1→4)-D-xylotetraose |
| C4 | β-(1→4)-D-xylopentaose |
| C5 | β-(1→4)-D-xylohexaose |
| C6 | D-galactose |
| C7 | β-(1→4)- D-galactobiose |
| C8 | $6^3,6^4$-α-D-*di*galactosyl-β-(1→4)-D-mannopentaose |
| C9 | α-(1→5)- L-arabinobiose, feruloylated |
| D1 | Alduronic acids (DP 2, 3 & 4) |
| D2 | Isoprimeverose D-xylose-α-(1→6)-D-glucose |
| D3 | Xyloglucan heptamer XXXG DP 7 |
| D4 | Xyloglucan octamer XXLG / XLXG DP 8 |
| D5 | Xyloglucan nonamer XLLG DP 9 |
| D6 | $6^3$-α- D-galactosyl-β-(1→4)-D-mannobiose |
| D7 | $6^3$-α-D-galactosyl-β-(1→4)-D-mannotriose |
| D8 | Lactose |
| D9 | α-(1→5)- L-arabinotriose, feruloylated |
| E1 | β-D-mannose |
| E2 | β-(1→4)- D-mannobiose |
| E3 | β-(1→4)- D-mannotriose |
| E4 | β-(1→4)- D-mannotetraose |
| E5 | β-(1→4)- D-mannopentaose |
| E6 | β-(1→4)-D-mannohexaose |
| E7 | glucomannan (konjac) DP 4-6 |
| E8 | $6^2$-β-D-galactosyl-β-(1→4)-D-galactotriose |
| E9 | galactomannan DP 4-6 |

| | Oligosaccharide conjugated to BSA |
|---|---|
| F1 | (1→3),(1→4)-β- D-glucotriose G3G4G |
| F2 | (1→3),(1→4)-β- D-glucotriose G4G3G |
| F3 | (1→3),(1→4)-β- D-glucotetraose G3G4G4G |
| F4 | (1→3),(1→4)-β- D-glucotetraose G4G4G3G |
| F5 | (1→3),(1→4)-β- D-glucotetraose G4G3G4G |
| F6 | (1→3),(1→4)-β- D-glucopentaose G3G4G4G4G |
| F7 | (1→3),(1→4)-β- D-glucohexaose G3G4G3G4G3G |
| F8 | (1→3),(1→4)-β- D-glucan (DP 2-4) (barley) |
| F9 | D-glucose |
| G1 | β-(1→3)- D-glucobiose |
| G2 | β-(1→3)- D-glucotriose |
| G3 | β-(1→3)- D-glucotetraose |
| G4 | β-(1→3)- D-glucopentaose |
| G5 | β-(1→3)- D-glucohexaose |
| G6 | α-(1→4)- D-glucobiose (maltose) |
| G7 | α-(1→4)- D-glucotriose (maltotriose) |
| G8 | α-(1→4)- D-glucohexaose (maltohexaose) |
| G9 | α-(1→4)- D-glucobiose, 6-phosphate |
| H1 | β-(1→4)- D-glucobiose |
| H2 | β-(1→4)- D-glucotriose |
| H3 | β-(1→4)- D-glucotetraose |
| H4 | β-(1→4)- D-glucopentaose |
| H5 | β-(1→4)- D-glucohexaose |
| H6 | α-(1→6)-D-glycosyl-α-(1→4)-D-maltotriose G6G4G4G |
| H7 | D-glycosyl-α-(1→6)- D-maltotriasyl-α-(1→6)- D-maltotriose G6G4G4G6G4G4G |
| H8 | α -(1:6),(1:4) -D-glucododecaose |
| H9 | α-(1→4)- D-glucobiose, 3-phosphate |
| I1 | *N*-acetyl- D-glucose-2-amine |
| I2 | *di*acetyl-chitobiose |
| I3 | *tri*acetyl-chitotriose |
| I4 | *tetra*acetyl-chitotetraose |
| I5 | *penta*acetyl-chitopentaose |
| I6 | *hexa*acetyl-chitohexaose |
| I7 | BSA |
| I8 | $6^2$-α-D-galactosyl-β-(1→4)-D-galactotriose |
| I9 | Arabinoxylan (DP 2-4) |

# Appendix J

## Standard cycloamylose

Standard cycloamylose from Amylomaltase from *Thermus aquaticus* ATCC 33923. was using to compare retention time. ($CD_n$, n is the glucose number of large ring cyclodextrin).

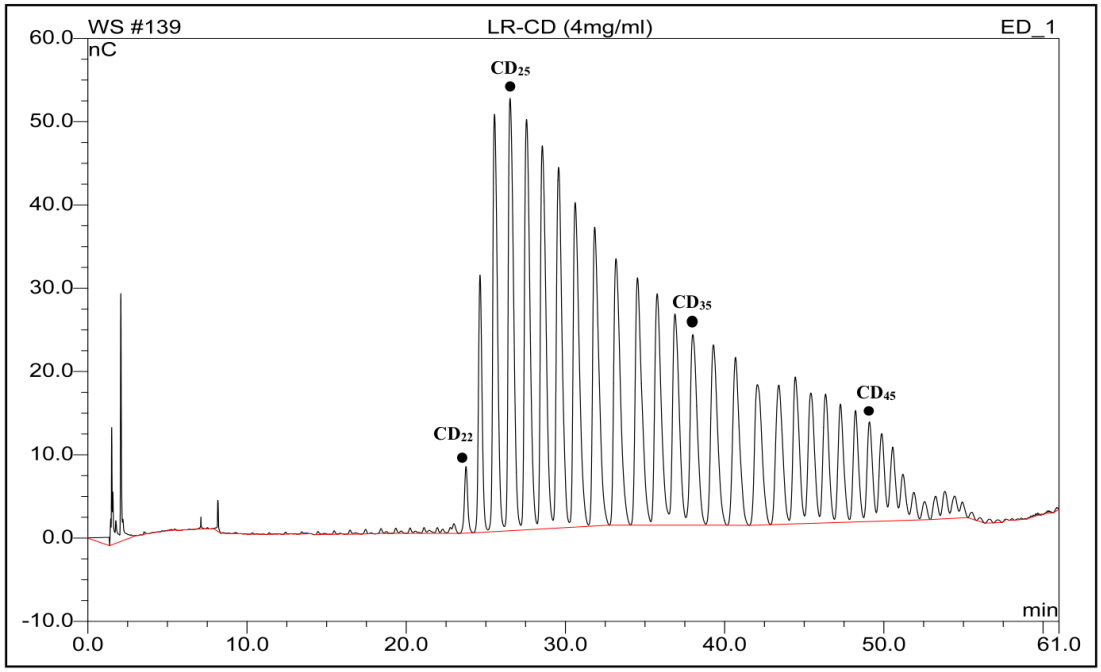

# BIOGRAPHY

Mr. Krit Tantanarat born on April 3, 1981. He graduated with the Bachelor Degree of Science in Biochemistry from Chulalongkorn university in 2004. He graduated with Master Degree of Science in Biotechnology from Chulalongkorn University in 2006. Then he further studied for the degree of PhD. in biochemistry at the department of biochemistry, faculty of science, Chulalongkorn university until 2012.